AD-A137 225 DESIGN OF GRAVITY DAMS ON ROCK FOUNDATIONS SLIDING STABILITY ASSESSMENT B..(U) ARMY ENGINEER WATERWAYS EXPERIMENT STATION VICKSBURG MS GEOTE.. G A NICHOLSON 1/2

UNCLASSIFIED OCT 83 WES/TR/GL-83-13 F/G 13/13 NL

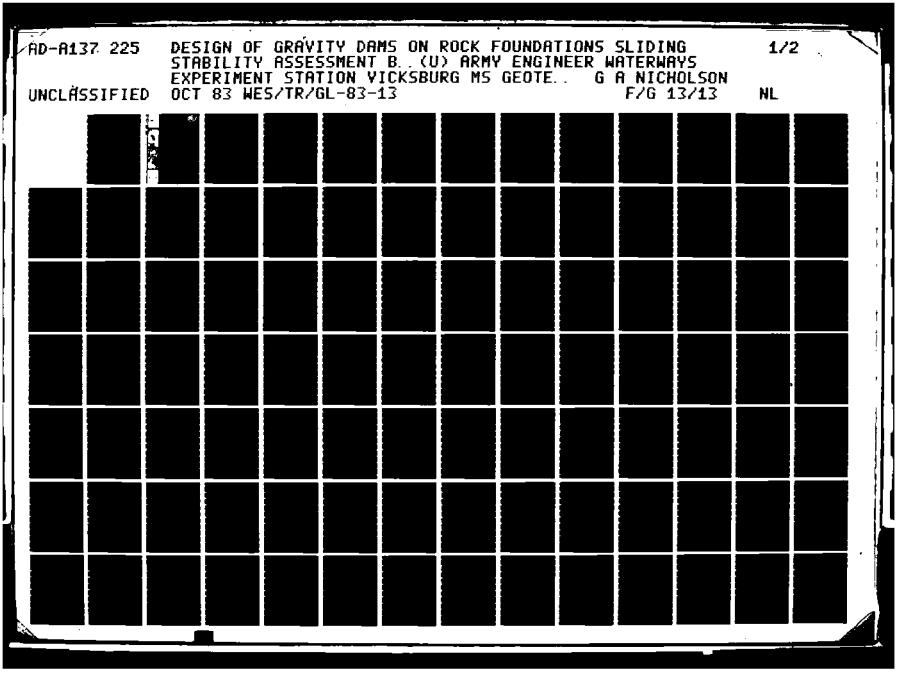

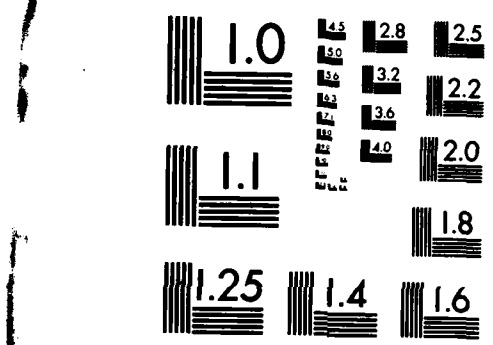

US Army Corps of Engineers

GEOTECHNICAL LABORATORY

TECHNICAL REPORT GL-83-13

16

DESIGN OF GRAVITY DAMS ON ROCK FOUNDATIONS: SLIDING STABILITY ASSESSMENT BY LIMIT EQUILIBRIUM AND SELECTION OF SHEAR STRENGTH PARAMETERS

by

Glenn A. Nicholson

Geotechnical Laboratory
U. S. Army Engineer Waterways Experiment Station
P. O. Box 631, Vicksburg, Miss. 39180

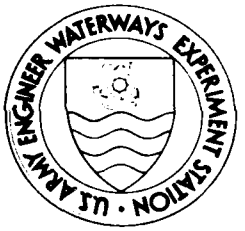

October 1983

Final Report

Prepared for Office, Chief of Engineers, U. S. Army
Washington, D. C. 20314

Under CWIS Work Unit 31668

Destroy this report when no longer needed. Do not return it to the originator.

The findings in this report are not to be construed as an official Department of the Army position unless so designated by other authorized documents.

The contents of this report are not to be used for advertising, publication, or promotional purposes. Citation of trade names does not constitute an official endorsement or approval of the use of such commercial products.

Unclassified

SECURITY CLASSIFICATION OF THIS PAGE *(When Data Entered)*

REPORT DOCUMENTATION PAGE

READ INSTRUCTIONS BEFORE COMPLETING FORM

1. REPORT NUMBER: Technical Report GL-83-13	2. GOVT ACCESSION NO.
3. RECIPIENT'S CATALOG NUMBER	
4. TITLE *(and Subtitle)*: DESIGN OF GRAVITY DAMS ON ROCK FOUNDATIONS: SLIDING STABILITY ASSESSMENT BY LIMIT EQUILIBRIUM AND SELECTION OF SHEAR STRENGTH PARAMETERS	5. TYPE OF REPORT & PERIOD COVERED: Final report
	6. PERFORMING ORG. REPORT NUMBER
7. AUTHOR(s): Glenn A. Nicholson	8. CONTRACT OR GRANT NUMBER(s)
9. PERFORMING ORGANIZATION NAME AND ADDRESS: U.S. Army Engineer Waterways Experiment Station, Geotechnical Laboratory, P. O. Box 631, Vicksburg, Miss. 39180	10. PROGRAM ELEMENT, PROJECT, TASK AREA & WORK UNIT NUMBERS: CWIS Work Unit 31668
11. CONTROLLING OFFICE NAME AND ADDRESS: Office, Chief of Engineers, U. S. Army, Washington, D. C. 20314	12. REPORT DATE: October 1983
	13. NUMBER OF PAGES: 140
14. MONITORING AGENCY NAME & ADDRESS *(if different from Controlling Office)*	15. SECURITY CLASS. *(of this report)*: Unclassified
	15a. DECLASSIFICATION/DOWNGRADING SCHEDULE

16. DISTRIBUTION STATEMENT *(of this Report)*

Approved for public release; distribution unlimited.

17. DISTRIBUTION STATEMENT *(of the abstract entered in Block 20, if different from Report)*

18. SUPPLEMENTARY NOTES

Available from National Technical Information Service, 5285 Port Royal Road, Springfield, Va. 22151.

19. KEY WORDS *(Continue on reverse side if necessary and identify by block number)*

Dam foundations
Dam safety
Gravity dam design
Rock foundations
Shear strength

20. ABSTRACT *(Continue on reverse side if necessary and identify by block number)*

The U. S. Army Corps of Engineers recently changed the method by which it assesses the sliding stability of gravity structures from the shear-friction method to the limit-equilibrium method. This report discusses the assumptions used in the development of and the limitations of the limit-equilibrium method for assessing the sliding stability of gravity hydraulic structures. The limit-equilibrium method applies the factor of safety directly to the least known parameters of sliding stability assessments; that is, the (Continued)

DD FORM 1 JAN 73 1473 EDITION OF 1 NOV 65 IS OBSOLETE

Unclassified

SECURITY CLASSIFICATION OF THIS PAGE *(When Data Entered)*

20. ABSTRACT (Continued).

shear strength of the founding material. Because shear strength forms an important part of any sliding stability assessment, this report also offers information on methods for the selection of design shear strengths for structures founded on rock mass.

Shear strengths selected for design must consider certain prerequisites. Prerequisites briefly discussed include: field investigations, loading conditions, shear tests, material stress-strain characteristics, failure criteria, linear interpretation of nonlinear failure criteria, and the level of confidence that should be placed in the selected design strengths.

Modes of potential failure for a structure founded on a rock mass may be through intact rock and/or along clean or filled discontinuous rock. Methods which form the bases of shear strength selection are dependent upon modes of potential failure. Currently acceptable methods, including shear tests, empirical concepts, and rational approaches, are discussed. Particular emphasis is given to alternative approaches in selecting design shear strength parameters c and ϕ as the approaches relate to the level of confidence that must be placed in the design strengths.

PREFACE

The study reported herein was performed under the Civil Works Investigation Studies (CWIS) Program, Materials - Rock, Work Unit 31668 entitled "Foundation Design Methods." The study was sponsored by the Office, Chief of Engineers (OCE), U. S. Army. The investigation was conducted by the U. S. Army Engineer Waterways Experiment Station (WES) during FY 81 and FY 82.

This report was prepared by Mr. G. A. Nicholson, Rock Mechanics Application Group (RMAG), Engineering Geology and Rock Mechanics Division (EGRMD), Geotechnical Laboratory (GL). Appendices A and B were prepared by Mr. Hardy J. Smith, RMAG. During the preparation of this report Mr. J. S. Huie was Chief, RMAG, GL. Dr. D. C. Banks was Chief, ECRMD, GL. Dr. W. F. Marcuson III was Chief, GL. Technical Monitor for OCE was Mr. Paul R. Fisher.

Commander and Director of the WES during the preparation of this report was COL Tilford C. Creel, CE. Technical Director was Mr. Fred R. Brown.

CONTENTS

CONVERSION FACTORS, U. S. CUSTOMARY TO METRIC (SI)
UNITS OF MEASUREMENT

U. S. customary units of measurement used in this report can be converted to metric (SI) units as follows:

Multiply	By	To Obtain
cubic feet	0.02831685	cubic metres
feet	0.3048	metres
inches	2.54	centimetres
kips (force)	4.448222	kilonewtons
kips (force) per square foot	47.88026	kilopascals
kips (force) per square inch	6894.757	kilopascals
pounds (force) per square foot	47.88026	pascals
pounds (force) per square inch	6894.757	pascals
pounds (mass) per cubic foot	16.01846	kilograms per cubic metre
square feet	0.09290304	square metres
tons (force) per square foot	95.76052	kilopascals

DESIGN OF GRAVITY DAMS ON ROCK FOUNDATIONS: SLIDING STABILITY ASSESSMENT BY LIMIT EQUILIBRIUM AND SELECTION OF SHEAR STRENGTH PARAMETERS

PART I: INTRODUCTION

Background

1. A gravity structure is designed so that the forces acting on that structure are primarily resisted by the structure's own mass. Examples of gravity structures include dams, spillways, weirs, lock walls, and retaining walls. In terms of economics and in terms of the consequences of a possible failure, gravity dams are the most important gravity structure of interest to the U. S. Army Corps of Engineers (CE).

2. Like most other engineering feats the design and construction of gravity dams was and still is an evolutionary process. Archaeological ruins indicate that gravity dams were constructed as early as 2000 B.C. These early dams were generally made of uncemented masonry with base widths as much as four times their heights. Construction was, no doubt, based on trial and error. With the passing of centuries, various types of mortar were used to bind the masonry together, thereby increasing the stability and water tightness and permitting smaller base-to-height ratios. As time went by, concrete and cement mortar were used in the construction of large masonry dams, which were the forerunners of the modern mass concrete gravity dams. The use of mass concrete gravity dams evolved around the mid-1800's.

3. Methods to evaluate sliding stability are the most recent design consideration to undergo change in the CE. Methods based on limit equilibrium replaced the shear-friction concept in a Department of the Army Engineering Technical Letter (ETL) 1110-2-256 (Department of the Army, Office, Chief of Engineers 1981). In addition to the conceptual differences between the two methods, the change was significant in that the minimum acceptable factor of safety was also lowered.

4. Hydraulic gravity structures in the past were generally either constructed on competent rock masses where the potential for sliding instability was not a primary concern or conservative shear strengths were used in design if the potential for sliding existed. Use of conservative design strengths in questionable stability cases reflected the lack of confidence in the geotechnical engineer's ability to predict prototype strength behavior of weak rock masses. Advances in rock mechanics over the past ten years have significantly increased the understanding of rock mass behavior and hence increased the confidence in prototype strength predictions.

Objectives

5. The objectives of this report are twofold. The first is documentation as to the assumptions used in the development of and the limitations of the limit equilibrium method for assessing the sliding stability of gravity hydraulic structures. A fundamental understanding of the assumptions used in the development of the method is of particular importance in the selection of appropriate design shear strengths. Second, this report is intended to offer information on methods for the selection of design shear strengths for the assessment of sliding stability of structures founded on rock. The methodology for shear strength selection is not all inclusive; other methodologies are developing which will be the topics of future reports.

Contents of Report

6. Part II of this report, "Development and Comparison of Sliding Stability Design Methods," gives a brief historical review of previous design practice and discusses the assumptions, development, and limitations of the shear-friction and the limit equilibrium methods for assessing the sliding stability of mass concrete hydraulic structures. Calculated factors of safety and base area requirements with respect to sliding stability obtained from the two methods are compared for specific cases.

7. Part III, "Prerequisites for Selecting Shear Strength," briefly discusses field investigations, loading conditions, shear tests, material

stress-strain characteristics, failure criteria, linear interpretation (as a function of c and ϕ shear strength parameters) of nonlinear failure criteria and the level of confidence in selected design strengths.

8. Parts IV, V, and VI--"Selection of Design Shear Strengths for Intact Rock," "Selection of Design Shear Strengths for Clean Discontinuous Rock," and "Selection of Design Shear Strengths for Filled Discontinuous Rock," respectively--discuss considerations and approaches for selecting design shear strength parameters. Each part briefly defines the meaning of the potential mode of failure (i.e., intact rock, clean, and filled discontinuous rock) and discusses failure mechanics necessary for a fundamental understanding of the various design strength selection approaches. Particular emphasis is given to alternative approaches in selecting design shear strength parameters c and ϕ as the approaches relate to the level of confidence that must be placed in the design strengths.

9. Part VII, "Conclusions and Recommendations," summarizes the significant findings of this study and recommends those areas in need of additional research.

PART II: DEVELOPMENT AND COMPARISON OF SLIDING STABILITY DESIGN METHODS

Historical Review

10. The International Commission on Large Dams (1973) recorded 487 major (over 45 ft* in height) concrete gravity dams, which is approximately 10 percent of the total number of major dams in the world. Prior to 1900, the only stability requirement was to assure that the resultant of the acting forces fell within the center one-third of the dam base. Compliance with this requirement was deemed to result in a factor of safety of 2.0 against overturning; this requirement is still in use today for assessing overturning potential. By the mid-1880's hydraulic uplift forces were recognized to be a significant factor. The failure of the Austin Dam in 1900 and the Bayless Dam in 1910 (International Commission on Large Dams 1973) called attention to the fact that failure of mass gravity dams was generally accompanied by downstream mass movement and that this was facilitated by uplift pressures at the base of the dam. The two new factors of sliding and uplift were generally considered in design after 1900.

11. Initially a gravity dam was considered safe with respect to sliding if the ratio of the horizontal driving force to the vertical structural force (i.e., weight) was greater than the coefficient of sliding friction between the dam's base and the foundation material. Uplift forces were relieved by installing drains in the base of the dam. However, experience showed that drainage could not be depended upon to completely relieve uplift. According to a historical review by Henny (1933), allowance was made in the design for both drainage and uplift and the following equation was developed:

$$F_s = \frac{P}{W - u} \tag{1}$$

in which, for a unit width of dam, F_s , was the sliding factor; P , the driving horizontal force; W , the weight of masonry above an assumed sliding

---

* A table of factors for converting U. S. customary units of measurement to metric (SI) units is presented on page 4.

plane; and u , the uplift force under the sliding base. The literature is not clear as to how the sliding factor, F_s , was selected.

12. Equation 1 was used for assessing sliding stability of gravity dams until the 1930's. Henny (1933) wrote a most significant paper concerning the stability of concrete gravity dams. The paper introduced the shear component for design against sliding. Henny's basic equation defining the factor of safety against sliding was of the form:

$$Q = \frac{S}{P} \tag{2}$$

in which Q was the factor of safety of shear; S , the total resisting shear strength acting over the failure plane; P , the water pressure on the projected area of the structure assumed to move and acting on a vertical plane normal to the direction of motion. The total resisting shear strength, S , was defined by the Coulomb equation:

$$S = s_1 + k\ (W - u) \tag{3}$$

in which s_1 was the total shear strength under conditions of no load; k was the factor of shear strength increase; W was the weight of the structure above an assumed sliding plane; and u the uplift force under the sliding plane.

13. Interestingly, Henny stated, "This theory [Coulomb's equation] has not been proven." Henny spent a significant proportion of the paper in summarizing test results on concrete and intact rock in an attempt to verify the correctness of Equation 3 and establish reasonable values for s_1 and k . Henny concluded that taking the correctness of Equation 3 for granted and combining it with Equation 2,

$$Q = \frac{s_1}{P} + k\,\frac{W - u}{P} \tag{4}$$

The paper did not make recommendations, present requirements, or establish an acceptable value for Q , although discussions repeatedly used a Q value of

4.0. It is also of interest to note that Henny considered only horizontal planes of potential sliding.

14. Although the approach proposed by Henny enjoyed considerable acceptance, the concept of resistance to sliding (see paragraph 11) continued to be used in design. EM 1110-2-2200 (Department of the Army 1956) states: "Experience has shown that the shearing resistance of the foundation or concrete need not be investigated if the ratio of horizontal forces to vertical forces ($\Sigma H/\Sigma V$) is such that a reasonable safety factor against sliding results. This will require that the ratio of $\Sigma H/\Sigma V$ be well below the coefficient of sliding friction of the material." The maximum ratio of $\Sigma H/\Sigma V$ was set at 0.65 for statically loaded conditions. This criteria generally required that the angle of friction, ϕ, be equal to or greater than 33° ($\tan 33° = 0.65$).

Shear-Friction Method

15. Some form of Equation 4 has been in general use from approximately 1935 to 1981 by the CE and other governmental agencies (Tennessee Valley Authority and the Bureau of Reclamation). Records cannot be located to indicate adaptation of Henny's work into CE sliding stability criteria. Nevertheless, the initial concept of defining the factor of safety (Equation 2) for sliding stability as the ratio of the total resisting shear strength acting along a horizontal failure plane to the maximum horizontal driving force can be attributed to Henny and thus 1933 technology. General forms of Equation 4 developed from the initial definition of the factor of safety (Equation 2) are commonly referred to as shear-friction equations.

16. The CE expanded the shear-friction factor of safety to include inclined failure planes and embedment toe resistance. The expanded shear-friction factor of safety in the general form was defined as:

$$S_{s\text{-}f} = \frac{R + P_p}{H} \tag{5}$$

where R was the maximum horizontal driving force which can be resisted by the critical potential failure path (beneath the structure); P_p was the maximum passive resistance of the rock wedge (if present) at the downstream

toe; and H was the summation of horizontal service loads to be applied to the structure. The structural wedge included the structure and any rock or soil beneath the structure but above the critical potential failure path. The minimum acceptable shear-friction factor of safety (S_{s-f}) required for CE design was specified as 4.0. No records can be located by the author which indicate that other governmental agencies adopted a general form similar to Equation 5.

17. The basic definition of the factor of safety for sliding stability (Equation 2) as proposed by Henny (1933) is valid. The various forms of the shear-friction equations developed from the definition have served the profession well. The United States Committee on Large Dams (1975) indicates that since its initial use in the mid-1930's not a single major gravity hydraulic structure has failed because of sliding instability. In fact, the sliding failure of a lock wall at Wheeler Lock and Dam is the only sliding failure of any CE permanent structure known to the author. The success of the shear-friction method can primarily be attributed to the conservative minimum factor of safety and to the fact that most mass concrete gravity structures constructed in the past were founded on competent foundation material. It should be noted that the CE practice has in the past waived the factor of safety requirement of 4.0, but only on a special case-by-case basis. Such waivers were made at the Office, Chief of Engineers (OCE), U. S. Army level and only after assurance that all possible modes of failure and associated foundation strength parameters were thoroughly investigated.

Shear-friction assumptions

18. The fundamental assumption necessary for the development of the shear-friction method is that the basic definition of the factor of safety as given by Equation 2 is correct. The method also assumes that a two-dimensional analysis is applicable and that the analytic mode of failure is kinematically possible.

Problems with the shear-friction method

19. The shear-friction method is based on 1933 technology. Much knowledge has been developed in the past 49 years concerning soil mechanics, rock mechanics, and foundation engineering. Design of structures should be based on the current state-of-the-art technology. In addition to being outdated,

the shear-friction method as given by Equation 5 has other fundamental problems relating to the mathematical formulation. Equations for R and P_p in Equation 5 were derived from static equilibrium conditions treating the passive rock wedge as a separate body from the structural wedge. The equation for R for upslope sliding was:

$$R = \Sigma V \tan (\phi + \alpha) + \frac{sA}{\cos \alpha (1 - \tan \phi \tan \alpha)} \tag{6}$$

for downslope sliding:

$$R = \Sigma V \tan (\phi - \alpha) + \frac{sA}{\cos \alpha (1 + \tan \phi \tan \alpha)} \tag{7}$$

The equation for P_p was:

$$P_p = W \tan (\phi + \alpha) + \frac{sA}{\cos \alpha (1 - \tan \phi \tan \alpha)} \tag{8}$$

where

ΣV = summation of vertical structure forces and any forces due to material between the structure and failure plane

ϕ = angle of internal friction of the material or, where applicable, angle of sliding friction

α = angle between inclined potential failure plane and the horizontal

s = unit shear strength at zero normal loading along potential failure plane

A = area of potential failure plane developing unit shear strength s

W = weight of downstream passive rock wedge above the potential failure surface, plus any superimposed loads

As a matter of note, the term ΣV in Equations 6 and 7 included the vertical component of uplift. The term H in Equation 5 included the horizontal component of uplift. Equations 5, 6, 7, and 8 and symbols are listed as they appeared in CE guidance by ETL 1110-2-184 (Department of the Army, Office, Chief of Engineers, 1974) dated 25 February 1974.*

---

* Note: ETL 1110-2-184, dated 25 February 1974, was superseded by ETL 1110-2-256, dated 24 June 1981.

20. Recalling that the structural and passive wedges were considered as separate bodies (paragraph 19), a schematic of a gravity dam with forces acting on the dam and passive wedge according to the shear-friction convention is shown in Figure 1. For the case shown the shear-friction factor of safety may be determined by combining Equation 6 (for upslope sliding) with Equation 5 as follows:

$$S_{s-f} = \frac{\Sigma V \tan (\phi_s + \alpha_s) + \frac{s_s A_s}{\cos \alpha_s (1 - \tan \phi_s \tan \alpha_s)}}{H} + \frac{W \tan (\phi_p + \alpha_p) + \frac{s_p A_p}{\cos \alpha_p (1 - \tan \phi_p \tan \alpha_p)}}{H} \quad (9)$$

If the dam illustrated in Figure 1 rested on a single horizontal potential failure plane ($\alpha_s = 0$) without a passive wedge acting at the toe ($P_p = 0$) Equation 9 reduces as follows:

$$S_{s-f} = \frac{\Sigma V \tan \phi}{H} + \frac{sA}{H} \quad (10)$$

Equation 10 is basically the same equation (Equation 4) initially proposed by Henny (1933).

21. A detailed study of Equations 6, 7, 8, and 9 and Figure 1 will reveal the following problems relating to the mathematical formulation of the shear-friction method:

a. The R and P_p forces as illustrated in Figure 1 are imaginary forces required for static equilibrium at maximum shear strength (T in Figure 1). With the inclusion of inclined potential failure planes R and P_p are also a function of ΣV and W, respectively. Because R and P_p become functions of ΣV and W with inclined planes and because of the mathematics required for the solution of R and P_p it can be seen from Equations 6, 8, and 9 for upslope sliding that the factor of safety approaches infinity as the angle of inclination, α, approaches the tangent of 90° minus ϕ as illustrated for a hypothetical structure in Figure 2. The inclination angle at which S_{s-f} approaches infinity is independent of material unit

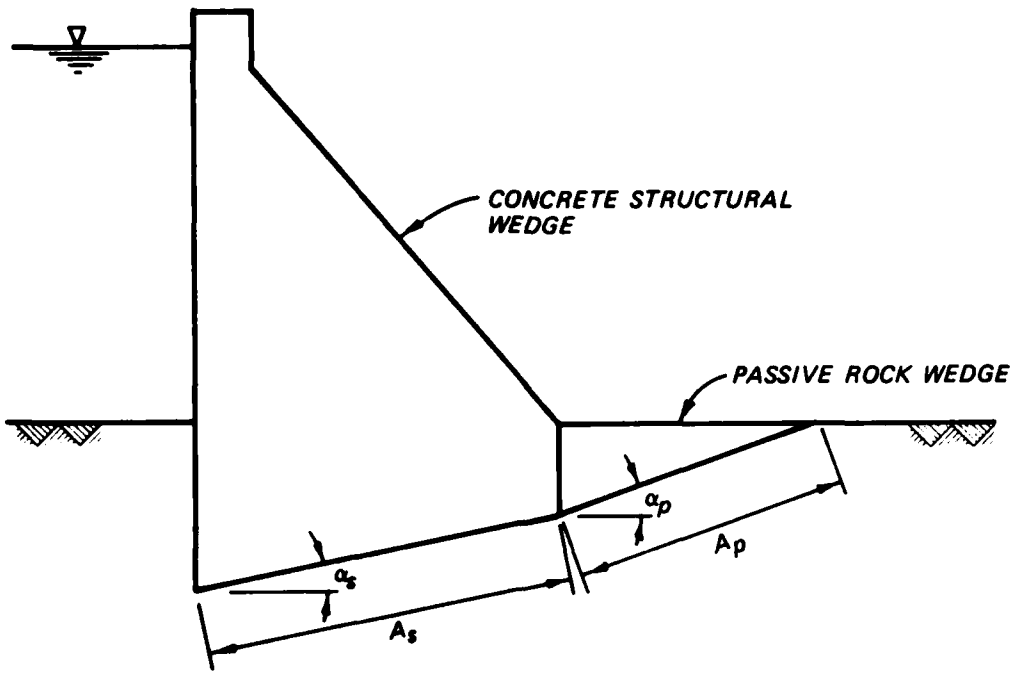

a. SCHEMATIC OF A CONCRETE GRAVITY DAM WITH PASSIVE WEDGE TOE RESISTANCE

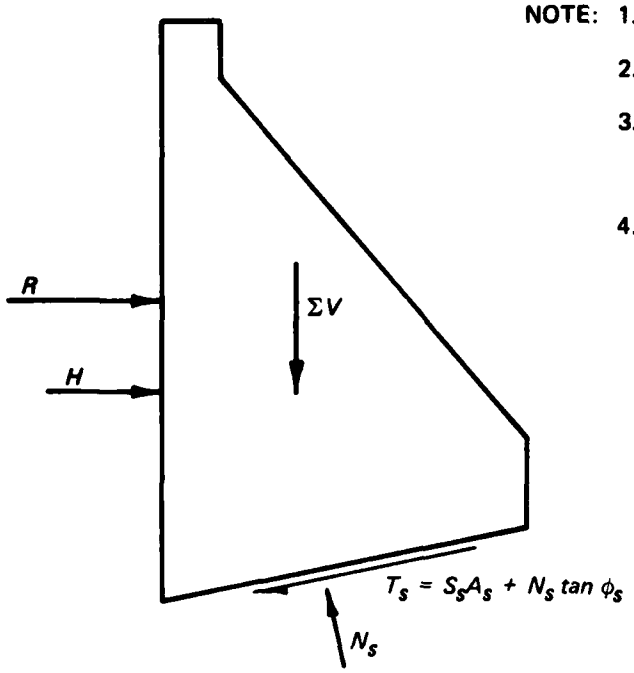

NOTE:
1. SUBSCRIPTS (s) AND (p) REFER TO STRUCTURAL AND PASSIVE WEDGE.
2. FORCES AND AREA ARE IN TERMS OF UNIT WIDTH.
3. VERTICAL AND HORIZONTAL COMPONENTS OF UPLIFT ARE INCLUDED IN THE (ΣV) AND (W) AND (H) TERMS.
4. THE INCOMPLETE FREE BODY DIAGRAM IN FIGURE 1.b. IS DUE TO THE FACT THAT THE STRUCTURAL AND PASSIVE WEDGES WERE CONSIDERED AS SEPARATE BODIES.

b. SHEAR-FRICTION FORCES ACTING ON DAM AND PASSIVE WEDGE

Figure 1. Schematic and forces acting on a hypothetical dam according to the shear-friction criteria

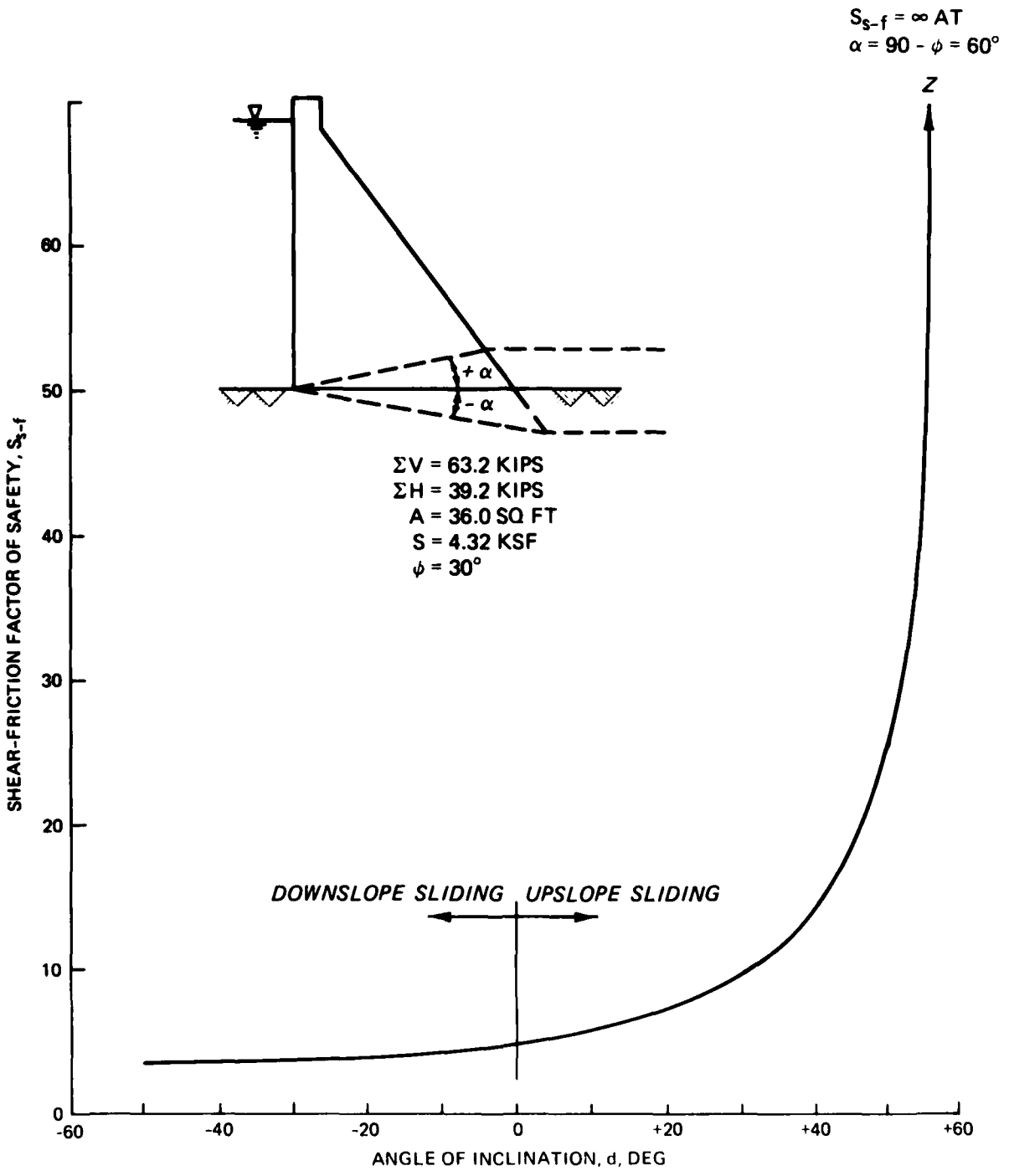

Figure 2. Plot of S_{s-f} versus α for hypothetical structure

shear strength (provided $s \neq 0$) or acting forces. Although Figure 2 illustrates a hypothetical case with no toe embedment, the probability of S_{s-f} approaching infinity in design is greater with a passive wedge present since the angle of inclination for a passive wedge is more likely to be defined by relatively steeply dipping (on the order of 60° or greater with respect to the horizontal plane) discontinuities in rock.

b. The passive wedge force component, P_p , in Equations 8 and 9 was derived assuming that P_p is the maximum force that can be resisted by the wedge at a given inclined failure plane. Because of this assumption, the P_p component is independent of the forces acting on the structure. Therefore, the structure and wedge considered as a single block are not in static equilibrium except where S_{s-f} is unity.

c. The application of the shear-friction Equations 6, 7, 8, and 9 is limited to modes of potential failure along one ($P_p = 0$) or two planes.

Limit Equilibrium Method

Definition of factor of safety

22. The current CE guidance for limit equilibrium sliding stability assessment was established by ETL 1110-2-256 (Department of the Army, Office, Chief of Engineers 1981). The method is based upon presently acceptable geotechnical principles with respect to shearing resistance of soils and rock. The basic principle of this method applies the factor of safety to the least known conditions affecting sliding stability, that is, the material strength parameters. Mathematically, the factor of safety is expressed as:

$$\tau = \frac{\tau_F}{FS} \tag{11}$$

in which τ is the shear stress required for equilibrium; τ_F is the available shear strength and FS is the factor of safety. The minimum factor of safety required by the new guidance is 2.0 for static loading conditions. Design cases with factors of safety of less than 2.0 require specific OCE approval.

23. According to this method, the foundation is stable when, for any potential slip surface, the resultant of the shear stresses required for

equilibrium is smaller than the maximum mobilizable strength. The ratio of these quantities, expressed by Equation 12, is called the factor of safety:

$$FS = \tau_F/\tau \tag{12}$$

in which all terms are the same as expressed in Equation 11. The ratio of τ_F/FS (Equation 11) can be thought of as the degree of shear strength mobilized.

Limit equilibrium assumptions

24. The fundamental assumptions required for the development of the stability equations are listed below. Where necessary for the comprehension and application of the principles involved in stability analysis, the implication and validity of the assumptions will be explored in following sections of this report.

a. The factor of safety is defined by Equation 12.

b. Impending failure occurs according to the requirements imposed by elastic-plastic failure theory.

c. The maximum shear strength that can be mobilized is adequately defined by the Mohr-Coulomb failure criteria.

d. Failure modes can be represented by two-dimensional, kinematically possible planes.

e. The factor of safety computed from the stability equations is the average factor of safety for the total potential failure surface.

f. To derive easy, simple-to-use equations, the vertical stresses/forces acting between wedges or slices are assumed to be negligible.

g. The structural wedge must be defined by only one wedge.

General wedge equations

25. Figure 3 illustrates the necessary geometry, forces, and coordinate system for a hypothetical i^{th} wedge in a wedge system. The initial step in the factor of safety solution requires that the difference in the horizontal P forces acting on each wedge in the system be determined. The general equation for the i^{th} wedge in any wedge system is as follows:

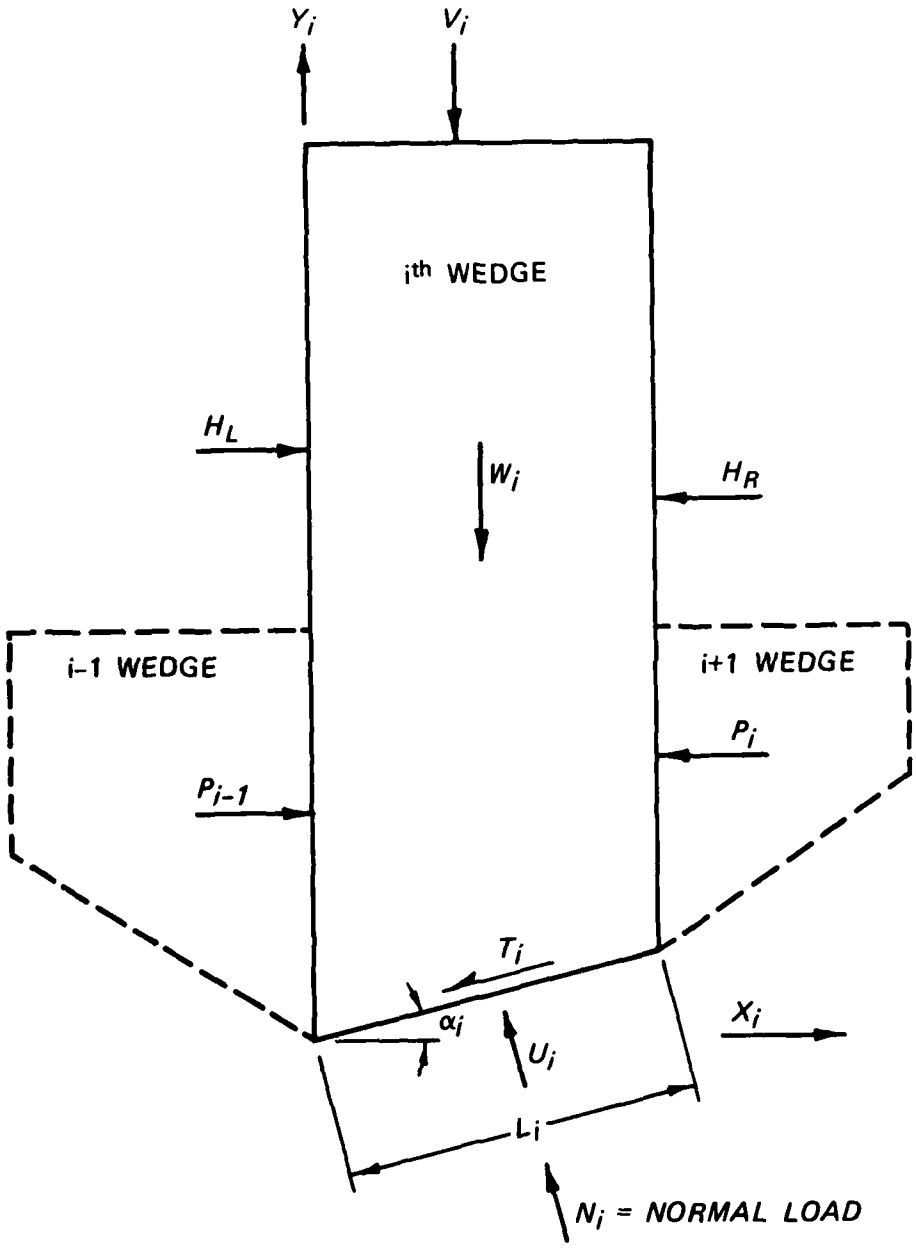

Figure 3. Geometry, forces, and coordinate system for an i^{th} wedge in a hypothetical wedge system

$$(P_{i-1} - P_i) = \frac{[(W_i + V_i)\cos\alpha_i - U_i + (H_{Li} - H_{Ri})\sin\alpha_i]\ \frac{\tan\phi_i}{FS_i}}{\left(\cos\alpha_i - \sin\alpha_i\ \frac{\tan\phi_i}{FS_i}\right)}$$

$$- \frac{(H_{Li} - H_{Ri})\cos\alpha_i + (W_i + V_i)\sin\alpha_i + \frac{c_i}{FS_i} L_i}{\left(\cos\alpha_i - \sin\alpha_i\ \frac{\tan\phi_i}{FS}\right)} \qquad (13)$$

where:

P = the resultant horizontal force acting on a vertical face of a typical wedge

W = the total weight of water, soil, or concrete in the wedge

V = any vertical force applied above the top of the wedge

α = negative for downslope sliding, positive for upslope sliding

U = the uplift force exerted on the wedge at the failure surface

H = in general, any horizontal force applied above the top of the adjacent wedge (H_L and H_R refer to left and right hand forces as shown in Figure 3)

L = the length of the wedge along the failure surface

FS = the factor of safety

c = cohesion

All other parameters are the same as in Equations 6, 7, and 8. Parameter symbols W , V , U , and H have been used previously with slightly different definitions. Symbols and definitions used in the above equation are as they appear in ETL 1110-2-256 (Department of the Army, Office, Chief of Engineers, 1981).

26. An observation of Equation 13 reveals that for a given wedge there will be two unknowns (i.e., $(P_{i-1} - P_i)$ and FS). In a wedge system with n number of wedges Equation 13 will provide n number of equations. Because FS is the same for all wedges (paragraph 24e) there will be n + 1 unknowns with n number of equations for solution. The solution for the factor of safety is made possible by a conditional equation establishing horizontal

equilibrium of the wedge system which states that the sum of the differences in horizontal forces ($P_{i-1} - P_i$) acting between wedges must equal the differences in the horizontal boundary forces. Since boundary forces are usually equal to zero, the conditional equation is expressed as:

$$\sum_{i=1}^{i=n} (P_{i-1} - P_i) = 0 \tag{14}$$

27. The solution for the factor of safety from $n + 1$ number of equations obtained from Equation 13 and 14 requires a trial-and-error procedure. A trial value for the factor of safety, FS , is inserted into Equation 13 for each wedge to obtain values of the differences in horizontal P forces acting between wedges. The sum of the differences in P forces is obtained from Equation 14. The process is repeated until the inserted FS value results in an equality from Equation 14. The value of FS which results in an equality is the correct value for the factor of safety. If trial values of FS are plotted with respect to the $\sum_{i=1}^{i=n} (P_{1-i} - P_i)$ values obtained from Equation 13, the number of trial-and-error cycles can be reduced.

Alternate equation

28. An alternate approach general equation for a system of n wedges defining a given potential failure surface is given below:

$$FS = \frac{\sum_{i=1}^{i=n} \frac{c_i A_i \cos \alpha_i + (V_i - U_i \cos \alpha_i) \tan \phi_i}{n_{\alpha_i}}}{\sum_{i=1}^{i=n} [H_i - V_i \tan \alpha_i]} \tag{15}$$

where

A = area of the potential failure surface

V = total vertical force acting on the potential failure surface

U = uplift force acting on the potential failure surface

$$n_\alpha = \frac{1 - \frac{\tan \phi \tan \alpha}{FS}}{1 + \tan^2 \alpha}$$

H = total external horizontal force acting on the slice

All other parameter symbols are the same as given in Equation 13. Symbols and definitions are listed as they appear in CE guidance. A plot of n_α versus α for values of $\tan \phi/FS$ is given in Appendix A.

29. By using the sign convention of $+\alpha$ for upslope sliding and $-\alpha$ for downslope sliding, Equation 15 is completely adaptable to any geometric shape and may also be used for single-plane sliding. Since n_α is a function of FS the solution for FS requires an iteration process. An initial value of FS is inserted into the n_α term. The process is repeated until the calculated value of FS equals the inserted value of FS . Convergence to within two decimal places usually occurs in 3 to 4 iteration cycles. Expansion of Equation 15 for a hypothetical 3-slice system is illustrated in Figure 4.

Comparison of equations

30. The general wedge equation (Equation 13) was formulated in terms of the difference in horizontal boundary forces to allow the design engineer to solve directly for forces acting on the structure for various selected factors of safety. The procedure has an advantage for new structures in that it allows a rapid assessment of the horizontal forces for prescribed factors of safety without requiring an iterative solution. Derivations of the general wedge equation are given in current CE guidance. The alternate equation (Equation 15) solves for FS . Its advantage is in the assessment of stability for existing structures. Derivation of Equation 15 is given in Appendix A. Both equations are mathematically identical, as shown in Appendix B.

Comparison of the Limit Equilibrium and the Shear-Friction Methods

Factor of safety for a single horizontal potential failure plane

31. For the special case of a single horizontal potential failure surface with zero boundary forces, the alternate approach, Equation 15 reduces to the general form of shear-friction Equation 10. The general wedge approach equation (Equation 13) will also result in the same general form by solving

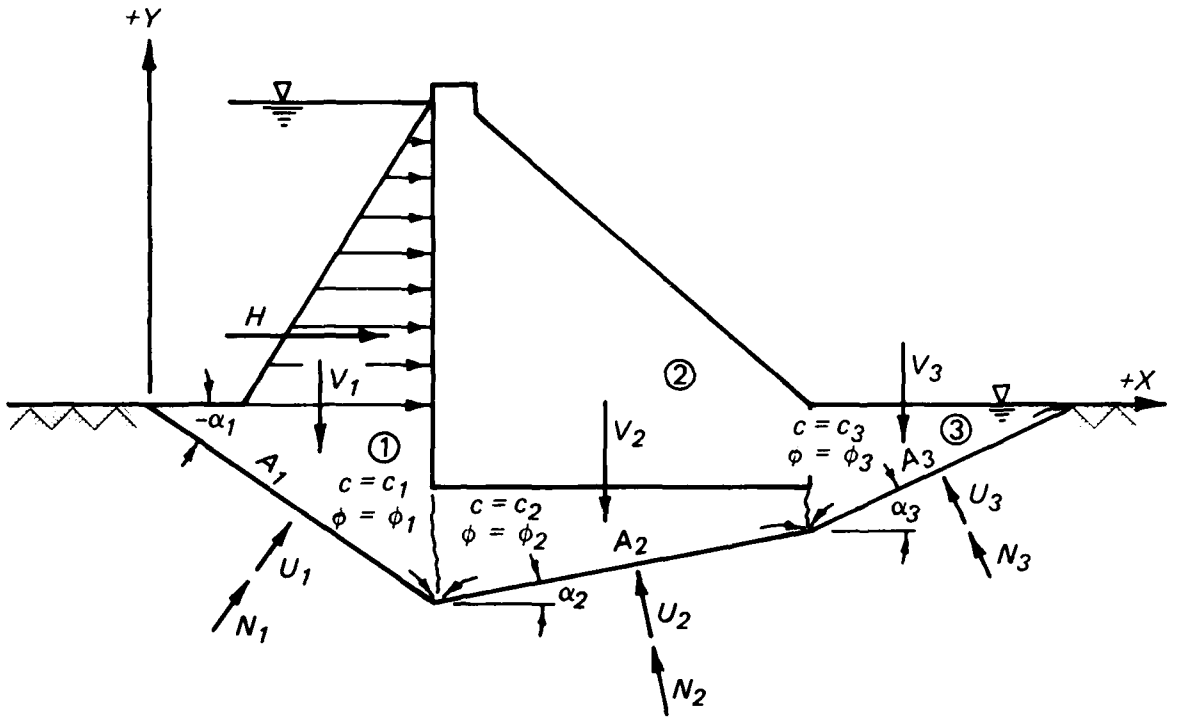

$$FS = \frac{\dfrac{c_1A_1 \cos(-\alpha_1) + (V_1 - U_1 \cos(-\alpha_1)) \tan \phi_1}{1 - (1/FS) \tan \phi_1 \tan(-\alpha_1)} + \dfrac{c_2A_2 \cos \alpha_2 + (V_2 - U_2 \cos \alpha_2) \tan \phi_2}{1 - (1/FS) \tan \phi_2 \tan \alpha_2} + \dfrac{c_3A_3 \cos \alpha_3 + (V_3 - U_3 \cos \alpha_3) \tan \phi_3}{1 - (1/FS) \tan \phi_3 \tan \alpha_3}}{1 + \tan^2(-\alpha_1) \quad 1 + \tan^2 \alpha_2 \quad 1 + \tan^2 \alpha_3}$$

$$H - V_1 \tan(-\alpha_1) - V_2 \tan \alpha_2 - V_3 \tan \alpha_3$$

Figure 4. Expansion of Equation 15 for a hypothetical structure with a given potential failure surface defined by three wedges

directly for the factor of safety. For this special case the solution for the factor of safety will be exactly the same for both the limit equilibrium and shear-friction methods.

Factors of safety for given cases

32. The limit equilibrium method specifies a minimum acceptable factor of safety of 2.0 as compared to the shear-friction requirement of 4.0. This does not necessarily imply that the overall factor of safety has been reduced by 50 percent. As a general rule, for a given structure with an inclined potential failure surface the limit equilibrium and shear-friction methods will result in a different and unique factor of safety. The magnitude of the difference is dependent on the geometry of the problem, loading conditions, and resisting shear strength parameters. The exception to the general rule occurs for a single-inclined failure surface when $\tan \phi$ is equal to the ratio of V/H ; in this case $S_{s-f} = FS$.

33. To illustrate the possible variations in the two factors of safety (S_{s-f} and FS) consider the plot of factors of safety with respect to c and $\tan \phi$ for a given hypothetical structure subject to a single plane downslope failure as shown in Figure 5. As can be seen, the two factors of safety are equal for certain values of c and $\tan \phi$ corresponding to a factor of safety of 1.0 and at $\tan \phi = V/H$. For values of $\tan \phi$ less than V/H , a given value of c and $\tan \phi$ will result in a higher shear-friction factor of safety than that calculated by limit equilibrium. For values of $\tan \phi$ greater than V/H , a given value of c and $\tan \phi$ will result in a lower shear-friction factor of safety with respect to limit equilibrium. Another interesting observation from Figure 5 is that the shear-friction factor of safety for downslope sliding is more dependent upon the $\tan \phi$ friction parameter than cohesion parameter when compared to limit equilibrium.

34. Figure 6 illustrates a similar comparison between the two factors of safety and c and $\tan \phi$ for the same hypothetical structure except for upslope sliding. As in the downslope sliding case (Figure 5), the two factors of safety are equal for certain values of c and $\tan \phi$ corresponding to a factor of safety of 1.0 and at $\tan \phi = V/H$. However, for values of $\tan \phi$ less than V/H , a given value of c and $\tan \phi$ will result in a

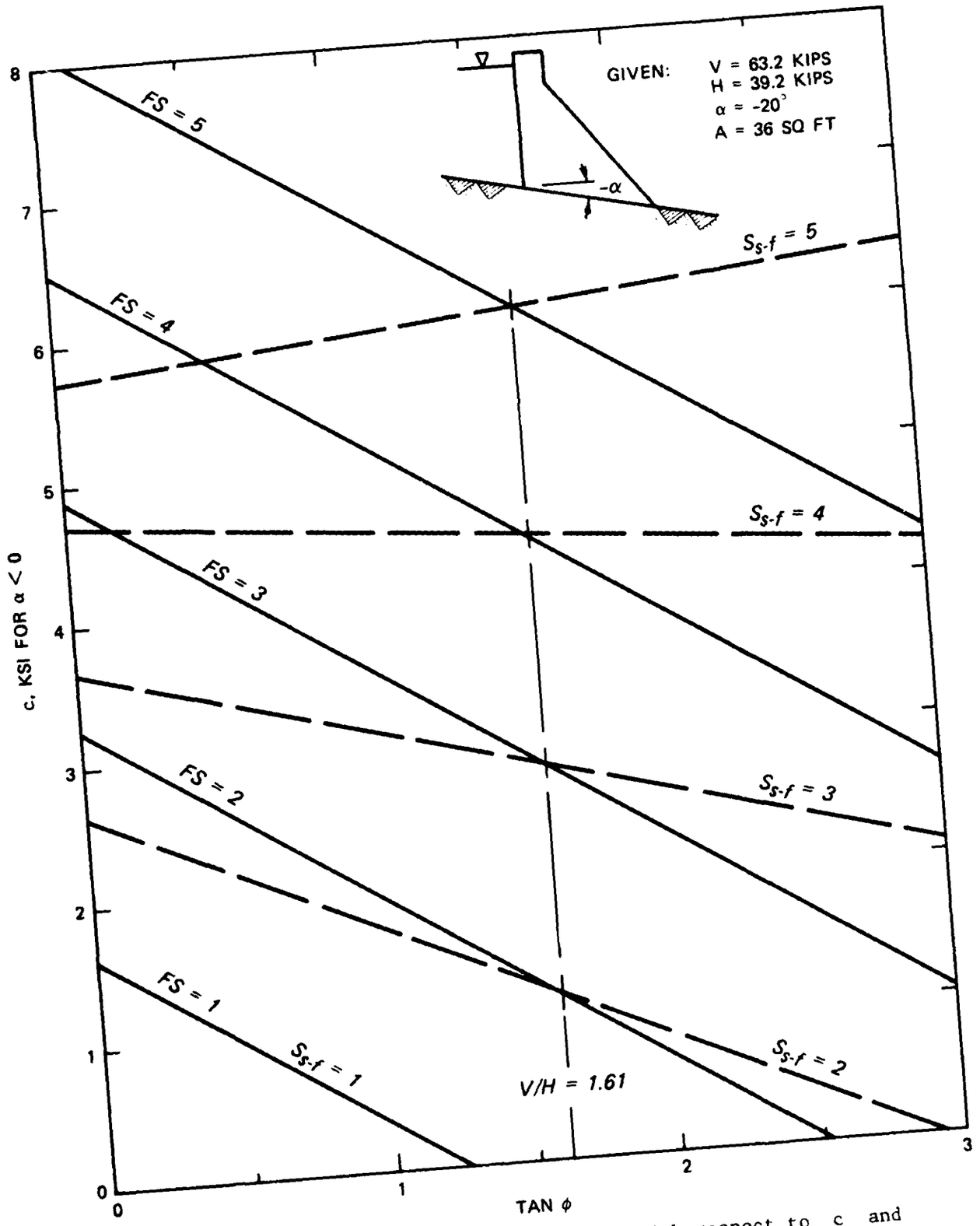

Figure 5. A comparison of FS and S_{s-f} with respect to c and tan ϕ for a hypothetical structure subject to a single plane downslope sliding

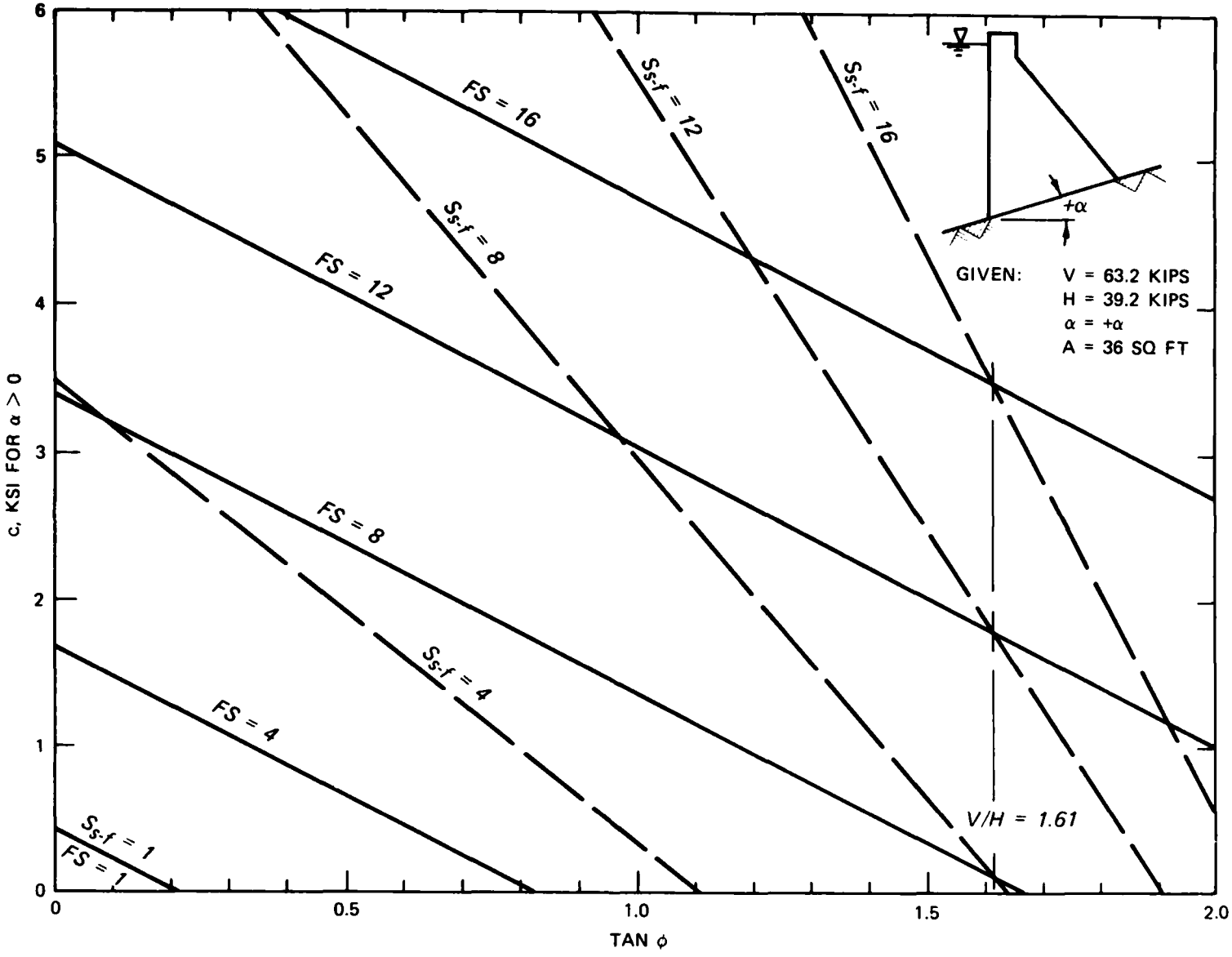

Figure 6. A comparison of FS and S_{s-f} with respect to c and tan ϕ for a hypothetical structure subject to downslope sliding. FS = factor of safety by limit-equilibrium method and S_{s-f} = factor of safety by shear-friction method

shear-friction factor of safety smaller than the limit equilibrium factor of safety. The reverse is also true for values of $\tan \phi$ greater than V/H. Also, for upslope sliding, the shear-friction factor of safety is more dependent on cohesion than friction when compared to limit equilibrium.

35. Comparisons of the two factors of safety for two potential failure planes (shear-friction limited to a maximum of two planes as shown in Figure 1b) can only be made for a given value of c and $\tan \phi$. For a given factor of safety greater than 1.0, there can exist unique values of c and $\tan \phi$ where the two factors of safety are equal. However, unlike single-inclined plane sliding, the conditions which result in equal factors of safety are dependent upon given values of the factor of safety, c and $\tan \phi$ for each plane, angle of inclination of each plane, and loading condition.

Comparison of required foundation base area

36. The design engineer responsible for the design of any structure is concerned with the impact a change in design criteria might impose on future design. The sliding stability of gravity structures is primarily a function of external loading acting on the structure, geometry, base area along which sliding occurs, resisting shear strength, and mass of the structure. Of the five factors influencing stability, mass of the structure, base area, and in some cases geometry are the factors most easily altered by the design process to achieve the optimum design with respect to cost and stability.

37. The height of hydraulic structures is generally fixed by design considerations. If the height is fixed, the mass of regular shaped structures is also a function of foundation base area. Therefore, the change in foundation base area is a convenient measure of the degree of impact caused by a change in design methods. Figure 7 shows triangular structures with a corresponding plot of the ratio of base areas required by the limit equilibrium, A_{FS}, and shear-friction, $A_{S_{s-f}}$, methods to generate specific values of factor of safety for varying angles of inclination, α. A triangular shape was chosen to simplify the relation between weight, V, and base area, A, and because a triangular shape closely approximates the shape of typical gravity dams. Curve 1 in Figure 7 shows the relationship between $A_{FS}/A_{S_{s-f}}$ and α for a required factor of safety of 4.0. Curve 1 indicates that for upslope

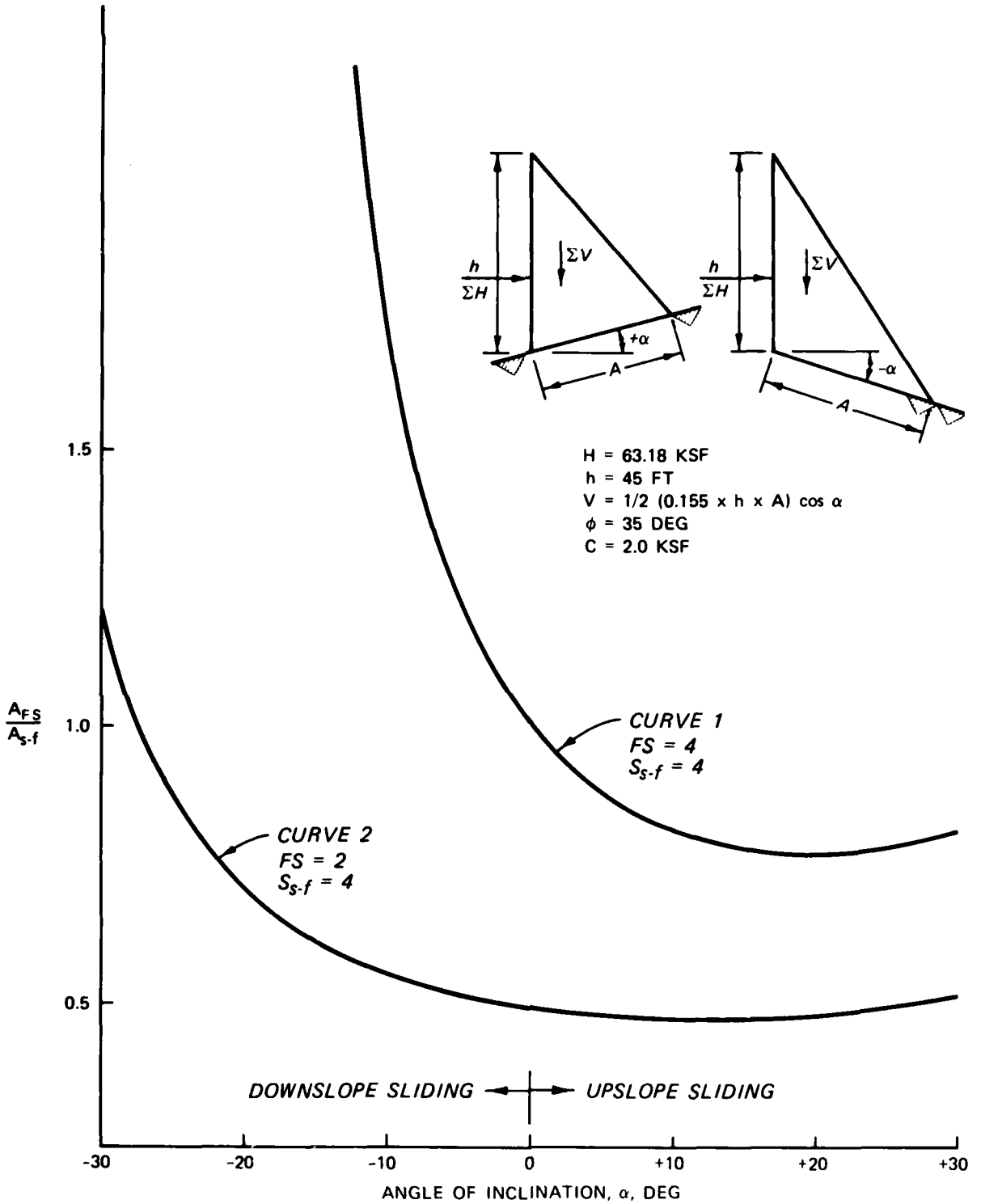

Figure 7. Comparison of the ratio of base areas required by the limit-equilibrium, A_{FS}, and shear-friction A_{s-f}, criteria for a hypothetical triangular-shaped structure subject to both upslope and downslope sliding

sliding, less base area is required by the limit equilibrium method to generate the same factor of safety (S_{s-f} = FS = 4.0) as the base area required for the shear-friction method. Conversely more base is required by the limit equilibrium method for downslope sliding.

38. Curve 2 shows the relationship between the ratio of $A_{FS}/A_{S_{s-f}}$, α, and the minimum acceptable factors of safety FS = 2 and S_{s-f} = 4 as dictated by the limit equilibrium and shear-friction criteria, respectively. For upslope potential sliding with α ranging from 0 to +30 deg the ratio of $A_{FS}/A_{S_{s-f}}$ only ranges from 0.497 to 0.502. Therefore, for upslope sliding, the minimum acceptable limit equilibrium sliding stability assurance requires approximately half the total base area as required by the minimum acceptable shear-friction assurance. For downslope potential sliding with α ranging from 0 to -30 deg the ratio of $A_{FS}/A_{S_{s-f}}$ ranges from 0.500 to 1.220. The range of the ratio of $A_{FS}/A_{S_{s-f}}$ for downslope sliding is heavily dependent on the magnitude of the $-\alpha$ angle.

39. Figure 7 illustrates the impact of change in methods on the parameter of base area for one hypothetical case. The illustration demonstrates that for a given case the relative change in the required base area is a function of the potential failure plane angle of inclination, α, and compared factors of safety, FS and S_{s-f}. Figure 7 also indicates, for the case shown, that the shear-friction factor of safety is unconservative for downslope sliding when compared to limit equilibrium factor of safety. For the general case the ratio of required base area is also a function of loading conditions and geometry of the structure.

40. It is important to realize that such comparisons as change in base area illustrated in Figure 7 or more generally comparisons in structure size address only the problem of sliding stability. The design of most hydraulic structures is not controlled by sliding stability requirements, but by assurance against overturning caused by external or internal loading conditions. For this reason it is doubtful that foundations of hydraulic structures will experience any radical design changes because of the limit equilibrium sliding stability method.

Special conditional cases of the limit equilibrium equations

41. There are three special conditional cases of the limit equilibrium equations that should be briefly discussed. Two cases pertain to upslope sliding, $+\alpha$, and one case to downslope sliding, $-\alpha$.

42. Upslope sliding. First, for upslope potential sliding the factor of safety will be infinity (FS = ∞) for the special case of $\alpha = \tan^{-1} (\Sigma H/\Sigma V)$. The special case of FS = ∞ does not mean that the assurance against sliding as measured by a calculated factor of safety is undefined. For the special case it simply means that the external horizontal driving loads and the horizontal components of the internal wedge loads are in static equilibrium thereby assuring stability independent of available resisting shear strength. Second, for upslope potential sliding there can exist certain cases where the calculated factor of safety may be negative. A negative factor of safety will occur when the horizontal external driving forces acting on the structure are less than the horizontal components of the internal wedge loads. A negative factor of safety does not necessarily imply a measure of stability in the reverse direction. Nor does it necessarily mean lack of stability in the original direction. A negative factor of safety will occur when the forces acting upstream are greater than the forces acting downstream. A negative factor of safety implies that stability should be checked in the reverse direction (i.e., change sign convention with upstream direction being positive).

43. Downslope sliding. The third case that may warrant special consideration is when a potential downslope sliding plane exists under the structure and the structure is acted upon by an active wedge. The limit equilibrium Equations 13 and 15 were derived based on a number of assumptions (see paragraph 24). One of the assumptions necessary for the derivation of simple sliding stability equations is that the vertical forces acting between wedges are assumed to be zero. The inclusion of this assumption into sliding stability equations will generally result in slightly conservative calculated factors of safety compared to factors of safety determined from complete equilibrium (inclusion of vertical forces between wedges) solutions. However, for downslope potential sliding of the structural wedge an active wedge subject to

settlement caused by gravitational forces or compaction of backfill adjacent to the structure will generate downdrag forces on the structure thereby contributing to the total driving forces acting on the structure. The factor of safety calculated using the limit equilibrium equations for this special case will be on the unconservative side.

PART III: PREREQUISITES FOR SELECTING SHEAR STRENGTH

44. Meaningful shear strength parameters used in the assessment of sliding stability are generally selected based upon shear testing techniques which attempt to model prototype loading conditions and either observe or predict material applied stress versus resisting shear stress behavior. Appropriate shear testing techniques require that all potential modes of failure including material type(s) defining potential modes of failure are defined, that external and internal (uplift and load induced pore pressures) loading conditions are known, and that there is a knowledge of available modeling techniques. The necessary link between modeling techniques and selection of design strengths for stability analysis must include an appreciation for material-dependent stress-strain characteristics and application of appropriate failure criteria. Figure 8 illustrates the minimum prerequisites necessary before realistic design shear strengths can be selected.

Field Investigations

45. The field investigation is a most important feature in the planning, design, and construction of new structures or evaluation of existing structures. By necessity, the field investigation must be a continual process starting with the preliminary geologic review of known conditions, progressing to a detailed boring exploration and sampling program and concluding at the end of construction with a safe and operational structure.

Exploration program

46. The objective of the exploration program is to define critical geologic features controlling the stability of the structure and to determine the geometry of those features for possible modes of potential failure. The extent of the exploration should vary from quite limited where the foundation material is strong even along the weakest potential failure plane to quite extensive and detailed where weak zones or seams exist with a strength in the range which is marginally required for satisfactory stability against sliding. While design parameters must be assigned prior to construction, it remains the obligation of the field geologist, geotechnical engineer, and design engineer,

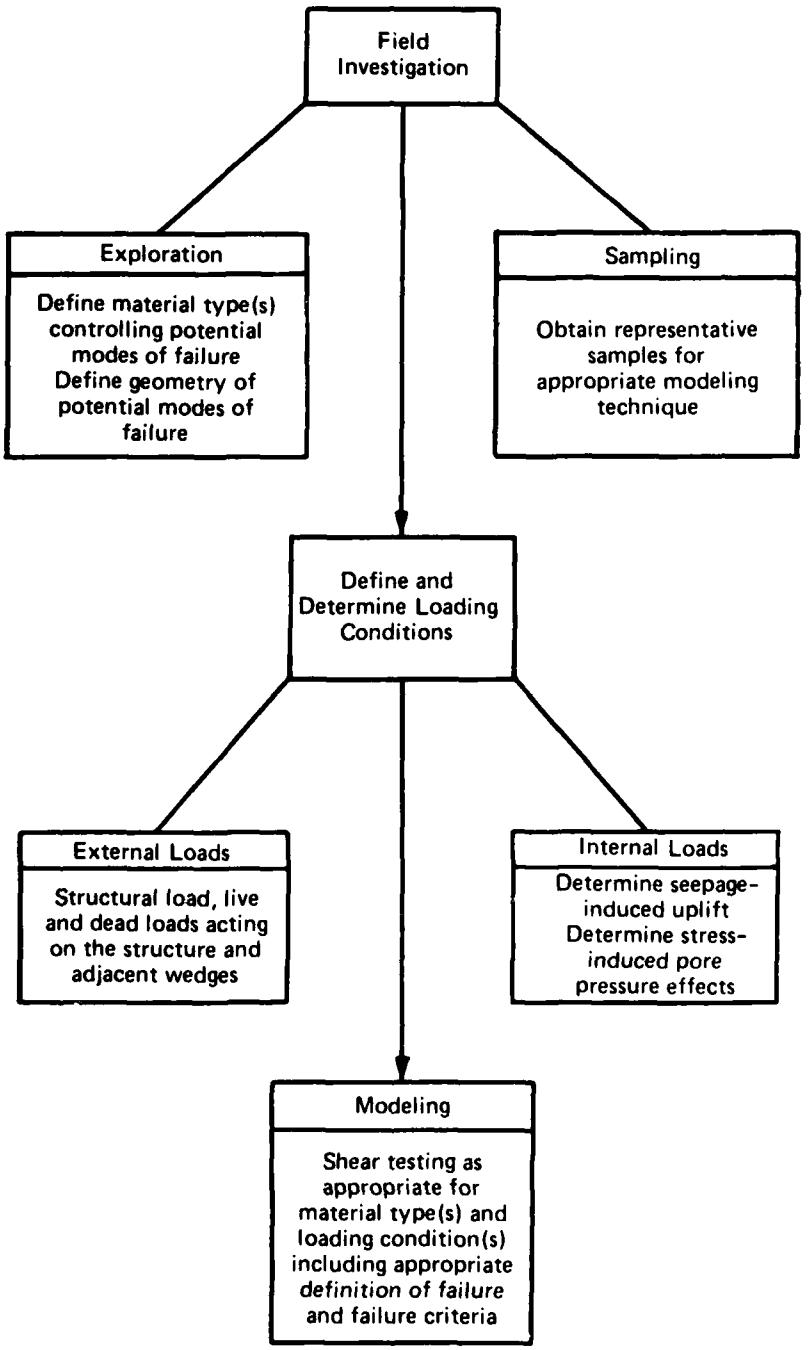

Figure 8. Minimum prerequisites for selecting design shear strengths

working as a team, to evaluate any critical feature that may become apparent during construction or for any other reason and, if necessary, make modifications to the design at that time.

Sampling program

47. Design shear strengths are usually based on appropriate shear tests on high quality, least disturbed "undisturbed" samples representative of potential failure surfaces (obtaining suitable samples may be congruent with or in addition to the exploration program). The selection of representative samples should be in coordination with the personnel conducting the field investigation and the geotechnical and design engineers involved in the design of the structure. Proper sampling is a combination of science and art. Many procedures have been developed, but alteration and adaption of techniques are often dictated by specific field conditions and investigation requirements. To obtain good quality samples whether for laboratory or in situ testing, there is no substitute for an experienced, competent, and conscientious field crew.

48. Soil sampling procedures are described in EM 1110-2-1803 (Department of the Army, Office, Chief of Engineers 1954) and in EM 1110-2-1907 (Department of the Army, Office, Chief of Engineers 1972). Rock sampling procedures are discussed in EM 1110-1-1801 (Department of the Army, Office, Chief of Engineers 1960).

Loading Conditions

49. Loading conditions may, for convenience of discussion, be separated into two categories--external and internal (pore water pressures). External loads include all loads acting on the structure and loads generated by the mass of the structure and/or material above the potential failure surface under consideration. Internal loads apply to unit area pore water pressures acting within the material defining the potential failure surface. Internal pore water pressures are among other factors dependent upon external loading conditions.

External loading conditions

50. Prior knowledge of external loading conditions are necessary for the

selection of design shear strengths for two reasons. First, external loading conditions define the stress range required for shear tests modeling prototype strength characteristics. Second, construction and reservoir filling schedules establish time rate requirements of shear test modeling.

Internal loading conditions

51. The total stress, σ , along any potential failure surface element of a saturated material consists of two parts. One part acts in the fluid filling voids (pores) and on the solid part of the material in every direction with equal intensity; this stress is commonly called the pore pressure, u_w . The remaining part acts exclusively between solid particles of the material and is the stress in excess of the pore pressure. The excess stress, σ' , is known as the "effective stress" and is defined by the following equation (Terzaghi 1936):

$$\sigma' = \sigma - u_w \tag{16}$$

A change in pore water pressure has no effect on the total stress conditions at failure. All the measurable effects on the shear stress conditions at failure are due to the effective stress σ' . Since the total stress σ is the stress observed in testing and in the field it is mandatory to make some determination as to the magnitude of the pore pressure to determine the effective stress σ' .

52. Pore water pressures can be generated by seepage conditions (commonly called uplift pressures in gravity dam design) and deformation characteristics of the foundation materials associated with external loading conditions. Both sources of pore water pressures are, among other factors, time dependent and are related to boundary conditions and the permeability of the material. In addition, deformation-related pore pressures are a function of material deformability. Designers of gravity dams routinely emphasize the importance of seepage (uplift) pressures. Uplift pressures are treated as forces separate from deformation-related pressures and incorporated directly into the stability equations. As long as proper consideration is given to deformation-induced pore pressures in the selection of strength parameters, the exclusion of these pressures in the stability calculations causes no problems.

53. Uplift. The sliding stability equations (Equations 13 and 15) include uplift pressures in terms of forces acting along the potential failure surfaces. CE guidance (ETL 1110-2-256) (Department of the Army, Office, Chief of Engineers 1981) prescribing the general criteria and guidance for assessing sliding stability states: "The effects of seepage forces should be included in the sliding analysis. Analyses should be based on conservative estimates of uplift pressures." The methods for estimating uplift forces are according to line-of-seepage method for structures with no drainage provisions for uplift reduction and the modified bilinear line-of-creep method for structures with drainage provisions.

54. The line-of-seepage method assumes that the head lost as water seeps under the structure is directly proportional to the length of the seepage path. The seepage path is generally defined as the distance from the point where water enters the upstream foundation material along the potential failure surface to the point where it emerges downstream along the potential failure surface.

55. Reduction of uplift pressures on the base of the structural wedge can only be attained by installing foundation drains. Drains generally become at least partially clogged with time. CE guidance specifies that preliminary estimates of drain effectiveness should not exceed 50 percent. The hydraulic gradient across the structural wedge from a line-of-seepage analysis should be modified to account for reduced uplift pressures due to foundation drains. A bilinear variation in the hydraulic gradient across the base of the structural wedge is usually adequate. Distribution of uplift pressures progress from a maximum pressure at the head to a 25 to 50 percent reduction in line-of-seepage pressure at the line of drains, and then from the line of drains to a minimum pressure at the toe.

56. An inspection of Equations 13 and 15 indicates that the net result of including uplift forces directly into the sliding stability equations is to reduce the total normal load acting on the potential failure surface considered. In gravity dam design, reductions in the foundation material shear strength that can be developed because of reductions in normal loads are generally more severe than potentional reductions in shear strength parameters because of load-induced deformation-related pore water pressure effects.

Therefore, a failure condition is most likely to occur at a critical loading condition of maximum uplift. Maximum uplift will occur at long-term steady state seepage flow conditions.

57. Load-induced pore pressures. Load-induced pore pressures are caused by a tendency for a material to undergo strain with change in applied stress. As a material tries to adjust (deform) to a change in applied stress the solid phase of the material attempts to rearrange in a more or less compact configuration thereby either decreasing (compress) or increasing (dilate) available void volume. If the voids are filled (saturated) with an almost incompressible fluid (water) the fluid will be subjected to an increase or decrease in fluid pressure in accordance with the tendency for void volume change. The magnitude of pore pressure change is a function of the material deformability characteristics under a given change in applied stress. With sufficient time and the availability of free drainage at some boundary these pore pressures dissipate and the material solid phase assumes a configuration compatible with the applied effective stress conditions and the material's deformability characteristics. Figure 9 illustrates the relationship between total and effective stress failure envelopes for materials that compress or dilate when sheared.

58. Shear tests modeling prototype loading conditions generally establish the relationship between load-induced pore pressures and their time-dependent effects on developed shear strength. A balanced design should be based on shear strengths selected to match corresponding time-dependent load induced pore pressure effects with time-dependent critical loading conditions.

Design loading conditions

59. EM 1110-2-2200 (Department of the Army, Office, Chief of Engineers 1958) lists three loading conditions applicable to the sliding stability of gravity dams:

a. Case I: Normal operating condition. Pool elevation at top of closed spillway gates, where spillway is gated, and at spillway crest, where spillway is ungated. Minimum tailwater elevation for gated and ungated spillways. Ice pressure if applicable.

b. Case II: Induced surcharge condition. Pool elevation at top of partially opened gate. Tailwater pressure at full value for nonoverflow section and 60 percent full value for overflow section. Ice pressure if applicable.

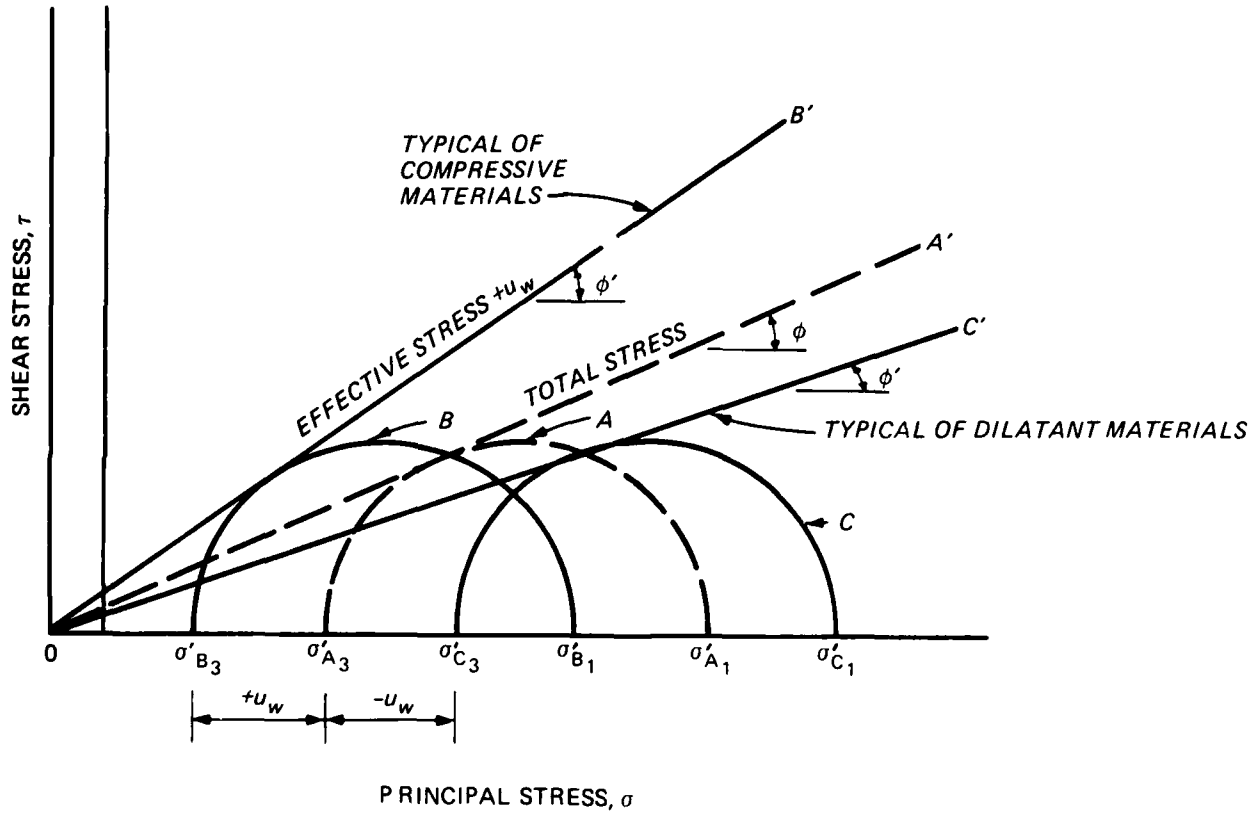

Figure 9. Relationship between total and effective stress failure envelopes for material that compresses or dilates when sheared

c. Flood discharge condition. Reservoir at maximum flood pool elevation. All gates open and tailwater at flood elevation. Tailwater pressure at full value for nonoverflow section and 60 percent of full value for overflow sections for all conditions of deep flow over spillway, except that full value will be used in all cases for computation of the uplift. No ice pressure.

60. The above design loading conditions are general in that they do not specify the details of time-related load occurrence. Because of the vast variations in foundation material types and loads typical of gravity dams and other structures, the time relationship between load occurrences and developed shear strength should be determined for each structure.

Shear Tests Used to Model Prototype Conditions

61. As noted above, the objective of any shear testing program is to model as closely as practical anticipated failure conditions that may occur in the field. Because of the enormous variety of soil and rock foundation materials and limitless combinations of loading and structural conditions that can exist, testing procedures for determining shear strength parameters of soils and rock cannot be standardized but rather must fit the specific needs of the design case. General guidance for soil testing procedures are discussed in EM 1110-2-1906 (Department of the Army, Office, Chief of Engineers 1970b). General methods and procedures for rock testing procedures are discussed in the "Rock Testing Handbook" (U. S. Army Engineer Waterways Experiment Station, 1980) and in "Suggested Methods for Determining Shear Strength" (International Society of Rock Mechanics 1974).

62. Shear strengths used in sliding stability analysis are generally determined from laboratory and/or in situ tests performed under three conditions of load-induced pore pressure drainage. These three drainage conditions are Q tests in which the water content is kept constant during the tests, R tests in which consolidation or swelling is allowed under initial stress conditions but the water content is kept constant during application of shearing stresses, and S tests in which full consolidation or swelling is permitted under the initial stress conditions and also during application of the shearing stresses.

63. Generally, Q , R , and S tests will be conducted on representative specimens for which design shear strengths are needed. The test conditions designated by the letters Q, R, and S provide limiting shear strength values corresponding to various prototype loading and drainage conditions. Shear strengths for design conditions not corresponding to these limiting strength values are usually obtained by interpolating between the limits depending upon loading and drainage conditions.

64. Certain combinations of initial and final in situ stress conditions and materials with anisotropic stress-strain-strength characteristics may require special tests or even research to adequately model field behavior. Special tests will not be discussed in this report because such tests are specifically tailored to fit individual project needs.

Material Stress-Strain Characteristics

Stress-deformation response

65. An important indicator of the field deformation behavior which may lead to failure is the laboratory-obtained material stress-deformation curve. Stress-deformation responses may be conveniently divided into three groups: elastic-plastic, strain-hardening, and strain-softening. Figure 10 illustrates the three groups of stress-deformation response curves. Sliding stability limit equilibrium solutions model ideal elastic-plastic material (assumption b in paragraph 24). Strain-hardening materials typically exhibit a constant increase in resisting shear stress up to a sometimes poorly defined break in the response curve, after which the stress-deformation slope may flatten somewhat, but with increasing deformation the resisting shear stress also increases as shown by curve C in Figure 10. Strain-softening materials or brittle elastic materials (curve A in Figure 10) exhibit a marked postpeak decline in resisting shear stress; that is, as deformation increases past peak, resisting shear stress will decrease. Generally, the amount of deformation required to generate peak (break for strain-hardening materials) resisting shear stress increases from strain-softening to elastic-plastic to strain-hardening materials as illustrated in Figure 10.

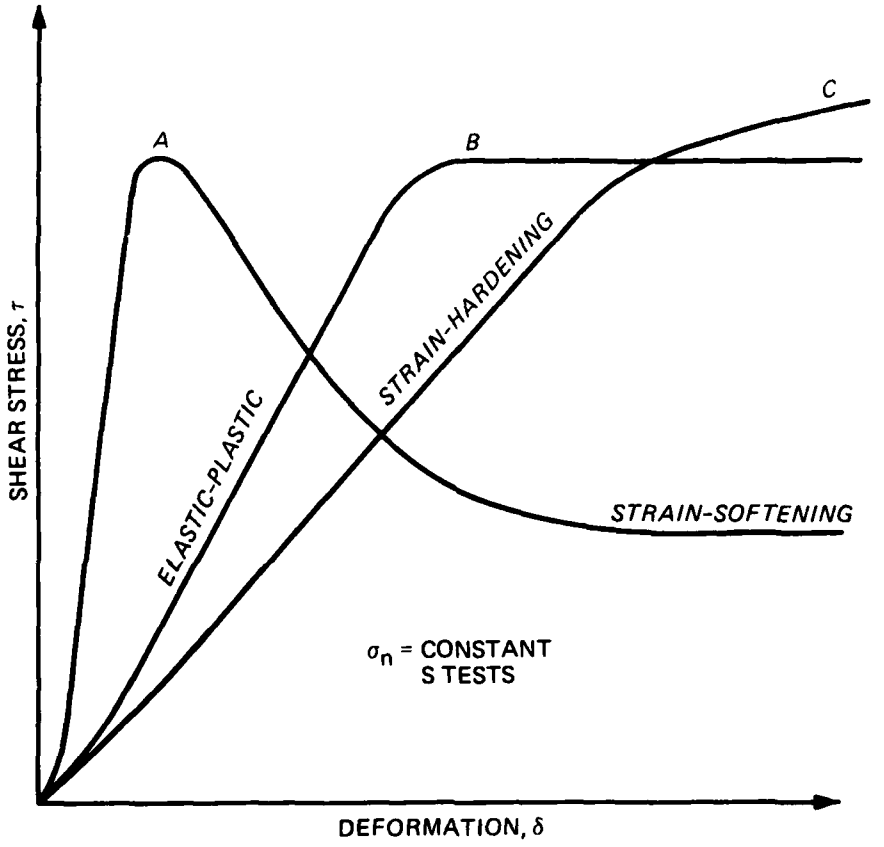

Figure 10. Hypothetical shear stress-deformation curves from drained direct shear tests on: (a) strain-softening; (b) elastic-plastic; and (c) strain-hardening materials

66. The designed performance of structures founded on or in materials characterized by elastic-plastic or strain-hardening presents few problems because these materials can sustain stress at least equal to design strengths regardless of the level of stress or deformation used to define failure. Strain-softening materials cannot offer this assurance. The safe and optimum design of structures founded on or in strain-softening materials using limit equilibrium techniques can be particularly difficult because analytic models are independent of strain or other factors that may cause a reduction in postpeak resisting shear stress. All strain-softening materials are susceptible to failure mechanisms commonly referred to as progressive failure.

Progressive failure

67. Conceptually progressive failure is explained in the following manner. If the maximum mobilizable strength of an element of material characterized by strain-softening behavior in the most stressed area along the potential slip surface is equal to or only slightly greater than the resisting stress needed for equilibrium, the material may strain past peak strength. The resisting shear stress of the most stressed element will decrease with increasing strain, resulting in a new distribution of applied stresses to the next element along the potential slip surface. Because of the steep stress-deformation gradient associated with strain-softening materials (Figure 10) the amount of strain required to exceed peak resisting shear stress will be small. Redistribution of stresses will, in turn, cause the new element to strain past peak strength and so on until the total slip surface progressively reaches the minimum value of resisting shear stress past peak that can be sustained by the material or until equilibrium is reestablished. If along the total slip surface the minimum resisting shear stress is not sufficient to establish equilibrium, failure occurs rapidly without time for remedial stabilization.

68. Bjerrum (1967) listed three conditions that must exist for a progressive failure to develop:

a. The development of a continuous failure surface by progressive failure is only possible if there exists, or can develop, local shear stresses exceeding the peak shear strength of the material.

b. The advance of a failure surface must be accompanied by local differential strain in the zone of shear failure sufficient to strain the material beyond failure.

c. The material must show a large and rapid decrease in shear strength with strain after the failure strength has been mobilized.

The problem with stability design of structures founded on or in strain-softening materials is recognizing potential conditions that might lead to a progressive failure. Once potential instability conditions are recognized, safe limit equilibrium designs can be achieved with the proper selection of stress and/or strain levels which appropriately defines failure of the model shear tests in accordance with the material's expected stress-deformation behavioral characteristics.

Definitions of failure for shear tests

69. Failure of a shear test specimen may be defined by any appropriate level of stress or strain along the stress-deformation curve. Four conditions commonly used to define failure are: peak stress, residual stress, ultimate stress, and a stress level associated with a limiting strain or deformation. Failure defined by peak, residual, and ultimate stresses are generally selected by visual interpretation of the stress-deformation curve, as illustrated in Figure 11. Failure defined by limiting strain (triaxial tests) or deformation (direct shear tests) sets a prescribed limit on the amount of strain or deformation that can be tolerated. Limiting strain is also used in some cases to define ultimate stress levels rather than from visual interpretation (see EM 1110-2-1906, pp IX-14) (Department of the Army, Office, Chief of Engineers 1970a).

70. Guidance for selecting the appropriate definitions of failure for soils are given in EM 1110-2-1906, Appendix IX (Department of the Army, Office, Chief of Engineers, 1970a). Similar guidance for rock is not available at the present. Therefore, the selection of conditions defining failure must be based on sound engineering judgment based on the particulars of the design and material failure mechanics.

Failure Criteria

71. Failure criteria link the shear stress to cause failure at a given normal stress with the mathematical model necessary for stability analyses.

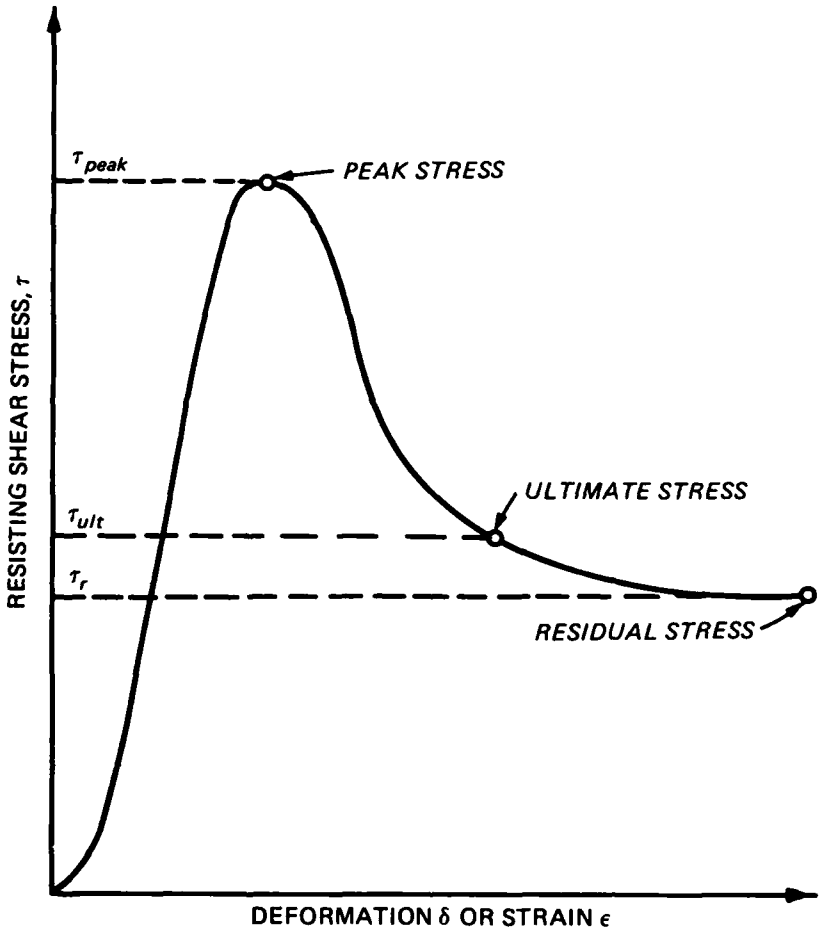

Figure 11. Shear test failure as defined by peak, ultimate, and residual stress levels

The link is independent of strain corresponding to the shear stress.

72. The Mohr-Coulomb criterion is the most common used for limit equilibrium solutions. The scope of this report will not permit a detailed discussion of failure criteria. However, to maintain continuity in discussions to follow, the basic principles of the Mohr-Coulomb criteria and bilinear and curvilinear criteria commonly used in rock mechanics will be briefly discussed.

Mohr-Coulomb failure criteria

73. Details of the Mohr-Coulomb failure criterion is presented in most soil mechanics textbooks. The Mohr-Coulomb criterion is directly applicable to triaxial (Bishop and Henkell 1962) or other test procedures where the principal stresses are known. Figure 12 shows a graphical representation of the Mohr-Coulomb relation between principal stresses and shear stress in the plane of failure for two hypothetical triaxial tests. In Figure 12, σ_n is the stress normal to the failure plane and σ_1 and σ_3 (assumes $\sigma_3 = \sigma_2$) are the major and minor principal stresses, respectively. The Coulomb equation (Equation 3) rewritten in the form familiar today becomes:

$$\tau_f = c + \sigma_n \tan \phi \tag{17}$$

where

τ_f = the shearing stress at failure

The c and ϕ parameters are the cohesion intercept and angle of internal friction, respectively.

74. In general, the failure envelope for a given series of tests under a given set of conditions is curved. However, for many soils and rocks, failure envelopes over most design stress levels can be closely approximated by the Coulomb equation as shown in Figure 12.

Bilinear failure criteria

75. Investigators have for some time noted that the failure envelope of some materials, in particular discontinuous rock, could not be adequately modeled by the linear Mohr-Coulomb failure criterion. Naturally occurring discontinuities exhibit surface irregularities (asperities) which contribute to the shearing resistance. Patton (1966) ran direct shear tests on

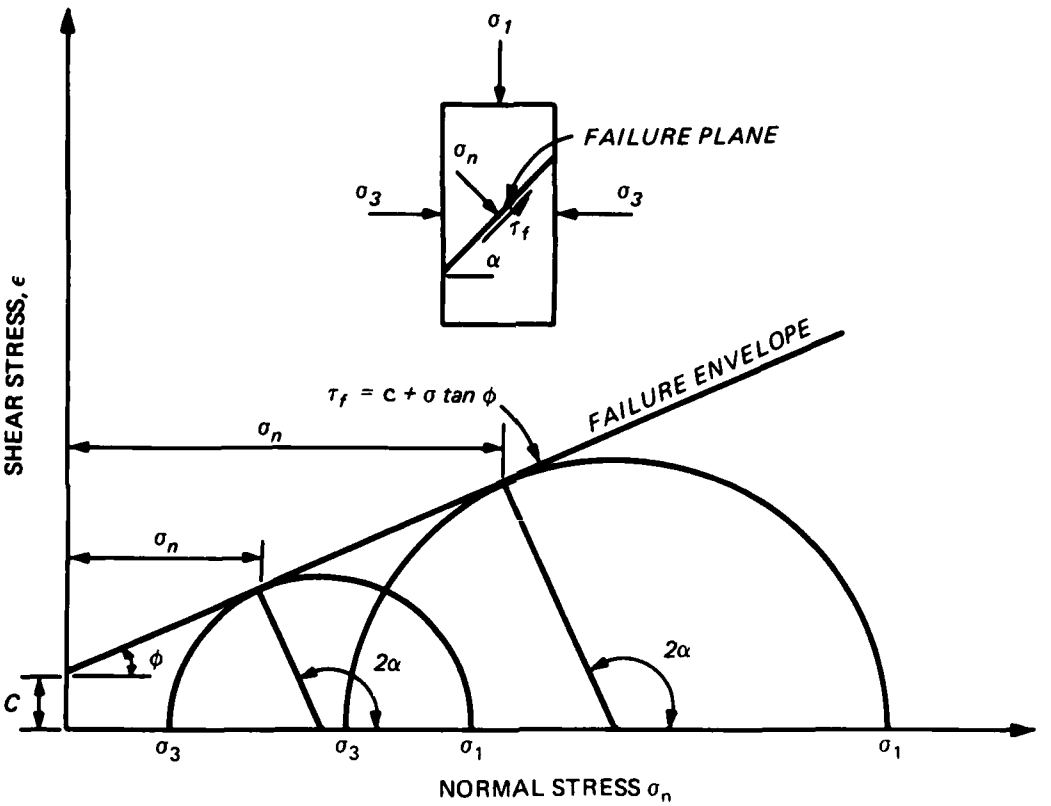

Figure 12. Mohr-Coulomb relationship with respect to principal stresses and shear stress

plaster-of-paris specimens to model the mechanisms of shear along an irregular rock surface. Specimens were cast with asperity surfaces inclined at the angle i measured with respect to the shear direction as shown in Figure 13. Both maximum and residual shear strength envelopes were constructed from the test results. The maximum shear strength was determined from the peak shear load. The maximum strength failure envelopes were actually curved, but were approximated by two straight lines. Line OAB in Figure 13 is a typical approximate bilinear maximum strength envelope. At normal stresses less than σ_T the expression for the approximate maximum strength envelope that can be developed is:

$$\tau_f = \sigma_n \tan (\phi_u + i) \tag{18}$$

while at normal stresses greater than σ_T

$$\tau_f = c_a + \sigma_n \tan \phi_r \tag{19}$$

where

ϕ_u = the friction angle on the sliding surface

ϕ_r = the residual friction angle of the material comprising the asperities

c_a = the apparent cohesion (shear strength) intercept derived from the asperities

A similar type of envelope was also proposed independently by Coldstein et al. (1966).

Curvilinear failure criteria

76. Actual rock surfaces obviously cannot always be adequately fit with such a simple model as the bilinear criteria. Attempts have been made to develop curvilinear criteria (Jaeger 1971, Ladanyi and Archambault 1969, and Barton 1971 and 1973) to more closely model actual rock behavior. Two criteria developed by Ladanyi and Archambault (1969) and Barton (1971 and 1973) have enjoyed some degree of acceptance in recent years.

77. Ladanyi and Archambault's criterion. The derivation of the Ladanyi and Archambault (1969) criterion follows the work of Rowe (1962), and Rowe, Barden, and Lee (1964) on stress dilatancy and energy components of dense

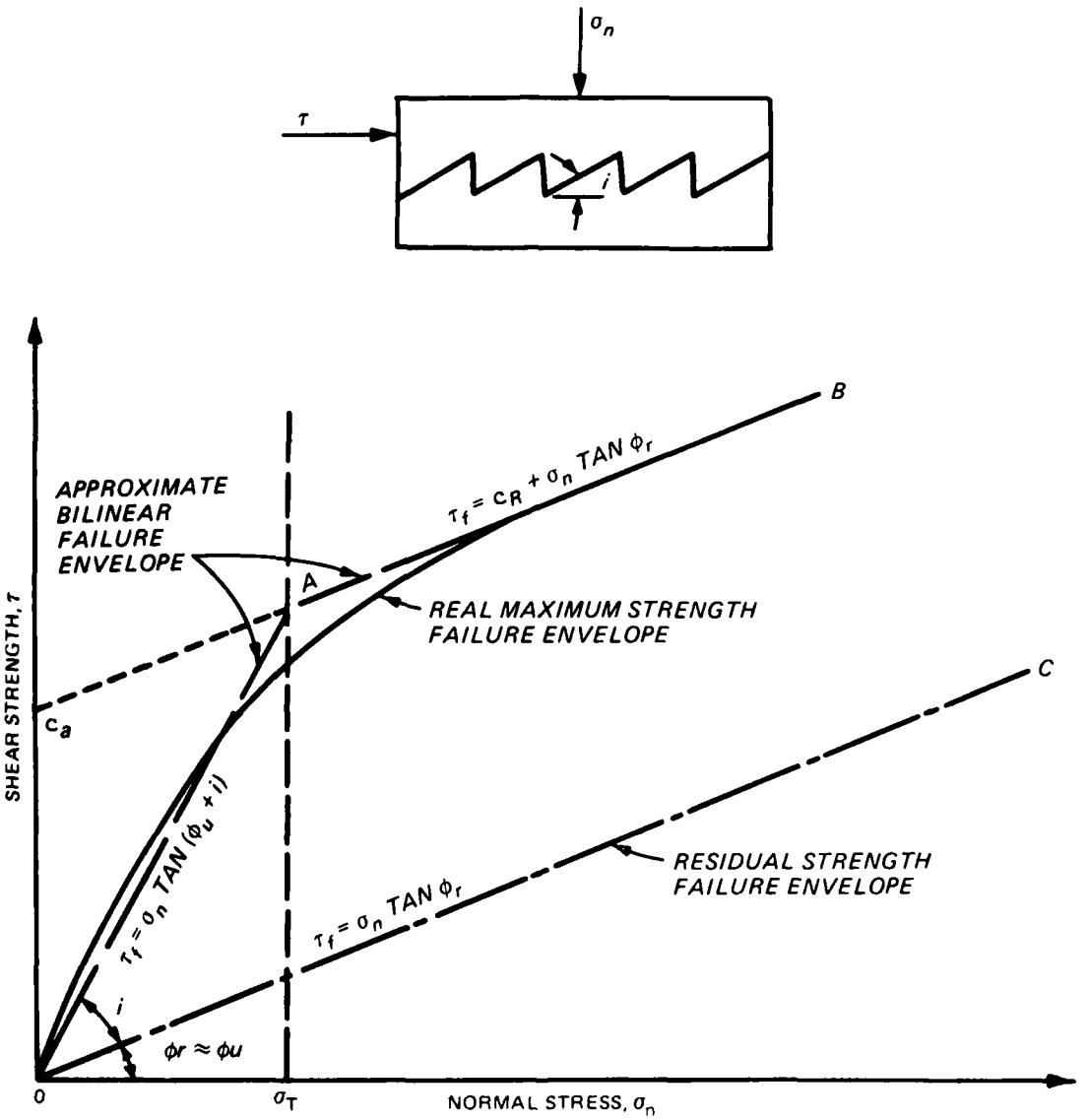

Figure 13. Typical approximate bilinear and real curvilinear failure envelopes for modeled discontinuous rock

sands. The criterion combined the friction, dilatancy, and interlock contributions to peak shear strength to derive a general strength equation for discontinuities which has proved accurate in studies on rock and simulated rock models (Ladanyi and Archambault 1969). The peak failure strength is given by:

$$\tau_f = \frac{\sigma_n (1 - a_s) (\dot{v} + \tan \phi_u) + a_s s_f}{1 - (1 - a_s) \dot{v} \tan \phi_u} \tag{20}$$

where

a_s = the proportion of joint area sheared through the asperities

$\dot{v}$ = the dilation rate at the peak shear stress

s_f = the shear strength of the rock composing the asperities

Equation 20 reduces to Equation 18 at low σ_n when $a_s = 0$ and $\dot{v} = \tan i$. Setting $s_f = \tau_f = c_a + \sigma_n \tan \phi_r$, Equation 20 reduces to Equation 19 at very high σ_n where all the asperities are sheared off, $a_s = 1$ and $\dot{v} = 0$. Ladanyi and Archambault recommended substituting a parabolic criterion developed by Fairhurst (1964) for s_f.

78. Barton's criterion. Barton (1971 and 1973) developed an empirical shear strength criterion for unfilled (clean) discontinuous rock accounting for the variation of dilatancy with normal stress and shear strength of the asperities. For the general case of weathered and unweathered rock joints (Barton and Choubey 1977) the peak failure strength is given by:

$$\tau_f = \sigma_n \tan \left[JRC \log_{10} \left(\frac{JCS}{\sigma_n} \right) + \phi_r \right] \tag{21}$$

where

JRC = Joint Roughness Coefficient which ranges linearly from 0 to 20 over the range from perfectly smooth to very rough

JCS = Joint wall unconfined compressive strength (in the same units as σ_n)

ϕ_r = residual friction angle expressed in degrees

Linear Interpretation of Bilinear and Curvilinear Failure Criteria

79. Many of the design shear strength failure envelopes corresponding to particular material behavioral characteristics are bilinear or curvilinear. Equations 13 and 15 for assessing sliding stability were developed assuming Coulomb's linear shear strength relationship which involves the determination of unique values of the shear strength parameters c and ϕ for particular values of average normal stresses acting along a critical potential failure surface. If the range of design normal stresses is small, linear approximations are straightforward. However, for certain design cases, the range of acting normal stresses must also be considered in the selection of linear c and ϕ strength parameters.

Bilinear failure criteria

80. In order to discuss the effects of normal stress distribution on sliding stability analysis for bilinear failure criteria, it is convenient to examine the simple hypothetical case of a block of unit width with potential for sliding down an inclined plane as illustrated in Figure 14a. The block and inclined plane are assumed to be perfectly rigid. The actual normal stress distribution is triangular as indicated in Figure 14a. Sliding stability analysis resolves normal stress distributions into resultant forces, which in effect assumes an average uniformly distributed normal stress distribution as shown. The particular type of normal stress distribution assumed makes no difference in the calculated factor of safety as long as the failure criterion is linear over the total range of the actual stress distribution. For example, if the failure criterion for block and inclined plane is defined by the linear envelope ABC in Figure 14b, the calculated factor of safety for both the triangular and uniform stress distribution will be 1.43.

81. Problems arise in sliding stability calculations when the shear strengths for a range of actual normal stress distributions are defined by a bilinear failure criteria. If the shear strength between the wedge and inclined plane shown in Figure 14a is defined by the bilinear failure criteria (line ABE) in Figure 14b, it can be seen that sliding stability is controlled by two separate failure criteria (τ_1 and τ_2). In typical designs, the criterion selected is often based on the magnitude of the average stress, σ_{na} .

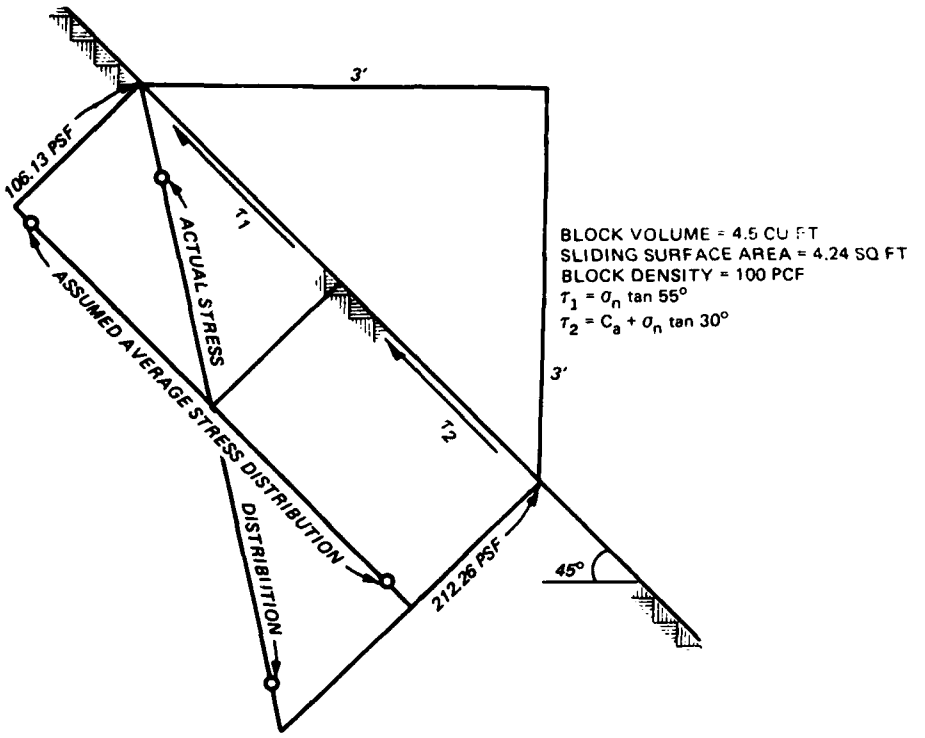

a. Assumed and actual stress distribution of a block subject to downslope sliding

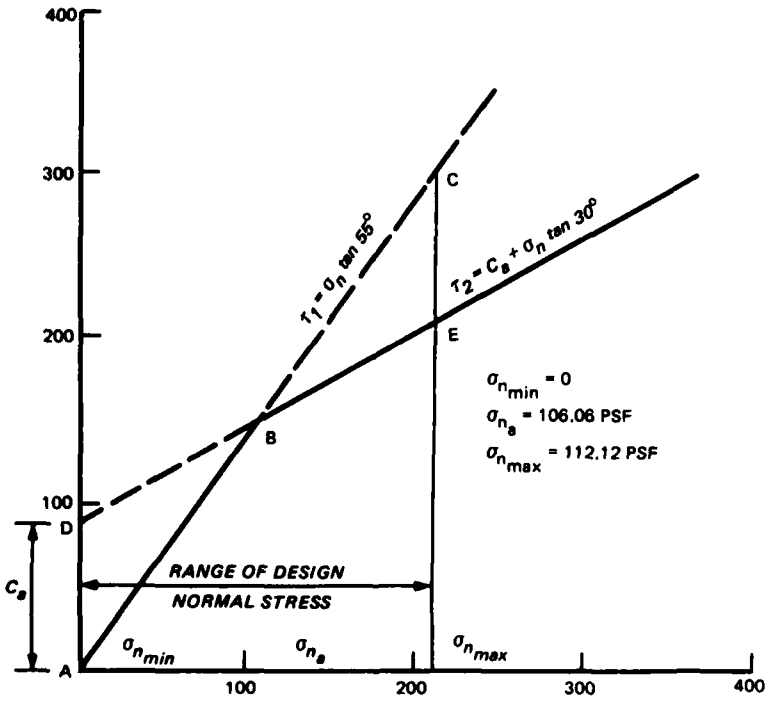

b. Range of normal stress distribution with respect to bilinear failure criteria

Figure 14. Factor of safety for bilinear failure criterion

The effects of the selected shear strength criterion on calculated factors of safety is dependent on which side of the bilinear break (point B, Figure 14b) the design average normal stress lies.

82. If the average design normal stress, σ_{na}, lies to the left of point B (Figure 14b), then the shear strength criterion commonly selected would be τ_1 (line ABC), which would result in an overestimate of strength for that segment of the block representative of τ_2. The amount of overestimate is bounded by the line BC and BE in Figure 14b. On the other hand, if σ_{na} lies to the right of point B, τ_2 strengths would overestimate the strengths for that segment of the block representative of τ_1 by the amount bounded by lines DB and AB in Figure 14b.

83. In the example illustrated in Figure 14, both assumptions of σ_{na} position (right or left) with respect to Point B will result in higher calculated factors of safety than the factor of safety based on a triangular normal stress distribution. Right and left assumptions of σ_{na} with respect to Point B will result in factors of safety of 1.78 and 1.43. The factor of safety considering actual normal stress acting over different areas of the block, each with its own shear strength (τ_1 and τ_2) is 1.38.

84. The reason for considering average normal stress distributions in design is that the actual normal stress distribution, to include range, is seldom known. Average stress distributions can be determined with a high degree of reliability since the average stress is a function of only body forces plus any surcharge forces and the area of the potential slip surface. Both forces and area can generally be determined rather accurately.

85. The actual normal stress distribution requires knowledge of the interaction between the potential sliding block and the founding material. If the potential sliding block and founding material are composed of materials with similar behavioral characteristics, reasonable estimates of normal stress distributions can be obtained from simple statics and the problem associated with stress ranges and bilinear failure criteria can be easily accommodated by breaking the potential sliding block into two or more segments with each segment having its own appropriate failure criterion.

86. Problems with assumed uniform normal stress distributions and bilinear failure criteria will generally be more severe where there is a large

difference in stiffness between the structure and foundation material. If the problem is deemed critical to the stability of the structure, principles of soil/rock structure interaction must be employed to determine stress distribution. Finite element techniques similar to the one developed by Varshney (1974) are commonly used to provide good approximations of actual normal stress distributions.

Selection of c and ϕ for curvilinear failure envelopes

87. Curvilinear failure envelopes compound the problems relating to the distribution of normal stress. Any given linear approximation of a curvilinear envelope will be valid only for a limited range of stress distributions. The applicable range of stress distribution for which a linear approximation can be made is dependent upon the curvature of the curvilinear envelope.

88. Hoek (1976) suggests that in order to apply curvilinear shear strength criteria to a sliding stability design of rock slopes, one can use either of the following approaches:

a. Approach 1. Calculate the effective (average) normal stress acting across each segment of a potential failure surface and use the corresponding shear strength value, either directly from a graph of shear strength versus normal stress or by calculation, in the factor of safety determination.

b. Approach 2. Draw a number of tangents to the curvilinear shear strength envelope and determine the apparent cohesion and friction angles for the (average) normal stress value at the tangent points corresponding to the normal stresses on each segment of the potential failure surface.

89. The two approaches are illustrated in Figure 15. Both approaches will result in the same calculated factor of safety because the design shear strengths for both approaches correspond to the shear strengths at the average normal stress. Unless the distribution of normal stresses is rather uniform or the curvature of the strength envelope flat, both approaches will overestimate the resisting shear strength.

90. As a matter of note, τ_d determined from approach 1 in Figure 15 is substituted for the cohesion parameter c in the sliding stability Equations 13 and 15 with the friction angle parameter ϕ assumed zero. Approach 2 gives shear strength parameters c_a and ϕ_a which substituted directly into the equations.

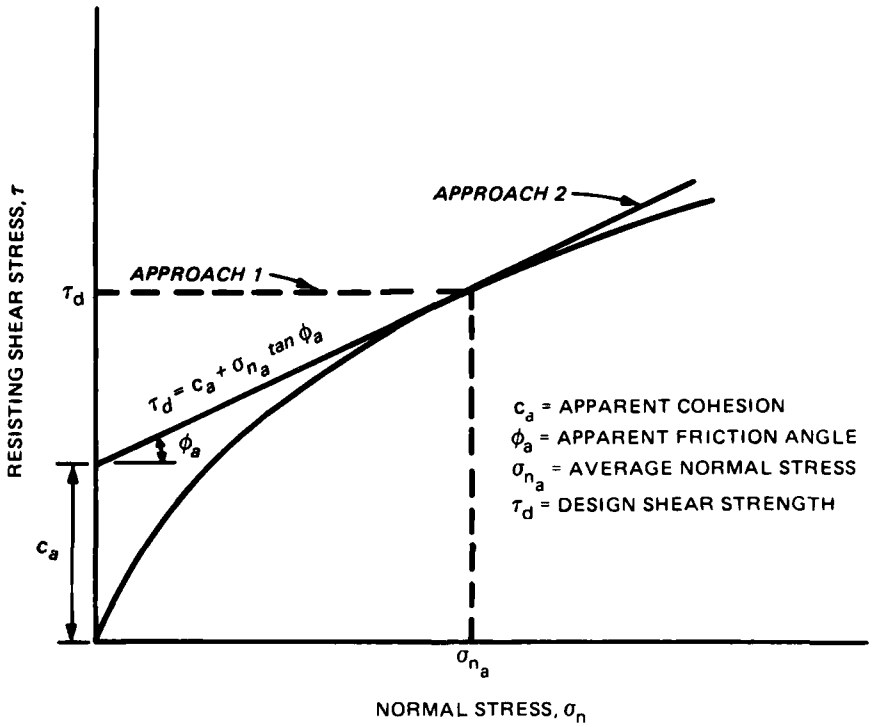

Figure 15. Shear strength parameters determined from curvilinear failure criteria using average normal stress

91. If the selection of resisting shear strengths along a potential failure surface is deemed critical to the sliding stability of the structure, the determination of actual normal stress distributions and ranges is necessary for accurate predictions of design shear strength. A knowledge of normal stress distribution will allow segmentation of the potential failure surface. ach segment of the failure surface would correspond to a given range of normal stresses, the shear strength parameters of which can be conservatively estimated by passing linear envelopes through the limiting normal stress ranges for each segment, as illustrated in Figure 16.

92. Segmented linear fits of curvilinear failure criteria can at best be only good approximations of actual strengths. Often, the selected linear approximations must be tempered with greater engineering judgment than typical for linear or bilinear criteria. Engineering judgment might include such factors as the reliability of observed shear strength from shear tests, the consequence of a possible failure, and the criticality of the observed strengths with respect to a potential failure.

Confidence in Selected Design Strengths

Considerations

93. The process of selecting design shear strengths for structures founded on rock masses involves the selection of appropriate shear tests (to include data interpretation) or available empirical techniques from which design strength selections are based. The process chosen is based on engineering judgment which assesses the degree of confidence that must be placed in the selected design strength. As a minimum, the assessed confidence must consider the mode of potential prototype failure, the factor of safety, the design use, the cost of tests, and the consequence of a failure.

94. Mode of failure. The mode of potential failure is perhaps the most important consideration in assessing the confidence that must be placed in selected design strengths. The mode of potential failure of rock masses may be conveniently divided into three groups: intact rock, clean discontinuous rock, and filled discontinuous rock. Resisting shear strengths that can be developed range from very high for strong intact rock to very low for

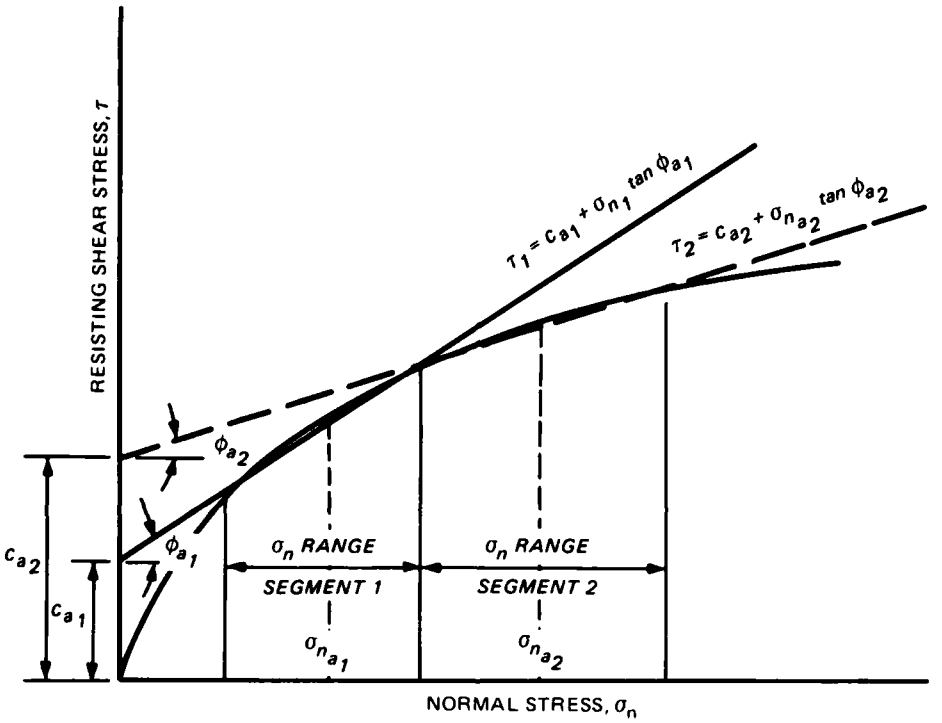

Figure 16. Shear strength parameters determined from curvilinear failure criteria using segmented ranges of normal stresses

discontinuous rock filled with weak filler material. If it is known that the only potential mode of failure is through massive and intact rock, the structure could be deemed safe against sliding without testing for rock strength (i.e., very conservative strength assumptions will lead to generous factors of safety). On the other hand, a weak discontinuous seam may require extensive in situ testing to obtain the necessary confidence that the selected design shear strength is representative of prototype strengths (i.e., conservative strength selection may result in unacceptably low factors of safety).

95. Factor of safety. The minimum acceptable calculated factor of safety for design provides some margin of error with respect to the degree of precision with which the selected shear strength represents prototype material strength behavior provided that the correct mode of failure has been selected for modeling. The calculated factor of safety is unique for given values of shear strength parameters c and ϕ. Although the c and ϕ parameters are unique for a given failure envelope or segment of a given failure envelope, the failure envelope in itself is not unique. The appropriate failure envelope judged to be representative of the upper limit of prototype resisting shear stress is dependent upon the failure criteria used to define the envelope, the definition of test specimen failure, and personal interpretation of test data. The failure envelope chosen and hence the calculated factor of safety reflects the assessed confidence to be placed in the selected design shear strengths.

96. Before the design strength selection process begins the designer should conduct at least an elementary parametric study to gain a feel for the magnitude of resisting strength required for safe stability. Such studies are referred to as sensitivity studies and relate the assessed confidence required of design strengths to the resisting strength required for safe stability.

97. Design use. The intended use of the design should also be considered in assessing confidence. Preliminary designs are frequently made for alternative evaluations before well defined geological or strength data are available. Such designs are usually based upon crude shear strength estimates.

98. Cost of tests. In general, cost of tests, which forms the basis of design strength selection, increases with increasing precision required of the

selected strengths. Cost of tests may or may not be a significant factor to consider in assessing the confidence to be placed in selected strengths. For example, high cost of tests should not be an important consideration where assessed confidence in selected design strengths require precise determinations of prototype strengths. On the other hand, if an inexpensive and easily obtained conservative strength selected for design results in an adequate factor of safety, the extra cost associated with tests that increase confidence (precision) could be assessed as not critical for design purposes.

99. Consequence of a failure. The assessed confidence should also reflect the social and economic impact should a failure occur. Design of dams located in populous areas where loss of life and/or extensive property damage will result should a failure occur demands a high degree of confidence that strengths selected for design will not exceed resisting prototype strengths that can be developed.

Assessed confidence

100. For the purpose of this report the assessed confidence in selected design shear strengths will be divided into three groups: low, high, and very high. In general, an increase in assessed confidence should either reflect increasing efforts to more closely define prototype shear strength at increasing cost or increasing conservatism in selected design strengths to account for the uncertainties of prototype strength. Figure 17 shows a flow diagram illustrating examples of factors to consider in assessing the confidence to be placed in shear strengths selected for design.

101. The following sections in this report will address the selection of appropriate shear tests (where necessary), interpretation of test data, and the approaches used in the selection of design shear strengths depending on the assessed confidence for each of the three major potential modes of failure associated with rock mass. The three major potential modes of failure are intact rock, clean discontinuities, and filled discontinuities. Because failure mechanisms form a necessary function in the selection of appropriate shear tests and interpretation of data depending on mode of failure each section will briefly discuss failure mechanisms relating to the major modes of failure.

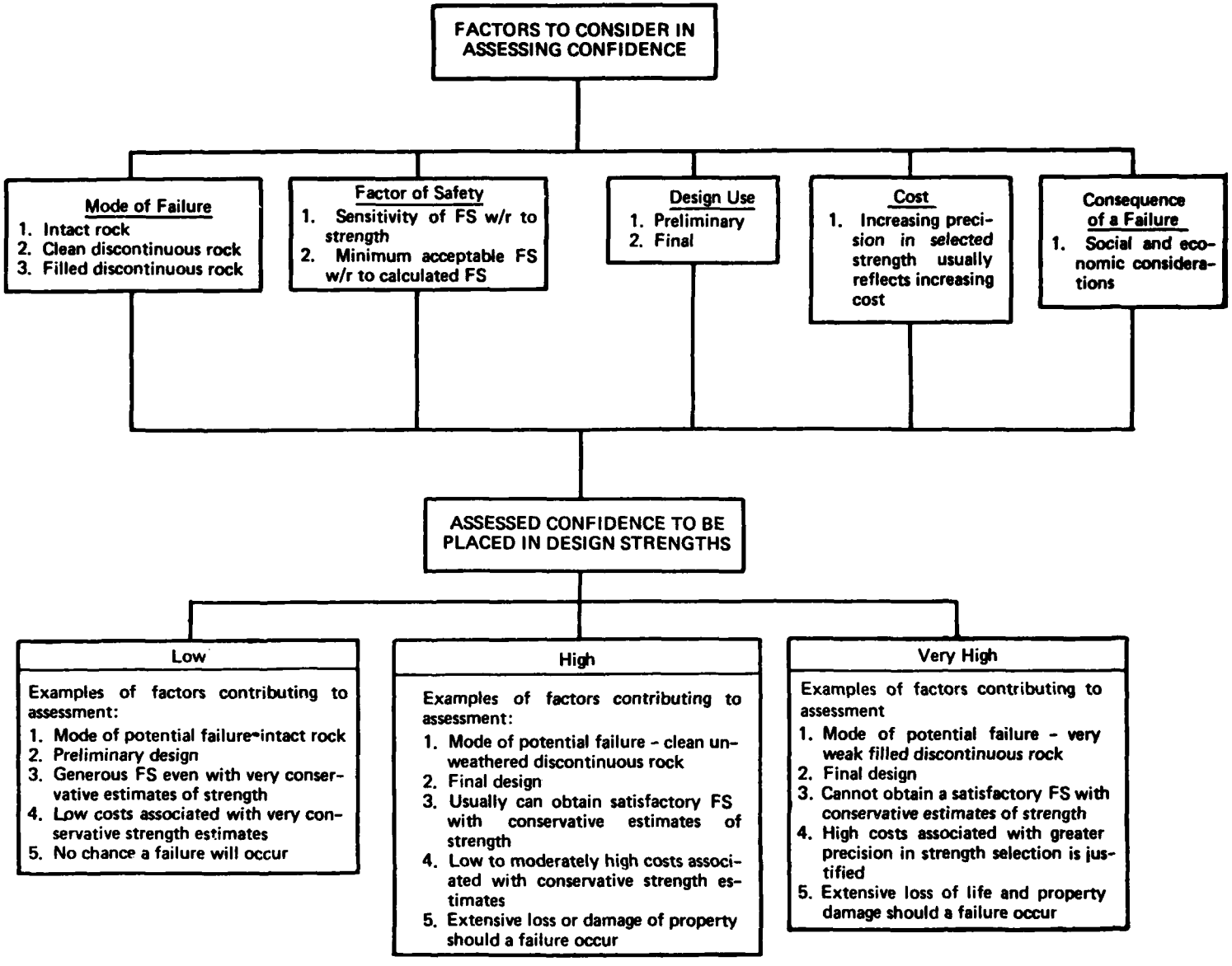

Figure 17. Flow diagram illustrating examples of factors to consider in assessing the confidence to be placed in selected design strengths

PART IV: SELECTION OF DESIGN SHEAR STRENGTH FOR INTACT ROCK

Definition of Rock

102. The word "rock" is a common term and yet the engineering distinction between rock and near-rock is vague. When does a stiff soillike material become rock? The American Geological Institute (1977) defines rock as any naturally formed, consolidated or unconsolidated material (but not soil) composed of two or more minerals, or occasionally of one mineral, and having some degree of chemical and mineralogic consistency. The term "consolidated" refers to any process whereby loosely aggregated, soft, or liquid earth materials become firm and coherent rock. The above definition might be suitable from a geological point of view; however, engineers are more concerned about behavioral characteristics rather than appearance. Many engineers think of rock as a strong and durable material that cannot be easily softened or weakened by weathering, and think of rock as not expanding or shrinking when subjected to wetting and drying cycles. Until a suitable engineering definition of rock is developed there will remain "gray areas" in the distinction between rock and soil, such as weakly cemented sandstones and clay shales.

Failure Mechanisms

103. Shear strengths of most intact rocks are sufficient to provide adequate resistance against shear failure for most loading conditions associated with hydraulic structures. There are exceptions; for example, an otherwise continuous plane of weakness might be interrupted by one or more relatively short segments of intact rock. Another example might be the potential failure of poorly cemented intact sandstones. The exceptions necessitate a fundamental understanding of intact rock behavior when subjected to a shear stress of sufficient magnitude to cause failure.

Failure modes

104. The typical confined peak strength failure envelope for intact rock is curvilinear. Figure 18 illustrates a hypothetical Mohr failure envelope typical of triaxial test results. The failure (commonly called "rupture" in

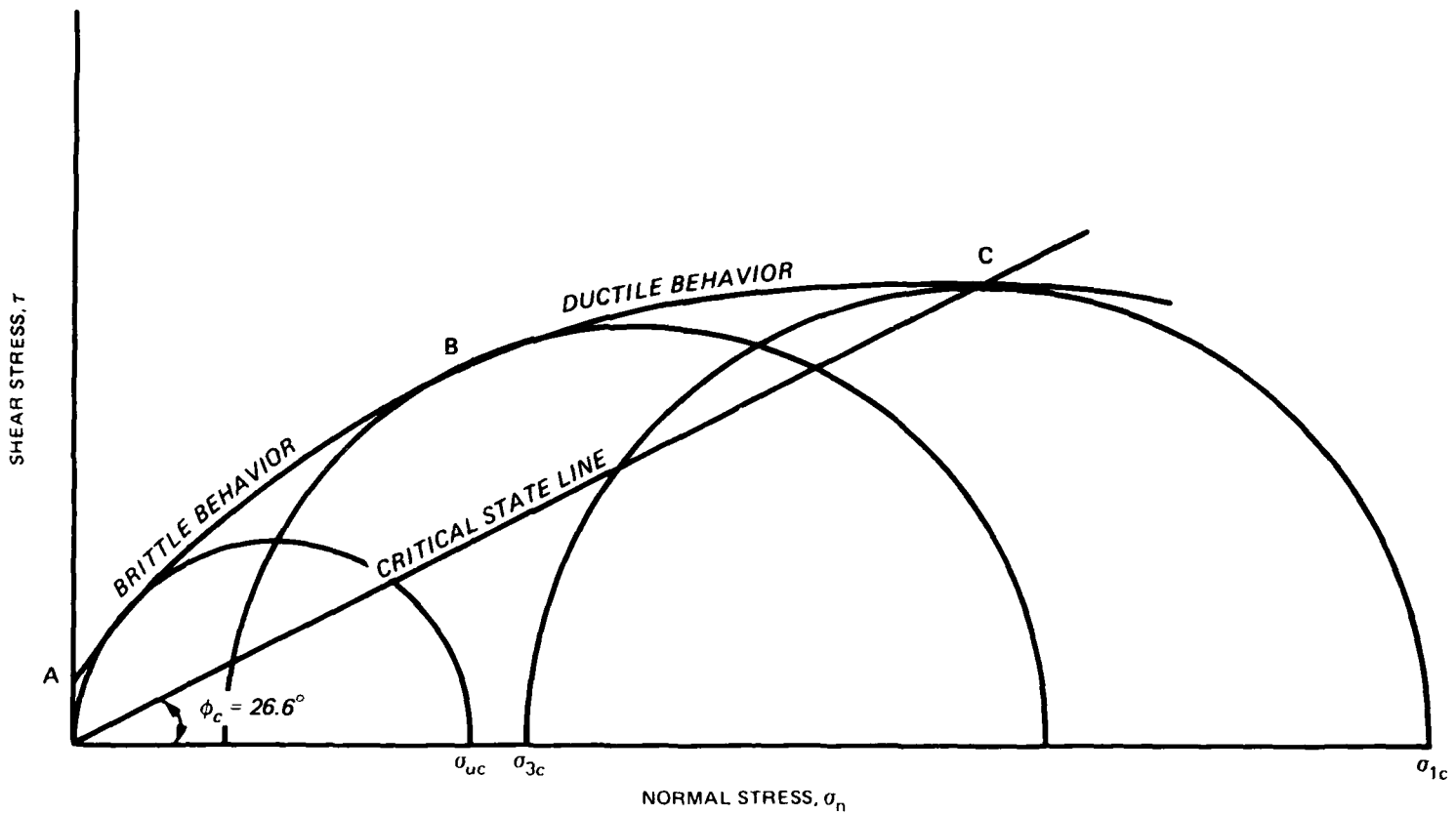

Figure 18. Hypothetical curvilinear Mohr failure envelope typically obtained from triaxial tests on intact rock specimens

rock) of intact rock is a function of confining pressure, temperature, and to some extent strain rate (particularly when saturated). For most surface or near surface engineering work, temperature is not a factor and therefore will not be discussed herein. At low confining pressures up to approximately the unconfined compressive strength (σ_{uc} and line AB in Figure 18) the rock behaves as a brittle material. With increasing confining pressures the material gradually exhibits ductile failure characteristics. The transition from brittle to ductile failure is approximated by point B in Figure 18, although in reality the transition occurs over a band or interval of stress. Finally, at a sufficiently high confining stress the material can no longer develop an increase in shear stress at failure as shown by point C in Figure 18. Barton (1976) defined this point (point C) of zero gradient as the critical state of stress. Barton (1976) demonstrated that the Mohr envelope intercepted the critical state of stress when the relationship between the major and minor principle stress is $\sigma_{1c} = 3\ \sigma_{3c}$ as shown in Figure 18. Barton (1976) also demonstrated that a line intercepting the origin and the critical state of stress will have an angle of inclination of 26.6 deg. The line was referred to as the critical state line. Barton (1976) suggested that the concept of the critical state of stress and critical state line is valid for all rock. At stresses beyond the critical state the shear strength will gradually decrease. Because the majority of engineering problems are at stress levels well below the brittle-ductile transition (typically less than 1/2 σ_{uc} even for very low strength rock) only brittle failure will be discussed herein.

Brittle failure

105. Bieniawski (1967) and Byerlee and Brace (1967) working independently developed a conceptual explanation of brittle failure. This conceptual explanation can best be explained by examining Figure 19a showing a hypothetical saturated intact rock specimen subjected to confined axial compression under drained shear conditions. According to Bieniawski (1967) and Byerlee and Brace (1967) (for uniaxial compression), as axial strain increases the initial microcracks first close (line oa, Figure 19a), then propagate for a limited stress range where the incurred strain is essentially elastic (line ab, Figure 19a). At higher stress levels (line bc) the crack propagation is stable but nonelastic. Over the stable crack propagation stress range

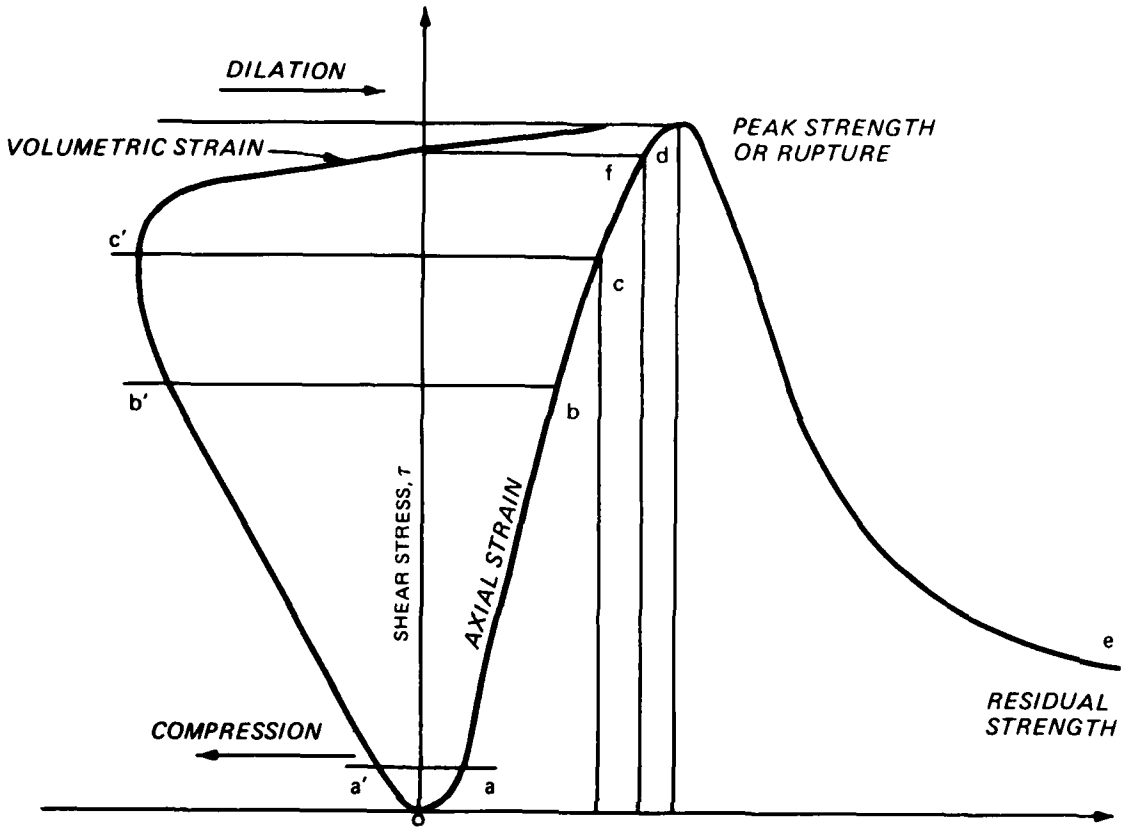

a. Relationship between volumetric and axial strain and shear stress under drained conditions

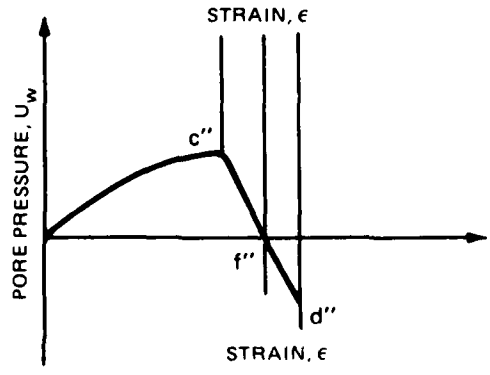

b. Relationship between pore pressure and axial strain for brittle failure of intact porous rock

Figure 19. Typical stress, strain, and pore pressure response of a rock specimen subjected to triaxial test conditions with low confining pressures

(line oc), the specimen undergoes volumetric compression. At stress levels above point c crack propagation becomes unstable and the strain nonreversible, resulting in progressive failure as the stress increases to peak strength and rupture (line cd). As the axial stress-strain progresses along line cd, volumetric strain decreases and finally dilates (for most rock) just prior to peak strength. In a sufficiently rigid system and for most rock there will be a marked decrease in strength past peak (point d) (brittle failure) down to the residual strength (line de). After rupture or peak strength three-dimensional dilation will cease followed by one-dimensional dilation along the formed failure surface.

106. If the specimen in Figure 19a is subjected to a triaxial test under very low confining pressure and is not allowed to drain during shear (volumetric strain equals zero) pore pressure response would be similar to that indicated in Figure 19b. Positive pore pressure will peak at the maximum stress level associated with stable crack propagation (point c, Figure 19a). At stress levels above point c pore pressure decreases and becomes negative just prior to rupture. Between rupture and residual strength pore pressure levels are largely determined by boundary drainage conditions. Figures 19a and 19b are offered as an illustration; in reality the shear stress-strain curve may not be the same for both drained and undrained tests.

107. Figure 19 demonstrates the presumption that intact rock behave according to the laws of effective stress. Triaxial tests by Robinson (1955) produced some of the first conclusive evidence of the validity of effective stress in reasonably porous rocks such as sandstone and limestone. Other investigators (Byerlee and Brace 1967, Lane 1969, and Byerlee 1975, and others) have since supported this evidence with similar test results on porous rock. For low porosity rock such as dolomite, siltstone, and dense granites the evidence is less conclusive. Supporting evidence for low porosity rock is difficult to obtain because of difficulty in saturating the specimen, and the extremely slow strain rates necessary to detect pore pressure response.

Scale effects

108. There are conflicting observations on the role of specimen size. Some investigators (Bieniawski 1968, Mogi 1962, Pratt et al. 1972, Koifman 1969, and Koifman et al. 1969) report a decrease in strength with increasing

specimen size, while others (Hodgson and Cook 1970) report no change in strength. The third possibility, an increase in strength with specimen size, has been reported by Koifman (1969) and Koifman et al. (1969), but only for small samples. The current consensus is that most intact rock experience at least some strength loss with increasing specimen size and that the amount of loss depends on comparable specimen size and material type. Figure 20 shows a plot of maximum uniaxial compressive stress versus specimen size for six material types. Pratt et al. (1972) and Bieniawski (1968) suggest, as indicated in Figure 20, that maximum strength values asymptotically approach a constant value for specimens greater than approximately 3 ft. The Weibull "weakest link" effect, stored strain energy within the specimen, and stress concentrations have been offered as possible explanations to strength loss. However, no single or combined explanation can yet explain the behavior of all material types.

Design Shear Strength Selection

Assessed confidence

109. The amount of effort and hence expense spent in defining meaningful design strengths need to properly reflect the probability that a failure might occur. If proper design is provided against overturning, sliding instability will not be a problem where the major mode of potential failure is through intact rock (except for possibly very weakly cemented rock). A high assessed confidence in selected design shear strengths is likely required only where a relatively small part of the total potential failure surface consists of intact rock. Table 1 presents a brief summary of assessed confidence to be placed in selected design shear strengths for various modes of potential failure, design use, and strength sensitivity. The terms "low," "high," and "very high" in Table 1 are in accordance with the discussions given in paragraphs 93 to 101. Table 1 is intended only as an illustrative example. It must be realized that assignment of confidence levels is a judgmental process. In some cases the quantity of intact rock is not known and need not be known if adequate factors of safety can be obtained by ignoring the extra contribution of resisting strength provided by the intact rock segments.

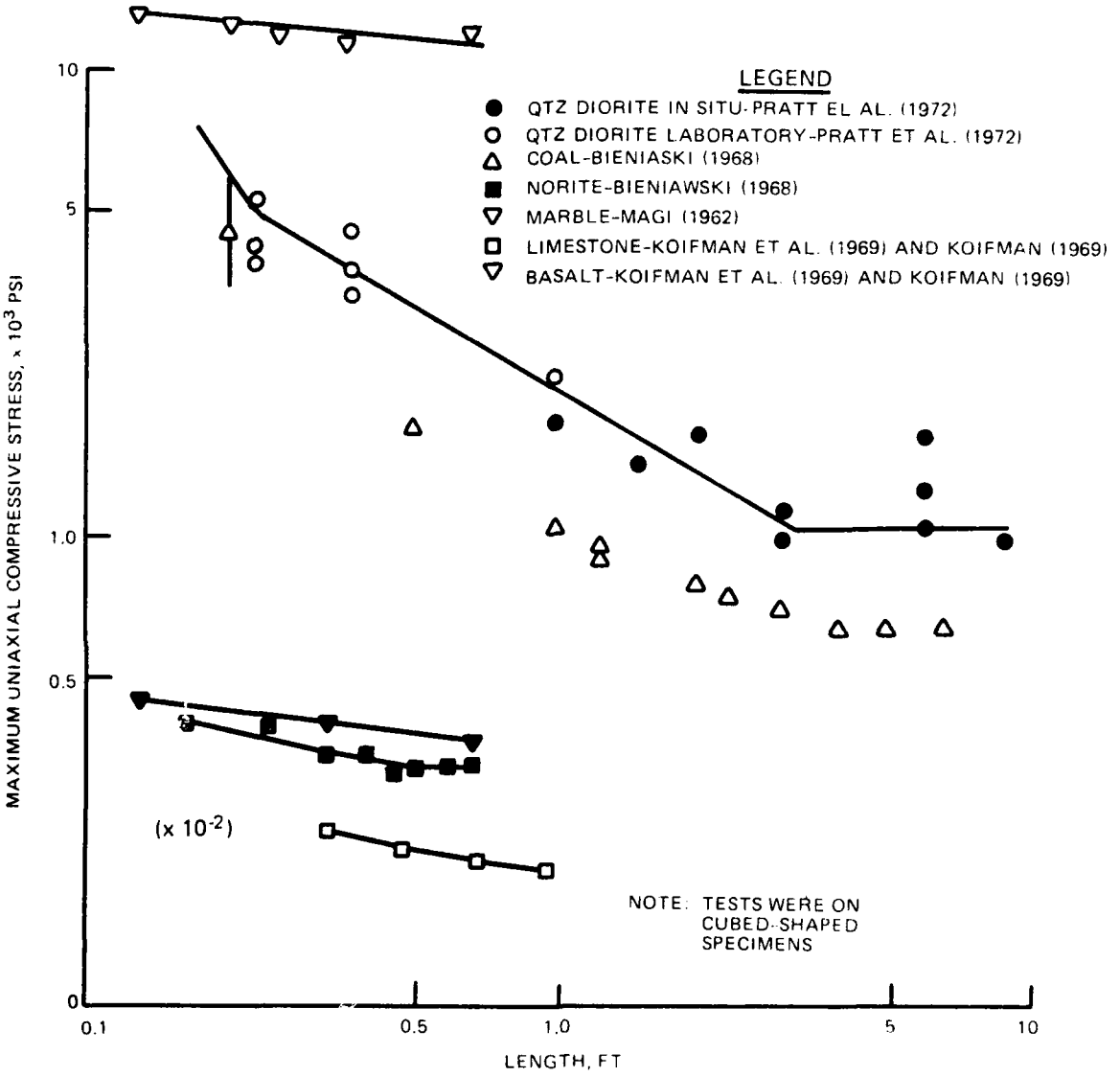

Figure 20. Maximum uniaxial compressive stress versus specimen size (after Pratt et al. 1972)

Shear tests
applicable to intact rock

110. General guidance for intact rock testing procedures discussed in the "Rock Testing Handbook" (U. S. Army Engineer Waterways Experiment Station 1980) and in the "Suggested Methods for Determining Shear Strength" (International Society of Rock Mechanics 1974) are for undrained tests. Because of the slow pore pressure response time associated with most rock, drained tests are not practical for most routine tests. For some porous rock drained test results can be obtained from $\bar{R}$ tests (undrained tests with pore pressure measurements) discussed in paragraph 61 and EM 1110-2-1906 (Department of the Army, Office, Chief of Engineers 1970a).

111. Typical laboratory shear devices are not sufficiently stiff to properly define postpeak shear-deformation characteristics. Failure in routine tests on intact rock is defined by peak strengths or predesignated levels of stress-deformation prior to peak strength.

112. Triaxial and direct shear devices have certain advantages and disadvantages depending on the needs of the test requirements and capabilities of the devices. Table 2 presents a summary of advantages and disadvantages of triaxial and direct shear devices for testing intact rock.

Interpretation of test results

113. Uniaxial compression test. The uniaxial compression test is simple and relatively inexpensive to perform. With proper interpretation test results will provide relative strength classification and approximations to shear strength.

114. Observed uniaxial compressive strengths from tests on seemingly identical intact rock specimens characteristically exhibit standard deviation of 15 to 20 percent or more for some rock types. The uniaxial compressive strength for a given rock type is obtained from the average of a series of tests. The number of tests may depend upon availability of specimens, but normally a minimum of ten tests is preferred.

115. The uniaxial compression (UC) test offers a quick and easy means of predicting the relative strength of intact rock. Table 3 (Deere and Miller 1966) presents a classification of intact rock strength with respect to ranges in uniaxial compressive strength, q_u .

116. Crude approximations of shear strength may be obtained by assuming that the friction angle is zero and cohesion is equal to one-half the uniaxial compressive strength as shown in Figure 21. This approximation will overestimate the actual shear strength since design normal stresses are typically below one-half the uniaxial compressive strength even for very weak intact rock.

117. Caution should be exercised in the use of design strengths obtained from uniaxial compression tests. However, for design situations which can tolerate order of magnitude approximations in shear strength, the uniaxial compression approach provides an inexpensive alternative.

118. Shear tests. Failure envelopes over normal stress levels up to the brittle ductile transition are usually strongly curvilinear. However, for normal stress ranges typical for design (0 to 20 tsf) linear approximations of curvilinear envelopes are in most cases adequate for design. Linear failure envelopes for direct shear tests are best obtained by a line of least squares best fit of shear stress, τ, versus normal stress, σ_n, plots. Linear failure envelopes for triaxial tests may be obtained by a line that visually best fits a family of Mohr's circles or by a line of least-squares best fit of a p-q diagram. The p-q diagram approach, illustrated in Figure 22, offers a rational means for statistically treating Mohr's circle data to obtain a least-squares best-fit failure envelope. The ϕ and c shear strength parameter corresponding to the failure envelopes best fitting the tangents of the family of Mohr's circles are obtained from the p-q line of least-squares best-fit α and a parameters (Figure 22) by the following equations:

$$\phi = \sin^{-1} (\tan \alpha) \tag{22}$$

$$c = a/\cos \phi \tag{23}$$

Paragraphs 86 to 91 describe considerations and procedures for linear approximations of $\tau - \sigma_n$ data that are curvilinear over the design normal stress range.

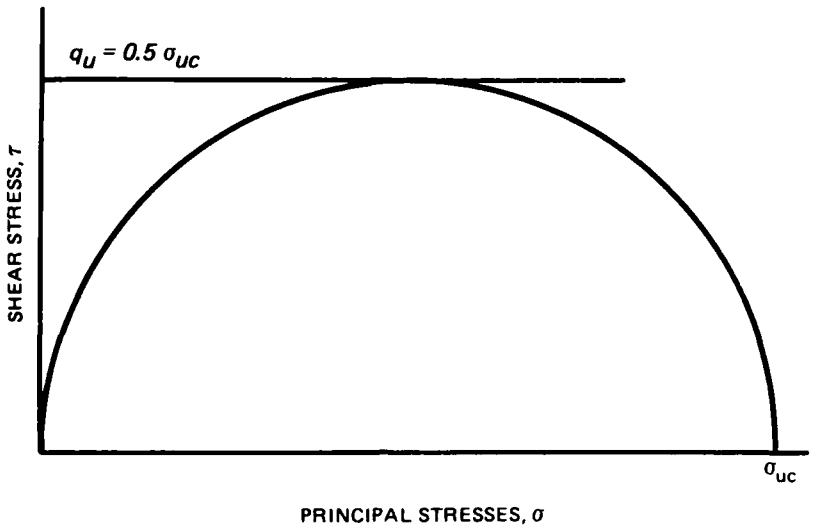

Figure 21. Estimates of intact rock shear strength from uniaxial tests

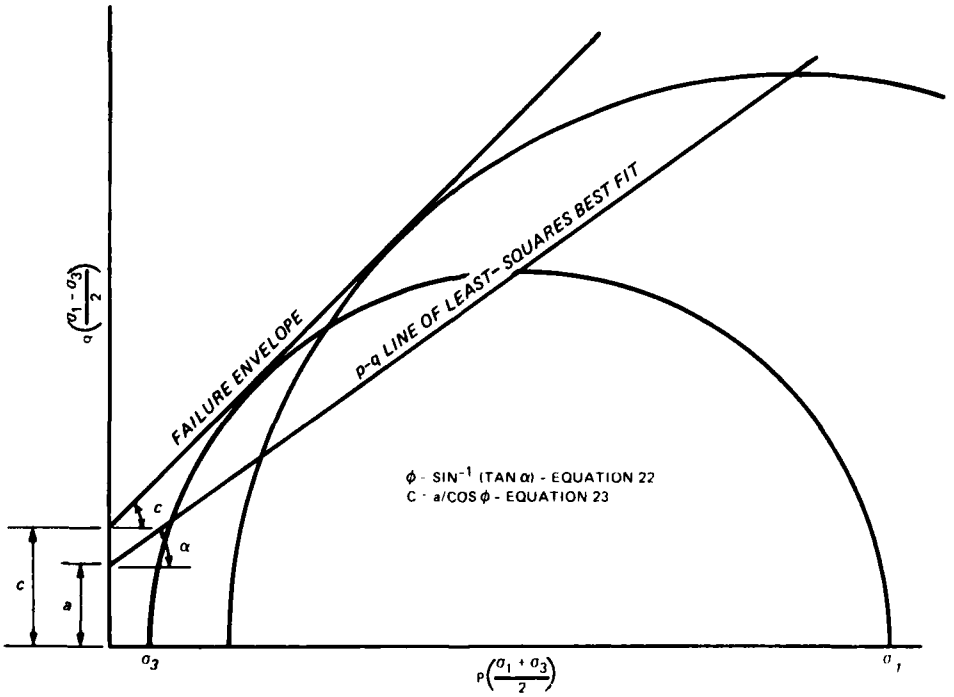

Figure 22. Determination of the failure envelope from p-q diagram

119. The $\tau - \sigma_n$ plots for intact rock generally exhibit considerable scatter. If a sufficient number of tests are conducted (usually nine or more), trends defining the upper and lower bounds of likely shear strength that can be mobilized become apparent. Figure 23 shows a $\tau - \sigma_n$ plot for direct shear tests on a very low-strength (average uniaxial compressive strength of 667 psi) intact limestone sheared parallel to bedding planes. Failure envelopes obtained from a least-squares best fit of upper bound, lower bound, and all data points are also shown in Figure 23. It is interesting to note that the cohesion value increases by 110.8 percent from the lower bound to upper bound envelope, while the variation in the friction angle for the three envelopes varies by only 4.7 percent. With a sufficient number of tests to define scatter trends over a given design normal stress range the assessed confidence that can be placed in the friction angle far exceeds the level of confidence that can be placed in the cohesion values.

Design shear strengths

120. Table 4 presents a summary of alternative approaches for the selection of c and ϕ shear strength parameters. The type of tests, specimen drainage conditions, definition of specimen failure, and alternative interpretation of test results are related to the assessed confidence required of the selected parameters and the mechanisms of failure associated with intact rock. The assessed confidence is in turn related to the mode of potential failure and intended use of the design strengths as discussed in paragraph 109 and summarized in Table 1.

121. Table 4 is intended only for general information. Special requirements of specific design cases may require modification of the alternative approaches. The column entitled "Comments" attempts to summarize the limitations and consequences of each approach.

122. It is important to note that while intact rock strengths from drained peak strength tests (long-term stability) are generally critical for design because of both maximum uplift considerations and dilation tendencies at failure, the slow pore pressure response associated with all but porous rock makes drained testing impractical for most rock. Undrained test results are generally interpreted in a conservative manner to compensate for the unconservative tendencies of undrained tests.

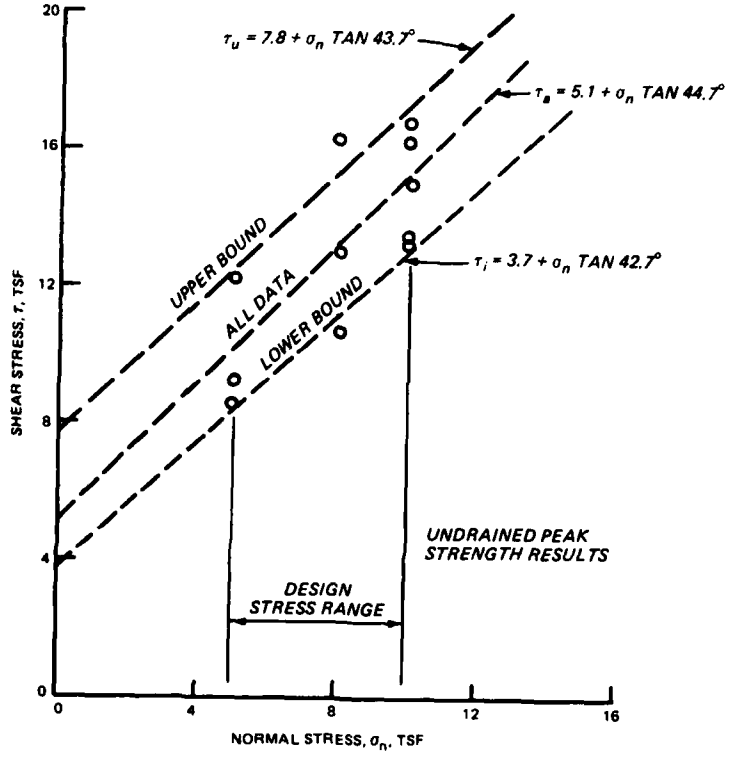

Figure 23. Direct shear tests on intact limestone (after U. S. Army Corps of Engineers, Nashville District 1974)

123. It is also important to note that Table 4 does not discuss specimen selection. Shear tests from which design shear strength are selected are only as valid as the specimens selected to be representative of potential prototype failure conditions. Specimen selection often reflects the assessed confidence to be placed in design strengths. For example, if the assessed confidence is considered to be very high, specimens selected for shear testing may reflect the worst average foundation conditions. The scope of this report will not permit a detailed discussion. However, the selection of test specimens judged to be representative of prototype material conditions and reflecting assessed confidence cannot be overly emphasized.

PART V: SELECTION OF DESIGN SHEAR STRENGTH FOR CLEAN DISCONTINUOUS ROCK

Definition of Clean Discontinuous Rock

124. The term "discontinuity" as used herein applies to any naturally occurring or man-induced fracture or break which extends through the element or unit of rock under examination. The term "joint" has in geotechnical engineering terminology come to be synonymous with "discontinuity." A clean discontinuity applies to any discontinuity that does not contain filler material.

125. A discontinuity may be weathered or unweathered. The degree of weathering is an important consideration in selecting appropriate testing techniques upon which shear strength selection may be based. Paragraphs 136 to 138 below will discuss how weathering effects influence the choice of testing techniques. Because of the vast range of weathering products derivable from intermediate stages of decomposition of rock no single index derived from simple field observations or laboratory tests can be expected to apply for all rock. The degree of weathering describing a particular joint wall is therefore primarily left to the judgment of the geologist. While descriptive terms such as unweathered, slightly weathered, moderately weathered, or severely weathered are frequently used to describe the degree of weathering, such terms are useful only in a relative sense. As long as the joint wall surfaces remain intact with the parent rock material regardless of weathering effects, the joint is deemed to be clean provided no other filler material is present between the joint wall surfaces.

Failure Mechanisms

Failure modes

126. The typical failure envelope for clean discontinuous rock is curvilinear as illustrated in Figure 24. The failure mechanics of discontinuous rock is complex. Surfaces of discontinuous rock are composed of irregularities or asperities ranging in roughness from almost smooth to sharply inclined

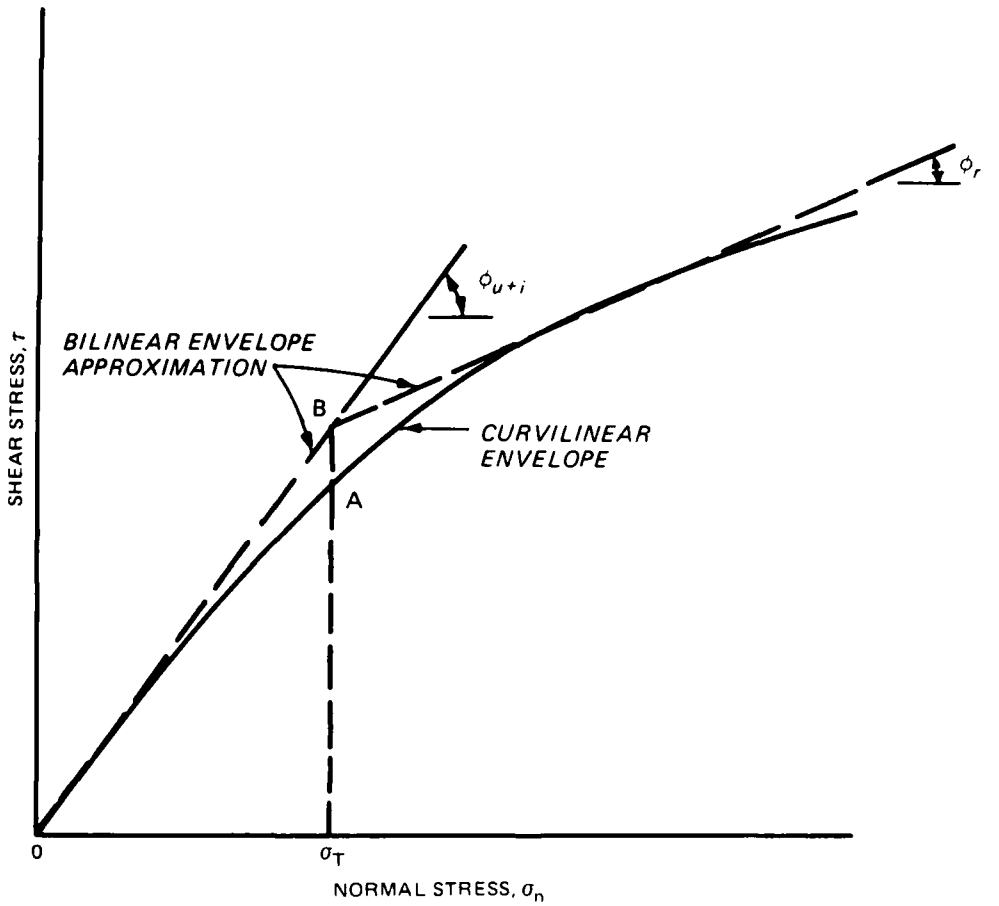

Figure 24. Typical curvilinear failure envelope for clean discontinuous rock with a bilinear envelope approximation superimposed

peaks. Conceptually there are three modes of failure--asperity override at low normal loads, failure through asperities at high normal loads, and a combination of asperity override and failure through asperities at intermediate normal loads. A bilinear approximation proposed by Patton (1966) and Goldstein et al. (1966) (discussed in paragraph 75) is based on the asperity override and failure through asperities modes of failure. A bilinear approximation is superimposed on the curvilinear envelope shown in Figure 24.

127. A discussion on failure modes must consider normal stress ranges. Before the onset of shearing opposing surfaces of a joint are matched (assumes no previous movement) and at low to intermediate normal stress ranges, the area of asperities in contact may be relatively large. Once shearing commences under a given overall normal stress (total area/total load), the contact area begins to reduce and causes the actual normal stress acting on individual asperities to increase. As the actual normal stress increases, the work required to override or dilate against the actual normal stresses will progressively exceed the work sufficient to fail through some asperities. Pure overriding of asperities probably does not occur except at zero normal load and then only if the maximum effective angle of asperity inclination is less than $90° - \phi$.

128. With increasing overall normal load, dilation will become completely suppressed and failure of asperities will occur without overriding when the actual normal stress acting on individual asperities approaches the unconfined compressive strength of the strongest asperities. Barton (1976) suggests that at sufficiently high normal stress levels discontinuous rock may exhibit a critical state of stress similar to intact rock although no supportive data are available.

129. The overall normal stress corresponding to complete surpression of dilation defines the stress level at which the break occurs in the approximate bilinear envelope as indicated by point B in Figure 24. The corresponding normal stress level, A , in Figure 24 cannot be detected by visual observation of the curvilinear envelope but can be observed with carefully controlled testing procedures. The overall normal stress level corresponding to points A and B (Figure 24) determines the stress level at which the bilinear failure criteria changes (from Equation 18 to 19) and determines the upper limit for which Barton's (Equation 21) curvilinear criterion is valid.

Shear deformation response

130. For normal stress intervals up to the unconfined compressive strength of the joint wall material, peak strength occurs at a shear deformation corresponding to peak dilation. Rough discontinuities typically exhibit a rapid rise in resisting shear stress up to a clearly defined peak followed by an irregular decline in resisting shear strength with additional shear deformation. Smooth discontinuities will also exhibit a rapid rise in resisting shear stress, but for comparable normal loads and material types the reduction in postpeak shear strength is less pronounced and smoother. Smooth discontinuities will also have smaller peak strength (and dilation) values.

Scale effects

131. Peak resisting stress versus normal stress failure envelopes are easily obtained from triaxial or direct shear tests on relatively small specimens. However, only rarely do tests on relatively small specimens adequately predict strength behavior of prototype material. This discrepancy between strength behavior of large and small failure modes is commonly referred to as scale effects and herein lies the difficulty in predicting design strengths. Pratt, Black, and Brace (1974) conclusively demonstrate scale effects from actual large- and small-scale in situ shear tests on jointed quartz diorite. Figure 25 shows the results of this study. As can be seen, peak shear stress versus normal stress failure envelopes decrease with increasing specimen size.

132. For a given normal load, two factors contribute to the observed strength--inclination angles of the asperities and the joint wall strength of the joint wall rock. Both the inclination angles (roughness) and strength are scale dependent. Patton (1966) and Barton (1971) found that as the joint length increases, the joint wall contact is transferred to the major and less steeply inclined asperities causing a decrease in effective asperity inclination angles as peak strength is approached. With the increased asperity contact area associated with major asperities, the joint wall compressive strength decreases in accordance with the compressive strength scale effects discussed in paragraph 108.

133. Bandis (1979) and Pratt, Black, and Brace (1974) demonstrated that the required shear displacement to generate peak strength is also scale

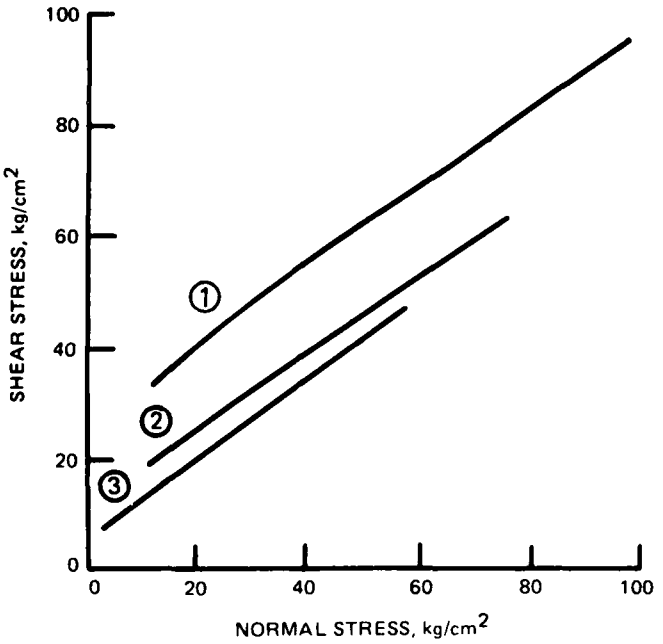

Figure 25. Failure envelopes developed from in situ tests on quartz diorite; each in situ envelope (1, 2, and 3) represents a series of tests on specimens with different joint orientations but having approximately the same joint area. Envelope 1 represents specimens with an average area of approximately 200 cm^2; 2, an average area of 1500 cm^2; and 3, an average area of 5000 cm^2 (after Pratt, Black, and Brace 1974)

dependent. The required displacement increases with increasing specimen size. In addition, as specimen size increases, the observed shape of the shear stress-shear displacement curves changes from brittle to elastic-plastic failure. Therefore, progressive-type failures are not a problem where the potential prototype mode of failure consists of a clean discontinuous rock.

Pore water effects

134. Most clean saturated joints are relatively free draining. Pore water pressures generated by compressive loads and shear loads dissipate rapidly. Therefore, most observed shear strengths selected for design are in terms of effective stress (no excess pore water pressure generated in a drained test). Partially healed joints or joints with boundary conditions which will not permit rapid dissipation of shear-induced pore water pressures are subject to time-dependent pore pressure effects. Triaxial and special direct shear devices (Goodman and Ohnishi 1973) can be used to evaluate pore water pressure effects but only for relatively small specimens. Since one-dimensional dilation of joints is scale dependent, the pore water pressures generated are no doubt also scale dependent. Very little research has been conducted into the scale dependency of load-induced pore water pressures. Time dependency of load-induced pore water pressures are, as a rule, not considered in design because the observed strengths are usually effective stress strengths due to rapid pore water pressure dissipation. Effective stress strengths of dilatant materials correspond to minimum resisting shear strengths (see Figure 9). Effective stress strengths also correspond to a condition of steady-state seepage (maximum uplift).

135. The presence of water does, however, significantly affect observed strength of joints. Unweathered joints typically have ϕ values 1 to 5 deg lower when wet than when dry. Weathered joints can exhibit a greater reduction in ϕ values depending on the degree of weathering. There are exceptions; Horn and Deere (1962) found that oven drying significantly lowered the friction angle of quartz, calcite, and feldspar at low confining pressures. As a rule most surfaces, however, are weaker when wet than when dry.

Friction characteristics

136. With the absence of asperities, all discontinuous rocks exhibit a fundamental frictional resistance to shear which is not scale dependent and

which establishes the minimum resistance to shear. For most fresh unweathered rock (rock mineral(s)), the frictional resistance, commonly referred to as the basic friction angle, is determined from shear tests on smoothly sawn specimens with relatively small shear displacements. Technical literature commonly use two symbols, ϕ_u and ϕ_b, to denote the basic friction angle. To avoid confusion this report will adopt the ϕ_u symbol. The basic friction angle for most rocks ranges from 23 to 35 deg (Barton 1974), and at moderate stress levels typical of hydraulic structures is not dependent on normal stress.

137. Another fundamental component of frictional resistance to shear is the residual friction angle, ϕ_r. The residual friction angle is commonly associated with weathered discontinuities or large shear displacements. Unless the zone of weathering is extensive, special specimen preparation, such as sawing, to provide a smooth surface will alter the weathered surface, resulting in unreliable test results. Therefore, residual friction angles are generally based on shear tests conducted on small specimens with unaltered joint wall surfaces. The amount of shear displacement required to establish ϕ_r is dependent on the surface roughness of the specimen tested.

138. The residual friction angle may be as low as 12 deg and in general $\phi_r < \phi_u$ for weathered discontinuities. For unweathered discontinuities, ϕ_r is approximately equal to ϕ_u. There are exceptions to this general rule. Coulson (1972) found that some unweathered rock (granite, basalt, gneiss, sandstone, siltstone, limestone, and dolomite) showed higher residual friction angles than basic friction angles, particularly at normal stresses greater than 500 psi. A similar behavior can be expected for low normal stress ranges typical of hydraulic structures for some low-strength rock. Higher residual friction angles for some unweathered rock can be explained by the fact that shear displacement will cause some rock shear surfaces to be coated with crushed material. The crushed material can result in higher residual friction than smoothly sawn surfaces.

Design Shear Strength Selection

Approach

139. In recent years a number of approaches have been developed and used successfully in selecting design shear strengths. Deere (1976) summarized three approaches: (a) use of traditional values of ϕ and c , (b) use of values obtained from test results, (c) use of rational values of ϕ and c based on evaluation of geological conditions and rock mechanics characterization of the surface roughness and weathering. An additional approach should be added to this list, (d) use of empirical shear strengths. While the chosen approach is largely a judgmental decision, some approaches may not be advisable for all levels of required confidence in the selected design shear strengths. Before discussing the four approaches the conceptual meaning of required level of confidence for clean discontinuous rock will be established.

Required level of confidence

140. The assessed confidence to be placed in design shear strengths for assurance against sliding of clean discontinuous rock surfaces must be considered as "high" or "very high" according to the discussions given in paragraphs 93-101. A "low" assessed confidence should be assigned only to preliminary designs. Table 5 presents a brief summary of the assessed confidence that might be assigned to selected design shear strengths for various rock types, weathering conditions, design use, and strength sensitivity. Assignment of confidence levels is a judgmental process. Table 5 is intended only as an illustrative example.

Traditional approach

141. Traditional values of ϕ and c were typically obtained from intact specimens which did not have a direct relationship to discontinuous rock strengths. In most cases, the strengths obtained were higher than those typical of discontinuities, particularly the cohesion c parameter. Recent advances in rock mechanics have led to the general discontinuation of this approach.

Testing approach

142. Design shear strengths based solely on test results have certain inherent limitations. While small-scale (NX to 6-in.-diam specimen size)

shear tests are relatively inexpensive, the tests do not address the problem of scale effects. Shear tests on large specimens attempt to address scale effects, but are expensive. With proper interpretation of test results, shear tests are a useful and necessary tool for selecting design shear strength. Table 6 briefly summarizes some of the more important advantages and disadvantages of triaxial and direct shear devices for testing clean discontinuous rock.

143. Small-scale shear tests applicable to clean discontinuous rock. At stress levels typical of hydraulic gravity structures most laboratory triaxial and direct shear devices are suitable for testing discontinuous rock. The primary requirement for any shear device used in testing discontinuous rock is provision for a constant normal load in direct shear tests or confining load in triaxial tests to accommodate corresponding normal vertical or lateral deformations.

144. Routine triaxial and direct shear tests on clean discontinuous rock specimens are considered to be drained (see paragraph 134), and therefore in conventional terminology are S tests. Because of wetting effects of joint walls (see paragraph 135) shear test specimens used for the selection of design shear strengths should be tested in a wet condition, preferably submerged. Failure envelopes (from which design shear strengths are selected) are usually based upon either peak strength or residual strength.

145. Large-scale shear tests applicable to clean discontinuous rock. Most large-scale shear tests are conducted in situ. However, large representative undisturbed specimens may be collected in the field and the tests conducted in the laboratory. In practice, nearly all large-scale shear tests are performed in direct shear devices. Because in situ direct shear tests are time-consuming, expensive, and usually conducted after construction excavation is in progress (delays final design), they are typically reserved for weak (severely weathered or filled) critically located geologic discontinuities. Zeigler (1972) offers an excellent summary of procedures and interpretation of data for in situ direct shear tests.

146. Most in situ direct shear tests have shear surface areas of less than 10 sq ft. The largest specimen known to be tested had a surface area of 1,000 sq ft (Evdokimov and Sapegin 1970). The cost of in situ testing

increases with increasing specimen size. Ideally, specimen size should be no larger than the size required to address the problem of scale effects. The International Society of Rock Mechanics (1974) recommends that test specimens should be 27.6 in. × 27.6 in. Barton (1976) concluded that the scale effect on the frictional strength of joints may die out when joint lengths exceed about 6 to 10 ft and that the scale effect on asperity failure appears to die out when sample size exceeds about 3 ft.

147. In general, test results converge down toward the prototype failure envelope with increasing specimen size. However, if the test specimen is not of sufficient size to account for scale effects, the geotechnical engineer and geologist are still faced with the problem of extrapolating prototype strengths. The problem of specifying specimen size must be weighed against the level of confidence that must be placed in the design strength values and cost of the test.

148. Interpretation of test results on natural joint surfaces. Failure envelopes over normal stress levels up to and in excess of the joint wall compressive strength are curvilinear. The degree of curvature depends on surface roughness, rock type, and degree of weathering. In most cases for normal stress ranges typical for design, linear approximations of curvilinear envelopes are adequate for design.

149. Triaxial specimens contain predetermined failure planes that rarely coincide with the theoretical failure plane for isotropic homogeneous material (inclination of the failure plane does not equal $45 + \phi/2$ deg). Failure envelopes should account for the actual angle of inclination at which the failure plane is inclined. Figure 26 illustrates the determination of linear failure envelopes and corresponding c and ϕ shear strength parameters from known angles of inclination, β_o, and p-q diagram a and α parameters (see paragraph 118). Equations 24 and 25 give the necessary trigonometric conversions:

$$\phi = \tan^{-1} \frac{\sin 2\beta_o \cdot \tan \alpha}{1 + \cos 2\beta_o \tan \alpha} \tag{24}$$

$$c = \frac{\tan \phi}{\tan \alpha} \cdot a \tag{25}$$

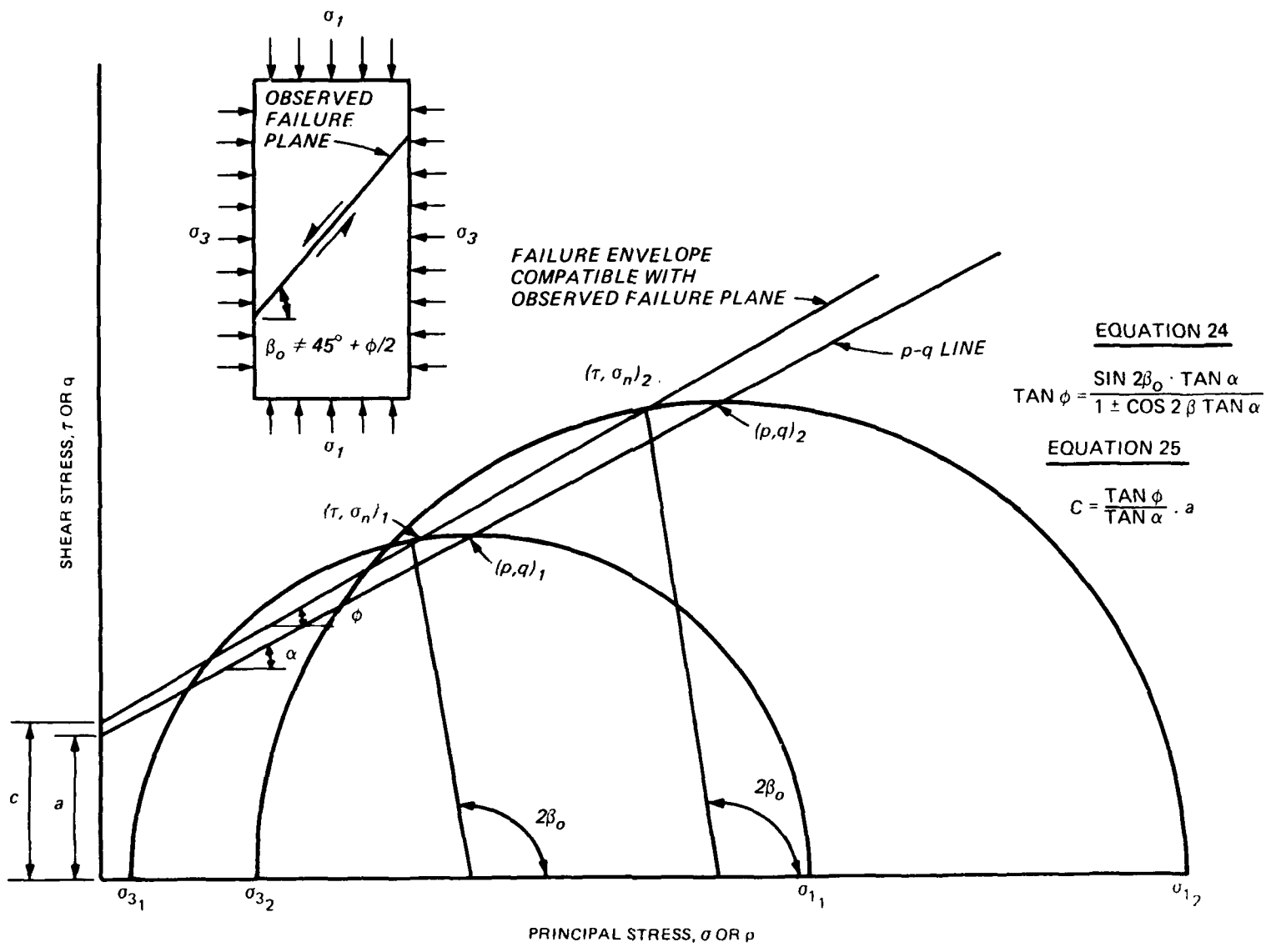

Figure 26. Relationship of failure envelope compatible with observed failure plane other than the theoretical failure plane and p-q diagram

150. Frictional restraint between the specimen and end caps may add new stress contributions on the joint that may require data corrections. Rosengren (1968) showed that corrections are necessary when friction coefficients between specimen and end caps are greater than 0.01. Rosengren (1968) derived equations which account for both frictional restraints and normal and shear stresses on the joint where β_o is not equal to the theoretical failure plane ($\beta_o \neq 45 + \phi/2$ deg).

151. Typical τ versus σ_n plots exhibit considerable scatter. Data scatter often obscures curvilinear trends. If a sufficient number of tests are conducted, upper and lower trends can be established similar to intact rock (see Figure 23). Experience has shown that at least nine tests are required to establish such trends.

152. If definite curvilinear trends are observed for which direct linear approximations cannot be readily made, considerations and procedures discussed in paragraph 79 to 91 can be used to extrapolate linear c and ϕ shear strength parameters for design. Extrapolation of linear parameters from curvilinear failure envelopes is particularly appropriate for large-scale specimen tests where the extra costs of such tests are justified by the need for rather precise determinations of prototype strengths.

153. Interpretation of test results for determining basic and residual friction angles. Failure envelopes from tests to determine basic and residual friction angles are typically linear over design normal stress ranges. Failure envelopes for direct and triaxial shear tests are obtained by methods discussed in the preceding paragraphs on natural joint surfaces. Although cohesion intercepts may occur, any contribution to shear strength due to cohesion should not be considered.

Rational approach

154. The rational approach is primarily based on sound engineering judgment which takes into account geological conditions and joint wall characteristics. In some cases, rational values of design shear strength may be selected by comparing the results of direct shear tests from other sites with similar rock types and joint wall characteristics. Another form of rational approach often employed today is to assume c is zero and increase either ϕ_r or ϕ_u depending on whether the joint wall is weathered or

unweathered by a rational estimate of the effective asperity angle of inclination (i angle in Equation 18). The ϕ_r or ϕ_u plus i angle approach requires some knowledge of the effective i angle which must be based on either judgment obtained from experience or actual measurements obtained from exposed discontinuities.

155. Tse and Cruden (1979) and Fecker and Rengers (1971) used numerical analysis of exposed joint surface coordinates to arrive at asperity roughness estimates. Such data can be obtained photogrammetrically as demonstrated by Ross-Brown, Wickens, and Marland (1973) and Patton (1966). The ratio of peak dilation to shear deformation is a measure of the true effective i angle. Effective i angles, then, may be obtained by measuring both dilation and shear deformation of joint blocks sliding across one another at low normal stress (weight of top block). Barton (1971) used this principle to develop his empirical shear strength criteria. The use of dilation principle to measure i can be accomplished in the laboratory using artificially simulated surfaces obtained from plaster, plastic, or rubber moldings of actual joint surfaces as suggested by Goodman (1974).

156. Deere (1976) states that the i value for most joints is often in the range of 5-15 deg but may range from 0-2 for planar joints, and 30-40 deg or greater for very irregular joint surfaces. The ϕ_r or ϕ_u plus i angle approach is only valid where the design range of normal stresses is within the initial linear (approximate) proportion of the failure envelope. As noted previously, the upper limit of the initial linear proportion is defined by the unconfined compressive strength of the joint walls for most rock. Hard crystalline rock and clay shales are the exception to this general rule. Crystalline rock can have transition stresses several times greater than the unconfined compressive strength. Stress levels for clay shales may reach a critical state similar to intact rock (point of zero τ/σ_n gradient) without first passing through the transition stress. With perhaps the exception of severely weathered joint surfaces or joints in very weak rock the transition stress will be greater than the typical upper range of design normal stresses.

Barton's empirical approach

157. One of the expense items associated with in situ testing of specimens of sufficient size to account for scale effects is the costs related to

the large hydraulic jacking systems and the necessary reaction requirements. The empirical shear strength relationship for unfilled rock joints developed by Barton (1971 and 1973) and refined by Barton and Choubey (1977) (Equation 21) provides an alternative to conventional in situ testing. Equation 21 contains three unknowns that must be evaluated--the residual friction angle ϕ_r, the joint roughness coefficient JRC, and the joint wall compressive strength JCS. As previously discussed, ϕ_r is not scale dependent and for unweathered surfaces can easily be evaluated by shear tests on small presawn specimens ($\phi_r \simeq \phi_u$). For weathered joint walls reasonable estimates of ϕ_r can be obtained from shear tests of small specimens containing the natural joint provided shear displacements do not extensively alter the weathered zone.

158. Both JRC and JCS are scale-dependent. Barton and Choubey (1977) describe simple procedures for determining full-scale (prototype) values of JRC and JCS. In addition, JRC may be estimated from numerical analysis of surface coordinates as demonstrated by Tse and Cruden (1979) and Fecker and Rengers (1971).

159. Estimating JRC. Barton and Choubey (1977) recommend that JRC be determined directly from tilt or push-pull tests. If the tilt or push-pull test specimens are of sufficient size, the JRC will be representative of the full-scale joint. Rearrangement of Equation 21 provides a simple equation for determining JRC from tilt tests:

$$JRC = \frac{\alpha^{o} - \phi_r}{\log_{10} (JCS/\sigma_{no})} \tag{26}$$

where

σ_{no} = normal stress induced by self weight of the upper sliding block ($\sigma_{no} = \gamma h \cos \alpha^{o}$; where h = thickness of upper block)

γ = rock density

$\alpha^{\bullet}$ = tilt angle at which sliding occurs

A similar rearrangement of Equation 21 provides an equation for JRC from push-pull tests:

$$JRC = \frac{\arctan \left[\left(\frac{T_1 + T_2}{N}\right)'\right] - \phi_r}{\log_{10} (JCS/\sigma_{no})} \tag{27}$$

where

T_1 = component of self weight of upper block acting parallel to the joint surface; T_1 is positive when acting with T_2 and negative when acting against T_2

T_2 = force required to slide upper block

N = component of self weight of upper block acting normal to the joint surface

160. Tse and Cruden (1979) demonstrated that small errors in estimating JRC could result in serious errors in predicting the peak shear strength from Equation 21. However, unlike mathematical profile analysis, tilt or push-pull tests result in JRC that exactly constitute the observed shear strength from the test for a given JCS value (ϕ_r can be determined accurately in most cases). Errors in predicting peak shear strength from Equation 21 because of errors in estimating JCS will be small due to the logarithmic formulation of the JCS term.

161. Estimating JCS . Barton and Choubey (1977) suggest that reasonable estimates of JCS can be made by the relationship between unconfined compressive strength of a rock surface, Schmidt hammer rebound number, and dry density of the rock developed by Miller (1965). The relationship is given in Equation 28:

$$\log_{10} (\sigma_c) = 0.00088 \ \gamma_d \ R + 1.01 \tag{28}$$

where

σ_c = unconfined compression strength of the rock surface in MN/m^2 (σ_c = JCS)

γ_d = dry density of rock in KN/m^3

R = rebound number

162. Schmidt hammer rebound numbers typically exhibit considerable scatter. Barton and Choubey (1977) recommend that the Schmidt hammer rebound number used in Equation 28 should be based on at least the average of the highest five readings out of ten. If JCS is determined from small specimens, scale reduction factors to account for scale effects should be applied to JCS . Barton and Choubey (1977) suggest reduction factors of 2.5, 5, and 10 depending on whether the rock is dense, moderately dense, or porous,

respectively. For example, if JCS is obtained from rebound readings on small specimens of dense rock such as basalt, the full-scale JCS would be JCS/2.5 . The automatic compensation of an underestimated full-scale JCS value with higher back-calculated value of JRC (and vice versa) from push-pull or tilt tests means that the correct estimation of an appropriate scale reduction factor is not as critical as might be expected.

163. Peak strength predictions. Barton's empirical approach is a relatively new development. Documentation of predicted versus prototype performance is sparse. However, Barton and Choubey (1977) believe that errors in arctan τ/σ_n are unlikely to exceed ± 2 deg provided the JRC is obtained from a sufficient number (4 or 5) of tilt or push-pull tests on large blocks and that the JCS is obtained from Schmidt hammer rebound readings as discussed above.

164. Conservative estimates of peak shear strength may be made by assuming a zero cohesion intercept and assuming the friction angle to be equal the arctan τ/σ_n equivalent to the maximum design stress as illustrated in Figure 27. Barton's curvilinear envelope in Figure 27 is representative of a rough joint surface (JRC = 20) with weak wall rock (JCS = 100 tsf).

165. The normal stress σ_n in Barton's equation (Equation 21) is in terms of effective stress. Design shear strengths selected from Barton's curvilinear criteria must be based on effective normal stresses. As discussed previously, clean discontinuous rock is free draining (except for confined systems) which implies that long-term drained conditions control design (maximum uplift). In conventional hydraulic structure design drained effective stresses are obtained by subtracting uplift pressures from the total stresses.

Strength selection

166. Scale effect is the primary difficulty in selecting design shear strengths for clean discontinuous rock. The geotechnical engineer and geologist seldom know with certainty that the strengths selected for design are representative of prototype conditions. Conservative strengths are typically employed in design because of this lack of certainty. Generally, the greater the level of confidence required of design strengths the greater the conservatism. The degree of uncertainty can be reduced with shear tests on increasingly larger specimens, but only with ever increasing cost.

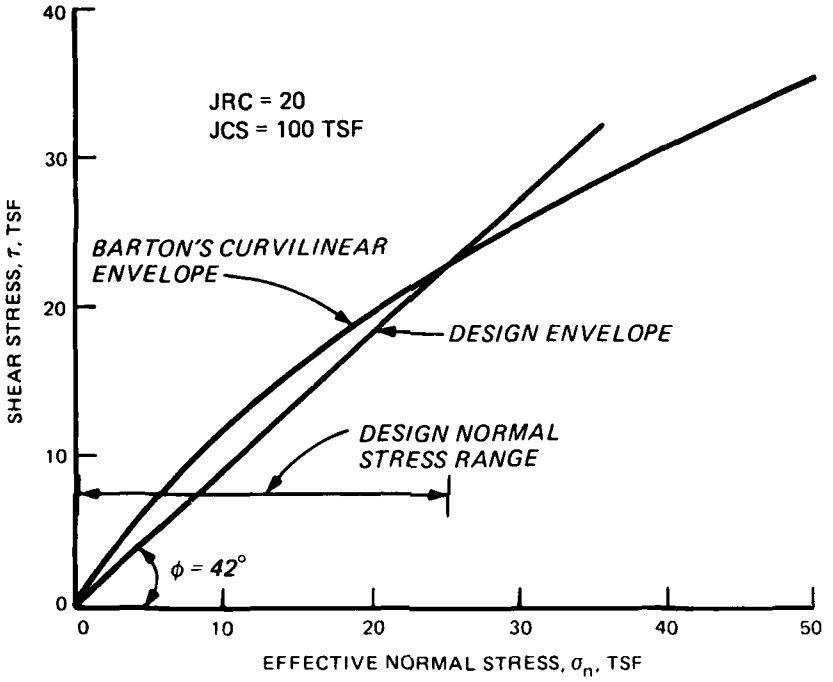

Figure 27. Design failure envelope from Barton's empirical curvilinear envelope

167. With a minimum of expense upper and lower limits of likely prototype strengths can be obtained. Upper limits can be established from small-scale tests on natural joint surfaces. Lower limits of strength come from determination of the basic or residual strength. It makes little sense to expend large sums of money to reduce prototype strength uncertainty if lower limit strengths are adequate for stability (reflects the importance of sensitivity analysis).

168. The preceding paragraphs discussed in some detail alternative approaches commonly used in design. Perhaps the optimum cost approach in selecting design strengths (in lieu of large-scale tests) would consist of a balanced design where strengths selected from one approach are checked and balanced against strengths from another approach. Table 7 summarizes various alternative approaches for selection of c and ϕ shear strength parameters according to the assessed confidence required of the selected parameters. Examples of assessed confidence as defined in paragraph 95 are given in Table 5. Table 7 is intended only for general information. Special requirements of specific design cases may require modification of the alternative approaches. The column entitled "Comments" attempts to summarize the limitation and consequence of each approach. It is important to note that the selection of test specimens is not discussed in Table 7. See paragraph 123 for comments.

PART VI: SELECTION OF DESIGN SHEAR STRENGTHS FOR FILLED DISCONTINUOUS ROCK

Definition of Filled Discontinuous Rock

169. The term "filled discontinuities" is an ambiguous term that is applied to all discontinuities with seams or layers of material weaker in strength than the parent rock. The range of filler materials covers the total spectrum of soil to weathered rock. Of all the possible materials the broad group of material labeled "clay" is the most troublesome and most frequently encountered.

170. The origin of the filler material is an important indicator of the type of material found and the strength characteristics of the joint. The finer products of weathering or overburden may be washed into open water conducting discontinuities and with time precipitate out as a weak normally consolidated clay with a high water content (sands and silts may also be deposited in this manner). In other cases the by-products of weathering may remain in place after weathering and result in a weak interface between two dissimilar rock types.

171. In sedimentary rocks filler material may consist of alternating seams of clay deposited during formation. In igneous and metamorphic rock the filler may result from alterations, for example, the alteration of feldspar to clay. Filler material can also be generated by crushing of parent rock surface due to tectonic and shear displacements. The crushed material may be subject to weathering and alteration.

Failure Mechanisms

Failure modes

172. Failure modes of filled discontinuities can range from those modes of failure associated with all soils to modes of failure associated with clean discontinuities. Because of the vast range of possible failure modes any discussion of failure mechanisms must be idealized. A mechanistic examination requires at least a brief discussion of four factors influencing their

strength behavior. These factors are: (a) thickness of the filler material, (b) material type, (c) stress history, and (d) displacement history.

Thickness of filler material effects

173. A large number of in situ direct shear tests have been conducted for various projects with the expressed purpose of defining shear strengths of filled discontinuities (Zeigler 1972). Despite the relatively large volume of data, there appears to be very little basic research to expand the state of the art. Most research has addressed the problem of the interaction between joint walls and filling material. Kanji (1970) showed that a smooth rock/soil interface could have a lower shear strength than the soil tested alone. Kutter and Rautenberg (1979) demonstrated that the actual shearing process is a combination of shear movements along the filler rock boundary and within the filler. Goodman (1970) found that for idealized regular sawtooth surfaces cast in a plaster-celite model material the thickness of the filling needs to be at least 1.5 times greater than the amplitude of the undulations for the strength of the composite sandwich to be as low as the filler alone. Barton (1974) suggests that for real joint surfaces the filler thickness should be on the order of 2.0 times greater than the amplitude of the undulations before filler strength fully controls.

174. The four grossly simplified shear characteristics examples given by Barton (1974) will help demonstrate the complexities associated with shear behavior with respect to filler thickness.

a. Almost immediate rock/rock asperity contact. Shear strength will be very little different from the unfilled strength because the rock/rock contact area at peak strength is always small. Normal stresses across the contact points will be sufficiently high to dispel the clay in these critical regions. Slight reduction in dilation component of peak strength may be more than compensated by "adhesive" action of the clay in zones which would be voids during shear of the unfilled joints. Dilation due to rock/rock contact will cause negative pore pressures to be developed in filling if shearing rate is fast.

b. May develop same amount of rock/rock contact as in a, but required displacement will be larger. Dilation component at peak strength greatly reduced since new position of peak strength is similar to position of residual strength for unfilled joints. Similar "adhesion" effect as a. Less tendency for negative pore pressures due to reduced dilation.

c. No rock/rock contact occurs anywhere, but there will be a build-up of stress in the filling where the adjacent rock asperities come closest together. If the shearing rate is fast, there will be an increase in pore pressures (normally consolidated soils) in these highly stressed zones and the shear strength will be low. If, on the other hand, the shearing rate is slow, consolidation and drainage will occur, the drainage being directed towards the low stress pockets on either side of the consolidating zones.

d. When the discontinuity filling has a thickness several times that of the asperity amplitude, the influence of the rock walls will disappear. Provided the filling is uniformly graded and predominantly soil the shear strength behavior will be governed by soil mechanics principles.

175. In general, the thicker the filler material with respect to the amplitude of the joint surface undulations, the less are the effects of scale associated with discontinuous rock.

Filler material type

176. Soil consists of discrete weakly bonded particles which are relatively free to move with respect to one another. Classification systems divide soil into individual groups. The Unified Soil Classification System, the widely-used system, divides soil into groups according to gradation, grain size, and plasticity characteristics. Although a gross simplification, soils are frequently divided into two broad groups: fine-grained cohesive soils and coarse-grained cohesionless soils. Fine-grained soils are more frequently found as fillers in discontinuous rock and are more troublesome in terms of stability problems. Therefore, fine-grained material (commonly referred to as clay in this report) will be discussed in greater detail than coarse-grained materials (commonly referred to as sands in this report).

Stress history

177. Stress-deformation response behavior of soils varies depending on soil characteristics. The past stress history of the material is a key indicator to stress-deformation behavior, with corresponding effects on shear strength, for a given loading condition. Consequently for this discussion it is convenient to separate soils into two general categories, normally consolidated and overconsolidated soils.

178. Normally consolidated soils. Normally consolidated soils are defined as those soils which have never been subjected to an effective

AD-A137 225 DESIGN OF GRAVITY DAMS ON ROCK FOUNDATIONS SLIDING STABILITY ASSESSMENT B..(U) ARMY ENGINEER WATERWAYS EXPERIMENT STATION VICKSBURG MS GEOTE.. G A NICHOLSON 2/2

UNCLASSIFIED OCT 83 WES/TR/GL-83-13 F/G 13/13 NL

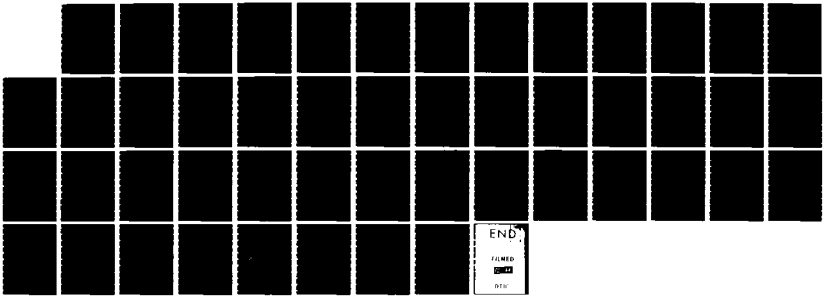

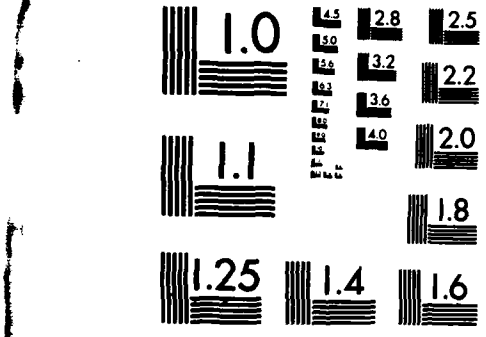

pressure greater than that which corresponds to the present overburden. Two behavioral characteristics are typical of normally consolidated materials. First, normally consolidated materials tend to consolidate or become more dense when subjected to shear strains under drained conditions. Secondly, shear stress-deformation curves are commonly of the elastic-plastic or strain-hardening type as illustrated in Figure 10. As a rule, normally consolidated materials are not susceptible to progressive failure.

179. Peak strength (elastic-plastic behavior) or limiting strain (strain-hardening behavior) failure envelopes, from which design shear strengths are selected, are typically linear for clays over normal stress level typical of design. Peak strength failure envelopes for sands and gravels tend to be curvilinear at high normal stresses due to the increase in the percentage of grains that are crushed as failure is approached. However, at normal stress levels typical of design, sand and gravels also exhibit linear envelopes. Consolidated undrained shear strengths are lower than consolidated drained strengths (Figure 9) because of positive pore pressures generated by the tendency for the solid phase to compress under load.

180. Overconsolidated soils. A soil is said to be overconsolidated if it has ever been subjected to an effective pressure in excess of its present effective overburden pressure. In the context of this report overconsolidated soils refers to those soils which undergo dilation (increase in volume) at failure under drained conditions. Typically, this category of materials is associated with clays and shales that have overconsolidation ratios in excess of 4 to 8 (approximate) and with dense silts, sands, and gravels. It must be recognized that there is a broad spectrum of materials between normally and overconsolidated materials as defined herein. The previous brief discussion on normally consolidated materials and the following discussion on overconsolidated materials are intended to illustrate the significant strength-related characteristics at two extreme ends of the spectrum.

181. Peak strength failure envelopes, from which design strengths are sometimes selected, are usually at least slightly curvilinear. However, over typical design normal stress ranges, adequate design strengths can be obtained from linear approximations. Because of negative pore pressures generated by the tendency for the solid phase to dilate under load, undrained shear

strengths are higher than drained strengths.

182. Shear stress-deformation response behavior is that of strain softening (brittle failure) as illustrated in Figure 10. The percentage of strength loss from peak to residual is less severe in sands and gravels than in silts and clays. In moving from peak to residual strength the cohesion intercept, c , of overconsolidated silts and clays decreases from a measurable value to a very small value or zero. Sands and gravels are cohesionless. Skempton (1964) observed that the angle of internal friction, ϕ , also decreases by as much as 10 deg or more for some clays.

183. All brittle materials are subject to progressive failure if applied stresses exceed peak resisting stresses along any point of the potential failure surface. However, some groups of clays and clay shales are particularly susceptible to progressive failure. In addition to strain softening, other primary factors causing strength reduction are fissures, weathering, latent strain energy, creep, and stress concentrations. These factors may act independently or together to cause strength reduction.

184. Some heavily overconsolidated clays contain a network of hair cracks. The removal of overburden, either by excavation or by geological processes, causes an expansion of the clay; thus some of the fissures open allowing water to enter. Water softens the clay adjoining these fissures and with time the mass is transformed into a softened matrix containing hard cores. The time required for the softening process is related to fissure spacing as well as other factors. The further apart the fissures are, the longer will be the time required for significant softening and associated reduction in strength. Fissures may also generate scale effects similar to intact rock.

185. Physical and chemical changes within the parent material are the two main causes of weathering. Physical weathering processes such as freeze-thaw cycles, temperature changes, increase in water content, and wetting and drying cycles are effective in breaking down the structure of the clay by generating strain. Increases in water content are the primary source of physical weathering under hydraulic structures.

186. There are two main types of chemical weathering in clay and clay shales. Solution is usually the first form of chemical weathering to occur.

Solution of cementing agents such as calcite and carbonates results in subsequent strength losses. Oxidation to form new chemical compounds within the soil mass can be accompanied by large volume changes; e.g., black shales usually exist in a reducing environment and contain appreciable amounts of pyrite. Upon exposure to water and air the pyrite reacts with the water and oxygen to form melanterite and sulfuric acid as a by-product. This chemical reaction results in a unit volume increase of over 500 percent. Sulfuric acid and water can react with calcite to form gypsum with a resulting 60 percent volume increase. Generally, soils containing magnesium, iron, or calcium are most susceptible to acid attack.

187. Most clays retain a certain amount of recoverable strain energy which will cause initial rebound when a given consolidation pressure is relieved. The amount of recoverable strain energy depends on the consolidation pressure and the properties of the clay. Some overconsolidated clays and clay shales can retain latent strain energy upon destressing. The extent to which latent strain energy is retained or released is dependent upon the strength of interparticle bonds and the processes acting to break the bonds. The release of strain energy, whether initial or latent, generates strain in the soil. If the strain levels are sufficient to strain past peak strength, strain softening will occur. Initial rebound strain can be accounted for in routine testing procedures. At the present time, the release of latent strain energy and its effects on shear strength cannot be determined with any degree of confidence. In general, the greater the plasticity and the greater the overconsolidation pressure, the greater will be the probability of progressive failure.

188. Laboratory observation of overconsolidated clay by Nelson and Thompson (1977) supports the possibility that resisting stresses can pass to the residual side of the stress-strain curve without ever reaching peak strength. This observation is explained by the occurrence of irreversible time-dependent deformations recognized as creep. Plastic creep deformations occur across the particle bonds resulting in their gradual deterioration.

189. Stress concentrations can act on the microscopic level or prototype level to cause overall reductions in average resisting shear strength in brittle materials. Hairline fissures typical of most overconsolidated clays

are the primary source of stress concentrations on the microscopic level. Thin seams of anomalous materials interbedded with overconsolidated clays and abrupt changes in foundation shapes are the primary sources of prototype stress concentrations.

Displacement history

190. An important consideration in determining the strength of discontinuities filled with fine-grained cohesive materials is whether or not the discontinuity has been subjected to recent displacement. If significant displacement has occurred, it makes little difference whether the material is normally or overconsolidated since they will no doubt be at their residual strength. Close to the surface there may be instances where silty-clay materials have subsequently been washed into the voids after displacement. These zones will not be at their residual strength. Nevertheless, the shear strength on the whole will be low, particularly in view of the additional softening that may occur due to increased water content. If displacement has not occurred, the filler material, whether normally consolidated or overconsolidated, will assume its characteristic behavior as previously discussed. Figure 28 presents a brief summary of the type of discontinuity, displacement history, and filler material stress history.

Design Shear Strength Selection

Approach

191. The selection of design shear strength parameters for filled discontinuous rock in the current state of practice is almost exclusively based upon results of shear tests. Because of the complex failure mechanisms and the potentially wide variations in strength behavior associated with filled discontinuities rational and empirical approaches commonly used for clean discontinuous rock are not readily adaptable to filled discontinuities.

Required level of confidence

192. Like clean discontinuities, the assessed confidence to be placed in design shear strengths for filled joints must be considered as "high" or "very high" according to the discussions given in paragraphs 93 to 101. A "low" required level of confidence should be assigned only to preliminary designs.

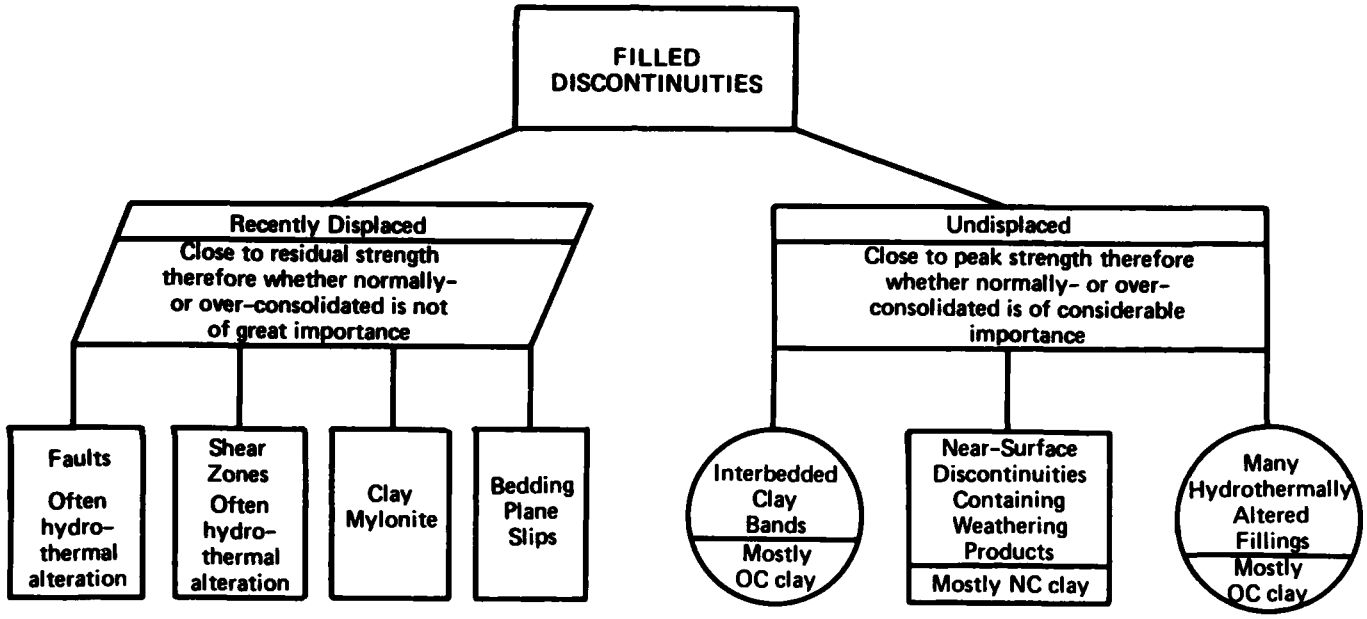

Figure 28. Simplified division of filled discontinuities into displaced and undisplaced and normally consolidated (NC) and overconsolidated (OC) categories (after Barton 1974)

Table 8 presents a brief summary of assessed confidence that might be assigned to selected design shear strengths for various filler material types, design use, and sensitivity. Table 8 is intended only as an illustrative example.

Shear tests

193. Shear tests are the only viable means of modeling the strength-dependent complex failure mechanisms associated with joint walls, filler material types, time-dependent pore pressure effects, and joint wall and filler material interactions. All four factors contributing to the failure mechanisms of filled joints are, to some extent, scale-dependent. While shear tests on large specimens attempt to address scale effects at increasing expense with specimen size, pore pressure control is difficult. Small laboratory shear tests are inexpensive and pore pressure control and measurement is a matter of routine, but small tests do not address scale effects. The appropriate shear testing program from which design shear strengths are selected should consider the limitation and applicability of the tests.

194. Small-scale shear tests. Most laboratory triaxial and direct shear devices are suitable for testing filled discontinuous rock. Because of the potential for joint wall dilation or compression, provisions must allow for a soft normal load (paragraph 143).

195. Triaxial and direct shear tests on filled discontinuous rock specimens may be unconsolidated-undrained (Q tests), consolidated-undrained (R tests or $\bar{R}$ with triaxial), or consolidated-drained (S tests). Test specimens may be saturated or partially saturated. In soils, drainage and saturation conditions are dictated by the sequence of prototype loading conditions and soil moisture content with respect to time. Design parameters are often interpolated from the Q , R , and S test conditions. However, small laboratory tests rarely model failure of filled joints. For this reason small tests on filled joints are used primarily to establish upper and lower bounds of design strength with drainage conditions chosen to reflect the filler material's minimum strength behavior.

196. Large-scale shear tests. Large-scale shear tests suitable for testing clean discontinuous rock specimens (discussed in paragraphs 145 to 147) are also suitable for testing filled joints. Unfortunately, the most commonly used test, in situ direct shear, involves several experimental

problems. A particular difficulty referred to by Drozd (1967) is that soft plastic fillings tend to be squeezed out of the joint during the course of a test. Squeezing can also occur during small specimen laboratory direct shear tests. Displacement of the filler is not likely to occur in the prototype case due to the continuous upper and lower rock surfaces. Another problem is the appropriate rate of shear displacement and degree of filler saturation to be compatible with Q , R , or S shear tests. The degree of saturation of in situ test specimens cannot generally be increased above undisturbed levels for practical tests. The rate of shear displacement can be controlled with proper choice of shear equipment.

197. Pore pressure control of large in situ direct shear tests has for the most part been neglected in the past. The case histories of in situ testing of both clean and filled discontinuous rock summarized by Zeigler (1972) indicated that of all the testing programs on filled joints only one program (James 1969) considered the drainage conditions of the filler material. There are three primary reasons for this neglect. First, pore pressures cannot be monitored in in situ direct shear tests. Second, shear loads are commonly applied with large hand-operated hydraulic jacks which provide, at best, crude control of shear deformation rates. Finally, test time (drained tests) to failure can be lengthy thus substantially increasing costs.

198. Basic research relating to times to failure of large filled joint specimens is lacking. In practice times to failure are based on approximations. Undrained in situ tests can be accomplished by ensuring shear rates are so fast as not to allow dissipation of pore water but slow enough to allow uniform transfer of shear stress over the failure area. Upper limits of shear displacement for large undrained in situ tests are on the order of a few hours to peak failure.

199. Time to failure for in situ drained tests on quartzite blocks along mudstone seams at Muda Dam reported by James (1969) were determined according to Bishop and Henkel (1957). Bishop and Henkel's method relates time to drained failure to the coefficient of consolidation and boundary drainage conditions by the following equation:

$$t_f = \frac{20h^2}{\eta c_v} \tag{29}$$

where

t_f = time to failure

h = one half of the height of the sample

η = a factor depending upon drainage conditions at the sample (filler) boundaries

c_v = coefficient of consolidation

The value of η is 0.75 for drainage along either top or bottom and 3.0 for drainage along both top and bottom. The average thickness of the filler material is equivalent to the height of the specimen. Boundary drainage factors, η, have been determined for radial and combinations of radial and top-bottom drainage conditions, but only for circular specimens.

200. Applications of Equation 29 have obvious limitations. The filler material must be confined by a porous rock (to permit drainage) on at least the top or bottom side. The filler must be sufficiently thick to obtain an undisturbed consolidation test sample for determining the coefficient of consolidation. Consolidation theories of soils do not account for possible joint wall contacts. The displacement required for failure must be estimated to determine the appropriate displacement rate. Because displacement at failure is dependent on both joint wall and filler material characteristics as well as filler thickness it may be necessary to shear one specimen to failure to form a basis for estimating displacement prior to commencement of the testing program. Installation of internal drains will decrease the time to failure, but techniques to predetermine their effectiveness are not available.

201. In an effort to reduce costs associated with in situ testing some investigators have conducted two- or three-stage tests on a single test specimen. Multiple-stage tests should only be considered for those joints containing nonsensitive normally consolidated filler materials with the specimen recentered after each shear cycle. As a rule, stage tests result in conservative peak strengths for all but the initial shear cycle.

202. Definition of failure. Definitions of failure used to select strengths from individual tests in order to construct design failure envelopes

are highly dependent upon the characteristics of the filler material and the required level of confidence in the selected strengths. In general, failure of filled joints containing normally consolidated cohesive materials and all cohesionless materials is defined by peak strengths. Failure of joints containing overconsolidated cohesive material of low plasticity is generally defined by either peak or ultimate strengths. Failure of joints containing overconsolidated cohesive materials of medium to high plasticity is defined by ultimate strength, peak strength of remolded filler, or residual strength depending on material characteristics.

203. Interpretation of test results. Interpretation of test results is essentially the same as the interpretation of test results on clean joints discussed in paragraphs 148 to 152. Data scatter is strongly related to the thickness of the filler material. As a rule, scatter increases with decreasing thickness of filler material. The number of tests should be sufficient to establish scatter trends.

204. Advantages and disadvantages of shear devices. Table 9 summarizes some of the advantages and disadvantages of shear devices commonly used for testing filled discontinuous rock specimens.

Strength selection

205. Design shear strengths of thickly filled discontinuities with filler thickness greater than approximately 1.5 to 2.0 times the amplitude of asperity undulations should be selected according to the principles of soil mechanics. As a rule, design strength selection is based on the results of small laboratory triaxial and/or direct shear tests on filler material specimens. Interpretation to obtain design strengths from Q , R , and/or S tests should be in accordance with expected prototype loading and pore pressure conditions; EM 1110-2-1902 (Department of the Army, Office, Chief of Engineers 1970b) offers guidance in interpretation. Although EM 1110-2-1902 applies directly to the stability earth- and rock-fill dam embankments, the principles, as outlined, are equally applicable to the stability of gravity structures.

206. The selection of design shear strengths for thinly filled discontinuous rock (filler thickness less than 1.5 times the amplitude of asperity undulations) is complicated by joint wall scale effects, filler material

behavioral characteristics, and interaction between filler material and joint walls. Because of these complications the geotechnical engineer and geologist seldom know with certainty that the strengths selected for design represent prototype conditions. As is the case with clean joints, the degree of uncertainty can be reduced with shear tests on increasingly larger specimens. Conversely, design strengths selected from small-scale tests results dictate conservative estimates to account for the uncertainty of prototype representation.

207. Test specimen drainage conditions (Q , R , or S) for tests on thinly filled joints usually reflect either critical material strength response or minimum strength response. The reasons for selecting drainage conditions corresponding to either the critical or minimum material strength response are twofold. First, the expense associated with large in situ tests restricts the number of tests. Case histories of in situ filled joints summarized by Zeigler (1972) indicate that the number of tests per testing program ranged from 1 to 12 with a median number of 3 to 4. If only a few tests can be run, most investigators will specify test conditions corresponding to a critical prototype condition of long-term stability with maximum uplift even though such a condition might be short-term in occurrence. For example, a short-term surcharge condition corresponding to maximum flood elevation in the reservoir would create a temporary redistribution of foundation stresses under partially consolidated and partially drained conditions with no appreciable increase in uplift. An optimum design would involve shear strengths selected from interpretation between both consolidated drained (S tests) and unconsolidated undrained (Q tests) tests (requires a greater number of tests) as described in EM 1110-2-1902 (Department of the Army, Office, Chief of Engineers 1970b). In the optimum design case uplift would not be increased above the level compatible with presurcharge conditions. A critical design would involve shear strengths selected from consolidated drained tests (assumes complete consolidation and zero shear-induced pore pressures) with maximum uplift compatible with the maximum flood elevation conditions substituted into the stability equations.

208. Drainage conditions for small laboratory tests on thinly filled joint specimens usually correspond to a condition of minimum filler material

strength response compatible with expected material behavior. Joint wall contacts of small test specimens result in higher observed strengths than large in situ tests or likely prototype strengths. Underwood (1964) reported an average decrease in ϕ values of 6 deg from small laboratory direct shear tests (ϕ = 14 deg) to large in situ tests (ϕ = 8 deg) conducted on thin bentonite seams in chalk. The specification of specimen drainage conditions compatible with minimum strength response attempts to partially compensate for the unconservative tendencies due to joint wall scale effects.

209. Table 10 attempts to summarize various alternative approaches for selection of c and ϕ shear strength parameters according to the assessed confidence required of the selected parameter. Examples of assessed confidence as defined in paragraph 100 are given in Table 8. Because the type of shear test and the selection process are highly dependent upon filler materi type and displacement history, alternative approaches are also listed accord ing to filler material type. Table 10 is intended only for general information. Special requirements of specific design cases and/or material behavior characteristics may require modification of the alternative approaches. The column entitled "Comments" attempts to summarize the limitations and consequence of each approach. It is important to note that the selection of test specimens is not discussed in Table 10. See paragraph 123 for comments.

PART VII: CONCLUSIONS AND RECOMMENDATIONS

Conclusions

Limit equilibrium

210. Limit equilibrium methods are currently the most accepted way of assessing sliding stability. All limit equilibrium methods of stability analysis use four basic assumptions, three of which are fundamental to all methods. The fourth assumption consists of a necessary conditional assumption required for static equilibrium solution.

211. Fundamental assumptions. The three fundamental assumptions common to all limit equilibrium methods of analysis are the same definition of the factor of safety, elastic-plastic failure, and that the calculated factor of safety is the average factor of safety for the total slip surface.

212. Limit equilibrium methods define the factor of safety as the ratio of the shear strength that can be mobilized to the shear strength required for equilibrium. The fundamental definition relates the factor of safety to the least known requirement, which is shear strength of the founding material.

213. Limit equilibrium methods involve the implicit assumption that the stress-strain characteristics of the founding material behave as elastic-plastic materials. The assumption of elastic-plastic behavior is necessary because there is no consideration of strains in the methods and no assurance that the strains will not vary significantly from point to point along the potential failure surface.

214. The calculated factor of safety for all limit equilibrium methods is the average factor of safety for the total potential failure surface. In addition, the average shear strength and average normal stress distribution for each segment of the potential failure surface are used in the solution for the factor of safety.

215. Conditional assumptions. In all limit equilibrium methods the number of static equilibrium equations available is smaller than the number of unknowns involved. Conditional assumptions are required to either reduce the number of unknowns or provide an additional equation or condition to permit equilibrium solution. The limit equilibrium equations given in this report

(Equations 13 and 15) reduce the number of unknowns by assuming that the vertical side forces acting between wedges are zero.

Validity of limit equilibrium

216. Extensive experience in slope stability assessment has demonstrated the effectiveness and reliability of limit equilibrium methods. Because the same principles and failure mechanisms applicable to slope stability are also applicable to the potential sliding of mass concrete gravity structures, limit equilibrium methods for assessing the stability of gravity structures are a valid approach.

217. Methods that consider complete force and moment equilibrium (with conditional assumptions) offer the more rigorous solutions for the factor of safety. However, these solutions are tedious and in some cases do not converge. The equations given in this report are based on the conditional assumption of zero side forces between slices. The equations generally result in slightly conservative (on the order of 5 to 10 percent), calculated factors of safety. Errors on the order of 5 to 10 percent are well within the permissible range of practical engineering.

218. Limit equilibrium methods mathematically evaluate the relative state or degree of equilibrium between forces resisting sliding and the forces acting on a body to cause sliding. The calculated factor of safety measures the relative state of equilibrium. Acting forces can be determined rather accurately. Resisting forces that can be developed are a function of c and ϕ shear strength parameters. The c and ϕ parameters provide the necessary link between the stress-strain-strength characteristics of the founding material and the mathematical state of equilibrium. The selection of shear strength parameters representative of prototype stress-strain-strength characteristics represents the greatest uncertainty in limit equilibrium assessments of sliding stability.

Prerequisites for selecting shear strength

219. The optimum design of new structures or evaluation of existing structures requires the close coordination of an experienced team. At a minimum such a team should consist of a design engineer, a geotechnical engineer, and a geologist. Although the geotechnical engineer is typically charged with the responsibility of the actual strength selection process, the

design engineer and geologist must provide vital information and services prior to and frequently during the actual selection process.

220. The geologist in coordination with the geotechnical engineer is responsible for the field investigation. Field investigations define the potential modes of failure to include material types from which the geologist and geotechnical engineer select and obtain representative specimens. Limit equilibrium assessments are valid only if all modes of potential failure have been defined and thoroughly investigated.

221. The design engineer provides information concerning the loads acting on and generated by the structure. Frequently this information may require inclusion of the time rate of load occurrence. Shear tests on specimens representative of potential failure modes attempt to model prototype loading conditions.

222. Prior to the actual strength selection process for design, the geotechnical engineer must have a fundamental appreciation of several factors. These factors are: (a) available shear tests and approaches used to model prototype conditions, (b) anticipated material stress-strain-strength characteristics, (c) failure criteria that may be used to establish failure envelopes representative of resisting strength that can be developed along the potential slip surface, and (d) techniques for linear interpretation of any nonlinear failure envelopes.

223. A sensitivity analysis should be performed prior to any strength selection process. Such an analysis is important in establishing the range of resisting shear strength required for stability. The analysis must be a team effort. The design engineer has knowledge as to the loading conditions and structural geometry required for design consideration other than sliding stability. The geotechnical engineer and geologist have knowledge as to the geometry of potential failure modes. The range of shear strengths required for stability and a fundamental appreciation of shear tests and approaches available to model expected prototype stress-strain-strength material characteristics form a basis for judging the level of confidence that must be placed in selected design strengths.

Selection of design shear strengths

224. The range of possible resisting shear strengths that can be

developed by a rock mass is large. The geotechnical engineer has at his disposal a variety of alternative approaches from which to predict prototype shear strengths. Most approaches are based on shear tests that attempt to model prototype loading conditions. Unlike soils, rock mass strengths are dependent on the size of the test specimens, particularly discontinuous rock. The relationship between strength and test specimen size is commonly referred to as scale effects. Scale effects are the primary difficulty in selecting design strengths representative of prototype strengths. As a rule, the degree of uncertainty in selected strengths can be reduced with increasing specimen size, but only with increasing cost.

225. To be cost effective the approach chosen for design strength selection must consider the assessed confidence in the selected design strengths relative to the actual prototype strengths. It is not cost effective to specify a costly testing program on large-scale specimens in an attempt to more closely define prototype strength when an easily obtained, but conservative, design strength may provide adequate assurance against sliding instability. In general, increases in assessed confidence required of design strengths reflect either an increasing effort and expense to more precisely define prototype strengths or increasing conservatism in selected strengths to account for the uncertainty of actual prototype strengths.

226. The alternative approach chosen to select design strengths is also dependent upon the material stress-strain-strength characteristics. The geotechnical engineer responsible for selecting design strengths must have an appreciation of the way in which material fails in order to judge which approach/approaches best model stress-strain-strength characteristics. Figure 29 shows a simplified flowchart of factors to consider in selecting design shear strengths.

Recommendations

227. Accurate prediction of shear strength is perhaps the most important aspect in assessing the sliding stability of gravity structures. Significant advances have been made in recent years toward improving the state of the art for predicting shear strength. Nevertheless, there remain areas where

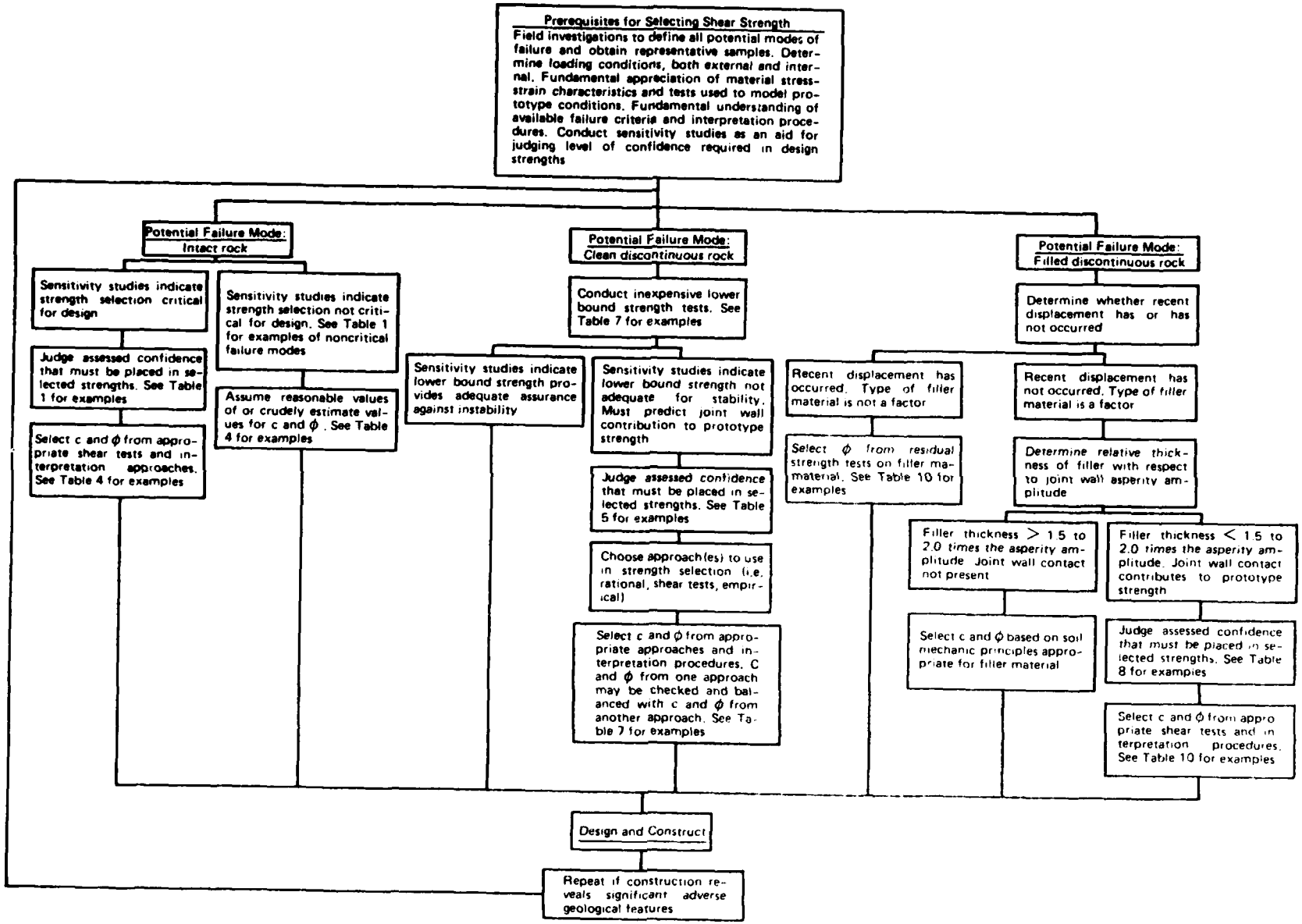

Figure 29. Simplified flowchart of factors to consider in selecting design shear strengths

capabilities are inadequate. This report briefly mentioned three areas that require additional research, including: (a) the development of techniques to permit reliable predictions of optimum shear strengths for materials subject to progressive failure, (b) scale dependency of shear-induced pore pressures along joints, and (c) verification of shear strengths of clean discontinuities predicted from empirical approaches.

228. The susceptibility of a material to progressive failure depends on four primary factors: (a) recoverable strain energy, (b) strength of interparticle bonds, (c) plasticity, and (d) the effects of various weathering agents. The effects of these four factors to reduce shear strength below peak strength can only be crudely quantified. The selection of optimum design shear strengths, upon which can be placed a reasonable degree of confidence, requires quantitative techniques to assess the interrelationship of the four factors with respect to prototype shear strength.

229. Research relating to pore pressures generated by shear strains along discontinuities, particularly filled discontinuities, is sparse. Shear strain-induced pore pressures and pore pressure effects for the most part are a matter of speculation. Research is needed to develop a practical understanding of the relationship between pore pressures and the dependent factors of scale effects, joint wall material characteristics, joint filler material characteristics, and time rate of shear load application.

230. The empirical curvilinear failure criterion developed by Barton (1974) offers an attractive alternative for determining shear strength of clean discontinuities. The criterion was developed from model studies. Good agreement exists between observed and predicted strengths from these studies. Research is needed to provide additional verification of the empirical criteria at the prototype scale level.

231. In some design cases the best predictions of prototype resisting strengths will not provide adequate assurance against sliding instability. The sliding stability of structures may be increased by construction or installation of features that provide extra resisting forces, by providing drains or other devices which reduce uplift forces, and altering the geometry of the structure to increase the normal load component and/or the base area. The stability of new structures may be conveniently increased by any or all of

these methods. The rehabilitation of aging structures to increase stability is usually limited to providing extra resisting forces and/or by reducing uplift forces.

REFERENCES

American Geological Institute. 1977. Glossary of Geology, Falls Church, Va., p 614.

Bandis, S. 1979. "Experimental Studies of the Shear Strength-Size Relationships and Deformation Characteristics of Rock Discontinuities," Ph.D. thesis, University of Leeds.

Barton, N. 1971. "A Relationship Between Joint Roughness and Joint Shear Strength," Rock Fracture Proceedings of the International Symposium on Rock Mechanics, Nancy, Vol 1, Theme I-8.

_____. 1973. "Review of a New Shear Strength Criterion for Rock Joints," Engineering Geology, Elsevier, 7, pp 287-332.

_____. 1974. "A Review of the Shear Strength of Filled Discontinuities," Norwegian Geotechnical Institute, NR 105, pp 1-38.

_____. 1976. "The Shear Strength of Rock and Rock Joints," International Journal of Rock Mechanics and Mining Sciences and Geomechanics Abstracts, Vol 13, No. 9, pp 255-279.

Barton, N. and Choubey, V. 1977. "The Shear Strength of Rock Joints in Theory and Practice," Journal, Rock Mechanics, The International Society for Rock Mechanics, Vol 10, No. 1-2, pp 1-54.

Bieniawski, Z. T. 1967. "Mechanism of Brittle Fracture of Rock," International Journal of Rock Mechanics and Mining Sciences and Geomechanics Abstracts, Vol 4, Parts 1 and 2, pp 395-423.

_____. 1968. "Propagation of Brittle Fracture in Rock," Proceedings, Tenth Symposium on Rock Mechanics, University of Texas at Austin, pp 409-427.

Bishop, A. W. and Henkel, D. J. 1962. The Measurement of Soil Properties in the Triaxial Test, 2d ed., St. Martin's Press, New York.

Bjerrum, L. 1967. "Progressive Failure in Slopes of Overconsolidated Plastic Clay and Clay Shales," Journal of the Soil Mechanics and Foundation Division, American Society of Civil Engineers, Vol 93, No. SM5, Part I, pp 3-49.

Byerlee, J. D. 1975. "The Fracture Strength on Frictional Strength of Weber Sandstone," International Journal of Rock Mechanics and Mining Sciences and Geomechanics Abstracts," Vol 12, No. 1, pp 1-4.

Byerlee, J. D. and Brace, W. F. 1967. "Recent Experimental Studies of Brittle Fracture of Rocks," Failure and Breakage of Rocks, C. Fairhurst, Ed., American Institute of Mining Engineers, New York, pp 58-81.

Coulson, J. H. 1972. "Shear Strength of Flat Surfaces in Rock," Proceedings, Thirtieth Symposium on Rock Mechanics, University of Illinois at Urbana, pp 77-105.

Deere, D. U. 1976. "Dams on Rock Foundations - Some Design Questions," Rock Engineering for Foundations and Slopes, Proceedings, Specialty Conference, American Society of Civil Engineers, Geotechnical Engineering Division, Boulder, Vol 2, pp 55-85.

Deere, D. U. and Miller, R. P. 1966. "Engineering Classification and Index Properties for Intact Rock," Technical Report AF WL-TR-65-116, U. S. Air Force Weapons Laboratory, Kirtland Air Force Base, N. Mex.

Department of the Army, Office, Chief of Engineers. 1954. "Subsurface Investigations - Soils (CH 1-2)," Engineer Manual 1110-2-1803, Washington, D. C.

_____. 1958. "Gravity Dam Design (CH 1-2)," Engineer Manual 1110-2-2200, Washington, D. C.

_____. 1960. "Geological Investigations (CH 1-2)," Engineer Manual 1110-1-1801, Washington, D. C.

_____. 1970a. "Laboratory Soils Testing," Engineer Manual 1110-2-1906, Washington, D. C.

_____. 1970b. "Stability of Earth and Rockfill Dams," Engineer Manual 1110-2-1902, Washington, D. C.

_____. 1972. "Soil Sampling," Engineer Manual 1110-2-1907, Washington, D. C.

_____. 1974. "Gravity Dam Design Stability," Engineering Technical Letter 1110-2-184, Washington, D. C.

_____. 1981. "Sliding Stability for Concrete Structures," Engineering Technical Letter 1110-2-256, Washington, D. C.

Drozd, K. 1967. "Variation in the Shear Strength of a Rock Mass Depending on the Displacement of the Test Blocks," Proceedings, Geotechnical Conference on Shear Strength Properties of Natural Soils and Rocks, Oslo, Vol 1, pp 265-269.

Evdokimov, P. D. and Sapegin, D. D. 1970. "A Large Scale Field Shear Test on Rock," Proceedings, Second Congress, International Society for Rock Mechanics, Vol 2, Theme 3, No. 17.

Fairhurst, C. 1964. "On the Validity of Brazilian Test for Brittle Materials," International Journal of Rock Mechanics and Mining Sciences, Vol 1, pp 535-546.

Fecker, E. and Rengers, N. 1971. "Measurement of Large Scale Roughnesses of Rock Planes by Means of Profilograph and Geological Compass," Rock Fracture, Proceedings of the International Symposium on Rock Mechanics, Nancy, Paper 1-18.

Goldstein, M. et al. 1966. "Investigation of Mechanical Properties of Cracked Rock," Proceedings of the First Congress of the International Society of Rock Mechanics, Lisbon, Vol 1, pp 521-529.

Goodman, R. E. 1974. "The Mechanical Properties of Joints," Proceedings of the Third Congress of the International Society of Rock Mechanics, Denver, Vol I, pp 124-140.

Goodman, R. E. and Ohnishi, Y. 1973. "Undrained Shear Testing of Jointed Rock," Rock Mechanics, Journal of the International Society for Rock Mechanics, Vol 5, No. 3, pp 129-149.

Henny, D. C. 1933. "Stability of Straight Concrete Gravity Dams," Transactions, American Society of Civil Engineers, Paper No. 1881.

Hodgson, K. and Cook, N. G. W. 1970. "The Effects of Size and Stress Gradient on the Strength of Rock," Proceedings of the Second Congress of the International Society of Rock Mechanics, Belgrade, Vol 2, Paper 3-5.

Hoek, E. 1976. "Rock Slopes," Rock Engineering for Foundations and Slopes, Proceedings, Specialty Conference, American Society of Civil Engineers, Geotechnical Engineering Division, Boulder, Vol 2, pp 157-171.

Horn, H. M. and Deere, D. U. 1962. "Frictional Characteristics of Minerals," Geotechnique, Vol 12, p 319.

International Commission on Large Dams. 1973. "World Register of Dams," Paris.

International Society of Rock Mechanics. 1974. "Suggested Methods for Determining Shear Strength," Commission on Standardization of Laboratory and Field Tests, Document No. 1, Lisboa Codex, Portugal.

Jaeger, J. C. 1971. "Friction of Rocks and the Stability of Rock Slopes - Rankine Lecture," Geotechnique, Vol 21, p 97.

James, P. M. 1969. "In Situ Tests at Muda Dam," Proceedings, Conference on In Situ Investigations in Soils and Rocks, British Geotechnical Society, London.

Kanji, M. A. 1970. "Shear Strength of Soil-Rock Interfaces," M. Sc. Thesis, University of Illinois.

Koifman, M. I. 1969. "The Size Factor in Rock-Pressure Investigations," Mechanical Properties of Rocks, translated by Israel Program for Scientific Translations, pp 109-117.

Koifman, M. I. et al. 1969. "Investigation of the Effect of Specimen Dimensions and Anisotropy on the Strength of Some Coals in Donets and Kuznetsk Basins," Mechanical Properties of Rock, translated by Israel Program for Scientific Translations, pp 118-129.

Kutter, H. K. and Rautenberg, A. 1979. "The Residual Shear Strength of Filled Joints in Rock," Proceedings, Fourth International Congress on Rock Mechanics, Vol 1, pp 221-227.

Ladanyi, B. and Archambault, G. 1969. "Simulation of Shear Behavior of a Jointed Rock Mass," Proceedings, Eleventh Symposium on Rock Mechanics, Society of Mining Engineers, pp 105-125.

Lane, K. S. 1969. "Engineering Problems Due to Fluid Pressure in Rock," Rock Mechanics - Theory and Practice, Proceedings, Eleventh Symposium on Rock Mechanics, CH 26, Berkeley, pp 501-540.

Miller, R. P. 1965. "Engineering Classification and Index Properties for Intact Rock," Ph.D. thesis, University of Illinois.

Mogi, K. 1962. "The Influence of the Dimensions of Specimens on the Fracture Strength of Rocks," Bulletin, Earthquake Research Institute, Tokyo University, No. 40, pp 175-185.

Nelson, J. D. and Thompson, E. G. 1977. "A Theory of Creep Failure in Over-consolidated Clay," Journal of the Geotechnical Engineering Division, American Society of Civil Engineers, Vol 103, No. GT11, pp 1281-1294.

Patton, F. D. 1966. "Multiple Modes of Shear Failure in Rock and Related Materials," Ph.D. thesis, University of Illinois.

Pratt, H. R., Black, A. D. and Brace, W. F. 1974. "Friction and Deformation of Jointed Quartz Diorite," Proceedings of the Third Congress of the International Society of Rock Mechanics, Denver, Vol II, Part A, pp 306-310.

Pratt, H. R. et al. 1972. "The Effect of Specimen Size on the Mechanical Properties of Unjointed Diorite," International Journal of Rock Mechanics and Mining Sciences and Geomechanics Abstracts, Vol 9, No. 4, pp 513-529.

Robinson, E. C. 1955. "Experimental Study of the Strength of Rocks," Geological Society of America Bulletin, Vol 66.

Rosengren, K. J. 1968. "Rock Mechanics of the Black Star Open Cut, Mount Isa," Ph.D. thesis, Australian National University, Canberra.

Ross-Brown, D. M., Wickens, E. H., and Markland, J. 1973. "Terrestrial Photogrammetry in Open Pits, Part 2 - An Aid to Geological Mapping," Transactions, Institute of Mining and Metallurgy, Section A, Vol 82, p 115.

Rowe, P. W. 1962. "The Stress-Dilatancy Relation for Static Equilibrium of an Assembly of Particles in Contact," Proceedings, Royal Society of London, Vol 269, pp 500-527.

Rowe, P. W., Barden, L., and Lee, I. K. 1964. "Energy Components during the Triaxial Cell and Direct Shear Tests," Geotechnique, Vol 14, No. 3, pp 247-261.

Skempton, A. W. 1964. "Long-term Stability of Clay Slopes," Geotechnique, Vol 14, No. 2, pp 77-102.

Terzaghi, K. 1936. "The Shearing Resistance of Saturated Soils," Proceedings of the First International Conference on Soil Mechanics and Foundation Engineering, Cambridge, Mass., Vol 1, pp 54-56.

Tse, R. and Cruden, D. M. 1979. "Estimating Joint Roughness Coefficients," International Journal of Rock Mechanics and Mining Sciences and Geomechanics Abstracts, Vol 16, pp 303-307.

Underwood, L. B. 1974. "Chalk Foundations at Four Major Dams in the Missouri River Basin," Transactions, 8th International Congress on Large Dams, Vol I, pp 23-48.

U. S. Army Corps of Engineers, Nashville District. 1974. "General Design Memorandum for Bay Springs N-11," Nashville, Tenn.

U. S. Army Engineer Waterways Experiment Station. 1980. "Rock Testing Handbook," Test Standards, Vicksburg, Miss.

United States Committee on Large Dams. 1975. "Lessons from Dam Incidents USA," American Society of Civil Engineers, New York.

Varshney, R. S. 1974. "Dams on Rocks of Varying Elasticity," International Journal of Rock Mechanics and Mining Sciences and Geomechanics Abstracts, Vol 11, No. 1.

Zeigler, T. W. 1972. "In Situ Tests for the Determination of Rock Mass Shear Strength," Technical Report S-72-12, U. S. Army Engineer Waterways Experiment Station, CE, Vicksburg, Miss.

Table 1

Level of Confidence Required in Selected Design Shear Strengths for Various Modes of Potential Intact Rock Failure and Design Use

Assessed Confidence	Mode of Potential Failure and Design Use	Sensitivity	Comments
Low	Major mode of potential failure - strong to moderately weak intact rock Preliminary design(s)	Stability not sensitive to strength determinations	Instability will not occur even with over-conservative estimates of strengths Preliminary design is often required for alternative comparisons before well defined strength data are available
High	Major mode of potential failure - very low strength poorly cemented intact rock Weak seams or discontinuities with significant amounts of intact rock separating an otherwise continuous trend Final design	Stability may be sensitive to strength determinations	Adequate FS can generally be obtained with confident estimates of conservative strength Strength selection should consider scale effects
Very high	Major mode of potential failure - weak seam or discontinuity with small segments of intact rock separating an otherwise continuous trend Final design	Stability is sensitive to strength determinations	Cannot achieve an adequate FS without considering contributions of total resisting strength from intact rock segments May require extensive field investigations (i.e., adits, trenches, etc.) to determine amount of intact rock Strength selection should consider potential for progressive failure, scale effects, and for porous rock time drainage conditions

Table 2

Summary of Advantages and Disadvantages for Triaxial and Direct Shear Devices for Testing Intact Rock

Device	Advantages	Disadvantages
Small triaxial	Capable of pore pressure control; monitoring, back pressure for saturation, etc.	Poor control of normal stress levels at which failure occurs
	Capable of monitoring volumetric changes in specimen	Generally more costly than direct shear tests
	Control over principal stresses	
Small direct shear	Good control of normal stress levels at which failure occurs	No pore pressure control capabilities for typical device
	Generally less costly than triaxial tests	No control of principal stresses
		Generally more scatter in test results
Large triaxial and direct shear	Same as small triaxial and direct shear, respectively, above	Same as small triaxial and direct shear, respectively, above
		Not recommended because devices of sufficient loading capacity for testing large intact rock specimens not readily available

Table 3

Classification of Intact Rock Strength
(After Deere and Miller 1966)

Description	Average Uniaxial Compressive Strength, q_u, psi	Examples of Rock Types
Very low strength	150-3500	Chalk, rocksalt
Low strength	3500-7500	Coal, siltstone, schist
Medium strength	7500-15000	Sandstone, slate, shale
High strength	15000-30000	Marble, granite, gneiss
Very high strength	>30000	Quartzite, dolerite, gabbro, basalt

Table 4

Summary of Alternative Approaches for Selection of c and ϕ Shear Strength Parameters for Intact Rock

Assessed Confidence	Test Type	Specimen Drainage Condition	Specimen Failure Definition	Alternative Approaches and Interpretation of Test Results for c and ϕ Selection	Comments
Low	No test	--	--	No analysis required or assumed value of c and ϕ	Use only in cases where a very high level of confidence exists for no failure
	Unconfined compression (UC)	Undrained Q	Peak strength	Assume ϕ = 0.0 and select c as one-half the average UC strength (see Figure 20)	Approach typically overestimates strength for most design σ_n ranges (see Figure 21) Number of UC tests should be sufficient to define general trend, usually 10 or more tests
	Direct shear (DS) or Triaxial (T)	Undrained Q	Peak strength	Select c and ϕ from DS or T $\tau - \sigma_n$ line of best fit see Figure 23)	C value will generally be unconservative DS preferred because of cost and σ_n control Number of DS or T tests should be sufficient to define general trend, usually 3 to 6 tests
High	Direct Shear (DS) or Triaxial (T)	Undrained Q	Peak strength	Select c and ϕ from lower bound DS or T $\tau - \sigma_n$ line of best fit adjust for any scale effects (see Figure 23)	C and ϕ from undrained peak strength tests will tend to be unconservative because of dilation tendencies (negative pore pressures, see Figure 9); however, selection of lower bound strengths and adjustment for scale effects will to some extent compensate for the unconservative trend Approach most applicable for routine design DS preferred because of cost and σ_n control Number of tests should be sufficient to define trend, usually a minimum of 9 tests
Very high	Direct Shear (DS) or Triaxial (T)	Undrained Q	Peak strength	Assume c = 0 and select ϕ from DS or T $\tau - \sigma_n$ line of best fit	Approach is the most conservative even though ϕ from undrained peak strength tests will tend to be unconservative because of dilation tendencies (see Figure 9) since "c" contributes a major part of the total strength of intact rock DS preferred because of cost and σ_n control Number of tests should be sufficient to define trend, usually a minimum of 9 tests

(Continued)

Table 4 (Concluded)

Assessed Confidence	Test Type	Specimen Drainage Condition	Specimen Failure Definition	Alternative Approaches and Interpretation of Test Results for c and ϕ Selection	Comments
Very high	Triaxial (T)	Undrained with pore pressure measurements, R	Stress level corresponding to peak in the pore pressure response curve - point of stable crack propagation (point C in Figure 19)	Select c and ϕ from lower bound $\tau - \sigma_n$ line of best fit and adjust for any scale effects	Approach is practical only for porous rock with relatively quick pore pressure response characteristics C and ϕ based on undrained test will be unconservative because of tendencies for volumetric compressive (positive pore pressures, see Figure 9), drained strengths can be obtained by pore pressure adjustments Triaxial tests are required for pore pressure monitoring but results in poor control of σ_n Number of tests should be sufficient to define trend, usually a minimum of 9 tests
		Drained S with volumetric strain measurements	Stress level corresponding to peak in volumetric compression - point of stable crack propagation (point C in Figure 19)	Select c and ϕ from lower bound $\tau - \sigma_n$ line of best fit and adjust for any scale effects	Approach is practical only for porous rock with relatively quick pore pressure response characteristics Approach requires precise monitoring of volumetric strain and not generally practical for routine testing. However, the best estimates of strength are obtained with this approach Triaxial tests are required for volumetric strain monitoring but results in poor control of σ_n Number of tests should be sufficient to define trend, usually a minimum of 9 tests

Table 5

Assessed Confidence to be Placed in Design Shear Strengths for Various Clean Discontinuous Rocks, Weathering Conditions, and Design Uses

Assessed Confidence	Rock Type, Weathering, Design Use	Sensitivity	Comments
Low	Preliminary design only	Stability not sensitive to strength determinations	Preliminary design is often required for alternative comparisons before well defined strength data is available
High	Most discontinuities with unweathered to moderately weathered surfaces Final design	Stability may be sensitive to strength determinations	Adequate FS can generally be obtained with confident estimates of conservative strength Strength selection may need to consider scale effects
Very high	Most discontinuities with severely weathered surfaces Most discontinuous rock of the sheet silicate minerals (mica, talc, serpentine, chlorite, etc.), particularly with smooth undulating surfaces Final design	Stability is sensitive to strength determinations	Cannot achieve an adequate FS with conservative estimates of strength Must consider scale effects

Table 6

Summary of Advantages and Disadvantages of Triaxial and Direct Shear Devices for Testing Clean Discontinuous Rock

Device	Advantages	Disadvantages
Small triaxial	Control over principal stresses	Poor control of σ_n at which failure occurs
	Capable of pore pressure control; though not usually necessary (see paragraph 134)	Requires special sample preparation to orient joint shear surfaces
		Generally more costly than direct shear tests
		May need to correct results for end friction effects between specimen and end platens and state of stress corresponding to actual failure plane
Small direct shear	Good control of σ_n levels at which failure occurs	No control of principle stresses
	Generally less costly than triaxial	
Large triaxial	Same as small triaxial	Same as small triaxial
		Not recommended because devices capable of testing specimens of sufficient size to address scale effects are not readily available
Large direct shear	Same as small direct shear	Same as small direct shear
	Only type of device routinely available currently capable of addressing scale effects	Very expensive

Table 7

Summary of Alternative Approaches for the Selection of c and ϕ Shear Strength Parameters for Clean Discontinuous Rock

Assessed Confidence	Approach and Type Test	Specimen Drainage Condition	Specimen Failure Definition	Alternative Approaches and Interpretation of Test Results for c and ϕ Selection	Comments
Low	Rational approach, no test	--	--	Assumed value of ϕ and $c = 0$	Assumed value of ϕ should be at least as great as typical values of ϕ_u or ϕ_r (unweathered and weathered surfaces, respectively) for rock type considered Assume a ϕ based on experience from similar projects and rock conditions
	Testing Approach, small-scale direct shear (DS) or triaxial (T)	Drained S	Peak strength	Assume $c = 0$ and select ϕ from DS or T $\tau - \sigma_n$ line of best fit. Tests conducted on natural joint surface	Except for smooth undulating joint surfaces this approach will overestimate strength DS preferred because of cost, σ_n control, no failure plane and/or no end restraints correction Number of DS or T tests should be sufficient to define general trend, usually 3-6 tests
High	Rational Approach, small-scale direct shear (DS) or triaxial (T)	Drained S	Peak strength (smooth sawn surfaces) or deformation corresponding to residual strength (natural surfaces) for unweathered and weathered surfaces, respectively	Assume $c = 0$ and adjust ϕ_u or ϕ_r (for unweathered or weathered surfaces, respectively) for an effective i angle, $\tau = \sigma_n \tan((\phi_u \text{ or } \phi_r) + i)$; $((\phi_u \text{ or } \phi_r) + i)$ value should not exceed ϕ value obtained from small-scale DS or T tests on natural joint surfaces	Approach most commonly used Adjustments for effective i angle must come from experience with similar projects and rock conditions, actual measurements and numerical analysis of exposed joint surfaces representative of actual rock conditions, or relationship between peak dilation/shear deformation for large representative blocks at low σ_n Should be used with caution for very low strength joint surfaces DS preferred because of cost, σ_n control, no failure plane and/or no end restraints corrections Number of DS or T tests should be sufficient to define trend, usually a minimum of 6 tests

(Continued)

Table 7 (Continued)

Assessed Confidence	Approach and Type Test	Specimen Drainage Condition	Specimen Failure Definition	Alternative Approaches and Interpretation of Test Results for c and ϕ Selection	Comments
High	Barton's Empirical Approach, large block push-pull or tilt tests; small-scale direct shear (DS) or triaxial (T) Schmidt hammer	Drained S	Stress at which sliding occurs (push-pull) angle at which sliding occurs (tilt). For tests, deformation corresponding to residual strength (natural surfaces or peak strength (smooth sawn surfaces) for weathered and unweathered surfaces, respectively	Assume c = 0 and select ϕ corresponding to the envelope obtained from the intersection of Barton's curvilinear envelope (Equation 21) and the maximum design σ_n (see Figure 27)	Approach should be used with caution because of lack of predicted versus prototype behavior data Requires knowledge of maximum σ_n Strengths selected in this manner will usually be conservative Number of push-pull or tilt tests to define JRC should be 4. Use Equation 26 or 27 to determine JRC. Test to be performed in a wet condition Schmidt hammer readings to define JCS should consist of at least the average JCS should consist of at least the average of the highest 5 out of 10 readings. Use Equation 28 to determine JCS Barton assumes ϕ_u or ϕ_r for unweathered joint surface. This assumption is not always correct (see *paragraph 137*). *Use* ϕ_u *for unweathered surfaces* Small-scale DS tests to determine ϕ_u or ϕ_r preferred because of cost, σ_n control, no failure plane, and/or no end restraints corrections Number of DS or T to determine ϕ_u or ϕ_r should be sufficient to define trend, usually a minimum of 6 tests.
Very high	Testing Approach, small-scale direct Shear (DS) or triaxial (T)	Drained S	Peak strength (smooth sawn surfaces) or deformation corresponding to residual strength (natural surfaces) for unweathered or weathered surfaces, respectively	Assume c = 0 and select ϕ corresponding to ϕ_u or ϕ_r for unweathered or weathered joint surfaces, respectively	Approach most conservative DS preferred because of cost, σ_n concontrol, no failure plane and/or no end restraints corrections Number of DS or T tests should be sufficient to define trend, usually a minimum of 6 tests

(Continued)

Table 7 (Concluded)

Assessed Confidence	Approach and Type Test	Specimen Drainage Condition	Specimen Failure Definition	Alternative Approaches and Interpretation of Test Results for c and ϕ Selection	Comments
Very high	Testing Approach, large-scale in situ or laboratory direct shear tests	Drained S	Peak strength	Select c and ϕ directly from linear approximation or curvilinear interpretation (see paragraphs 87-92) of $\tau - \sigma_n$ plots	Approach gives the best means of selecting design strengths representative of prototype conditions Tests are expensive and usually delay final design Number of tests should be balanced with cost and sufficient data to define trend. The minimum number of tests should be 3

Table 8

Level of Confidence Required in Design Shear Strengths for Various Filled Discontinuous Rocks, Filler Material Type, Displacement History, and Design Use

Assessed Confidence	Displacement History, Filler Material Type, and Design Use	Sensitivity	Comments
Low	Preliminary design only	Stability not sensitive to strength determinations	Preliminary design is often required for alternative comparisons before well defined strength data is available
High	Undisplaced joints with overconsolidated clays of low plasticity (lean clays) and silts Undisplaced and displaced joints with sands and gravels	Stability may be sensitive to strength determinations	Adequate FS can generally be obtained with confident estimates of conservative strength Strength selection may need to consider joint wall scale effects
Very high	Undisplaced and displaced joints with normally-consolidated clays Undisplaced and displaced joints with overconsolidated clays of medium to high plasticity	Stability (long and short term) is sensitive to strength determination	Cannot achieve an adequate FS with conservative estimates of strength or confidence in long-term strength prediction is poor Strength selection must consider joint wall scale effects and may need to consider filler material scale effects

Table 9

Summary of Advantages and Disadvantages of Triaxial and Direct Shear Devices for Testing Filled Discontinuous Rock

Device	Advantages	Disadvantages
Small triaxial	Control over principal stresses Capable of pore pressure control Capable of testing soft squeezing fillers	Requires special sample preparation to orient joint shear surfaces Generally more costly than direct shear tests May need to correct results for failure plane orientation and end friction effects between specimen and end platens Does not address scale effects
Small direct shear	Generally better soft normal load control than triaxial Generally less costly than triaxial Good control of normal stress levels at which failure occurs	Squeezing problems with soft fillers No control of principal stresses Does not address scale effects
Large triaxial	Same as small triaxial	Same as small triaxial Not recommended because devices capable of testing specimens of sufficient size to address scale effects are not readily available.
Large direct shear	Same as small direct shear Only type of device routinely available currently capable of addressing scale effects	Same as small direct shear items 1 and 2 Very expensive

Table 10

Summary of Alternative Approaches for the Selection of c and ϕ Shear Strength Parameters for Filled Discontinuous Rock

Assessed Confidence	Filler Material Type	Displacement History	Test Type	Specimen Drainage Condition	Specimen Failure Definition	Alternative Approach and Interpretation of Test Results for c and ϕ Selection	Comments
Low	All types	Both displaced and undisplaced	No tests	--	--	Assumed value of c=0 and ϕ based on experience with similar materials	Assumed value of ϕ should be at least as great as typical values of ϕ or ϕ_r of the filler material depending on whether the joint has not or has been previously displaced, respectively
	Clay and silt materials	Undisplaced	Small-scale direct shear (DS) or small-scale triaxial (T)	Drained S for overconsolidated materials, undrained R for normally-consolidated materials (triaxial)	Peak strength	Assume c=0 and select ϕ from DS or T $\tau-\sigma_n$ line of best fit, tests conducted on natural joint with filler	Approach may be conservative or unconservative depending on actual c values of filler material and joint wall contact contribution to ϕ T preferred because of better pore pressure and saturation control; T test results may need to be corrected for end effects and failure plane orientation Very thinly filled joints may exhibit considerable data scatter; number of DS or T tests should be sufficient to define general trend, usually 3-6 tests
	All cohesionless materials	Both displaced and undisplaced	Small-scale direct shear (DS) or small-scale triaxial (T)	Drained S	Peak strength	Assume c=0 and select ϕ from DS or T $\tau-\sigma_n$ line of best fit, tests conducted on natural joint with filler	Any observed c will be due to joint wall contacts, approach will usually be unconservative because of joint wall scale effects on ϕ Cohesionless materials are usually free draining, hence pore pressure control not critical; therefore, DS tests are preferred because of costs and no data correction required Very thinly filled joints may exhibit considerable data scatter; number of DS or T tests should be sufficient to define general trend, usually 3-6 tests
	Clay and silt materials	Displaced*	Small-scale direct shear (DS) or small-scale triaxial (T)	Drained residual	Strain (T) or deformation (DS) corresponding to residual strength	Select ϕ_r from DS or T $\tau-\sigma_n$ line of best fit, tests conducted on natural joint with filler	Any observed c will be due to joint wall contacts and should be neglected Some scale effects may still be present, particularly for very thinly filled joints Approach gives good estimates of prototype strengths for recently displaced joints DS preferred because of cost and ease of generating large displacements required for residual tests Generally little data scatter; usually requires a minimum of 3 tests
High	Overconsolidated clay of low plasticity and silt materials	Undisplaced	Small-scale direct shear (DS) or small-scale triaxial (T)	Drained S	Strain (T) or deformation (DS) corresponding to ultimate strength	Select c and ϕ from DS or T $\tau-\sigma_n$ line of best fit, tests conducted on undisturbed filler material	Approach most conservative because contribution to strength from any joint wall contact is not considered Value of c will generally be very small T tests preferred because of better pore pressure and saturation control Generally little data scatter; usually requires 6-9 tests

(Continued)

* Shear strengths of recently displaced joints are usually at or near residual. It may be difficult to determine from visual inspection of samples whether recent displacement has occurred. If the joint is at residual strength, peak strength from undisturbed filler material will be close to residual strength.

Table 10 (Continued)

Assessed Confidence	Filler Material Type	Displacement History	Test Type	Specimen Drainage Condition	Specimen Failure Definition	Alternate Approach and Interpretation of Test Results for c and ϕ Selection	Comments
						Assume c=0 and select ϕ from DS or T τ-σ_n line of best fit; tests conducted on natural joint with filler material	Approach is conservative except for very thinly filled joints with rough joint wall contacts and low actual c values of filler material, assuming c=0 usually offsets joint wall scale effects T tests preferred because of better pore pressure and saturation control; T test results may need to be corrected for end effects and failure plane orientation Generally little data scatter, usually requires 6-9 tests
					Peak strength	Select ϕ from DS or T τ-σ_n line of best fit, tests conducted on remolded filler material	Approach is applicable to very thinly filled joints where sufficient quantities of undisturbed filler cannot be obtained Approach will result in design strengths near those obtained from ultimate strengths of undisturbed filler material Values of c will generally be very small and generally assumed to be zero Approach not applicable to highly sensitive filler materials T tests preferred because of better pore pressure and saturation control Generally little data scatter, usually requires 6-9 tests
High	All cohesionless materials	Both displaced and undisplaced	Small-scale direct shear (DS) or small-scale triaxial (T)	Drained S	Peak strength	Select ϕ from DS or T τ-σ_n line of best fit, tests conducted on remolded filler material	Approach is conservative because contributions to strength from joint wall contacts not considered T tests preferred because of specimen confinement problem associated with DS tests Little data scatter, usually requires 3-6 tests
	All overconsolidated clay of low plasticity, silt and cohesionless materials	Undisplaced	Large in situ direct shear	Drained S	Deformation corresponding to ultimate strength for clay and silt materials, peak strength for cohesionless materials	Select c and ϕ from τ-σ_n line of best fit, tests conducted on natural joint with filler material	Conservative approaches listed above will result in adequate assurance against sliding for most typical designs; in situ tests are reserved for special design cases where a high order of confidence in design strengths are required and/or conservative estimate will not provide adequate assurance against sliding Tests are expensive and usually delays final design Very thinly filled joints may result in data scatter; number of tests should be balanced with cost and sufficient data to define trend; minimum number of tests should be 3

(Continued)

Table 10 (Concluded)

Assessed Confidence	Filler Material Type	Displacement History	Test Type	Specimen Drainage Condition	Specimen Failure Definition	Alternative Approach and Interpretation of Test Results for c and ϕ Selection	Comments
Very high	All clays and silts	Displaced*	Small-scale direct shear (DS) or small-scale triaxial (T)	Drained residual	Strain (T) or deformation (DS) corresponding to residual strength	Select ϕ_r from T or DS $\tau-\sigma_n$ line of best fit; tests may be conducted on natural joints with filler material or on undisturbed or remolded filler material	Any observed c value from tests on natural joints with filler will be due to joint wall contact effects and should be neglected Some scale effects may still be present for tests on natural very thinly filled joints Approach gives good estimates of prototype strengths for recently displayed joints DS preferred because of cost and ease of generating large displacements required for residual tests Generally little data scatter, usually requires 3-6 tests
	Normally-consolidated clays and silts	Undisplaced	Small-scale direct shear (DS) or small-scale triaxial (T)	Drained S	Peak strength	Select c and ϕ from T or DS $\tau-\sigma_n$ line of best fit; tests conducted on undisturbed filler material	Approach is conservative because contributions to strength from joint wall contacts are not considered For typical designs it is doubtful that conservative estimates of strength for materials in this group will provide adequate assurance against sliding; however, because the tests are inexpensive, strengths obtained in this approach should be checked against stability requirements prior to specifying expensive in situ tests if sufficient quantity of undisturbed filler material is available T tests preferred because of better pore pressure and saturation control Little data scatter, usually requires 3-6 tests
Very high			Large in situ direct shear	Drained S**	Peak strength	Select c and ϕ from $\tau-\sigma_n$ line of best fit; tests conducted on natural joints with filler material	Approach will give the best estimates of prototype strength Squeezing problems with very soft filler materials Tests are expensive and usually delay final design Very thinly filled joints may result in data scatter; number of tests should be balanced with cost and sufficient data to define trend; minimum number of tests should be 3
	Overconsolidated clay and clay shale materials of medium to high plasticity	Undisplaced	Small-scale direct shear (DS) or small-scale triaxial (T)	Drained residual	Strain (T) or deformation (DS) corresponding to residual strength	Select ϕ_r from T or DS $\tau-\sigma_n$ line of best fit; tests may be conducted on natural joints with filler material or on undisturbed or remolded filler material alone	Any observed c value from tests on natural joints with filler will be due to joint wall contact effects and should be neglected Some scale effects may still be present for tests on natural very thinly filled joints Conservatism in approach reflects lack of knowledge as to the potential for long-term decreases in strength and the potential for progressive failure associated with this group of materials; less conservative approaches require extensive experience with particular materials in this group Little data scatter, usually requires 3-6 tests

* Shear strengths of recently displaced joints are usually at or near residual. It may be difficult to determine from visual inspection of samples whether recent displacement has occurred. If the joint is at residual strength, peak strength from undisturbed filler material will be close to residual strength.

** Drained strength is usually critical for long-term stability. Undrained strength constitutes a minimum strength condition (see Figure 9) and should be used if unusual time sequence of loading so dictates.

APPENDIX A: DERIVATION OF SLIDING STABILITY EQUATIONS FOR THE ALTERNATE METHOD, SINGLE-PLANE AND MULTIPLE-PLANE FAILURE SURFACES

Definition of Factor of Safety

1. The factor of safety is defined as the ratio of available shear strength to shear stress which defines the factor of safety in terms of the least known conditions affecting sliding stability, the material strength parameters:

$$FS = \frac{\tau_a}{\tau} \tag{A1}$$

where

FS = the factor of safety

τ_a = the available shear strength

τ = the limiting shear stress for safe stability

The most accepted method for defining available shear strength, τ_a, is the Mohr-Coulomb failure criteria:

$$\tau_a = c + \sigma \tan \phi \tag{A2}$$

where

c = the cohesion intercept

σ = the normal stress on the shear plane

ϕ = the angle of internal friction

Then the limiting shear stress for safe stability may be written as:

$$\tau = \frac{c + \sigma \tan \phi}{FS} \tag{A3}$$

Notation, Forces, and Geometry

2. Consider the i^{th} wedge of a failure system as shown in Figure A1.

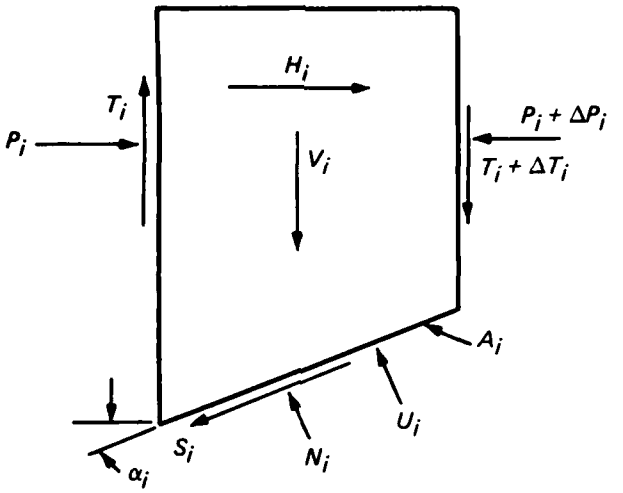

Figure A1. Free body diagram of an i^{th} wedge in a failure system

Symbols in the figure are defined as follows:

H_i = all applied horizontal forces acting on an individual wedge

V_i = all applied vertical forces (body and surcharge) acting on an individual wedge

P_i = all horizontal reactive forces with adjacent wedge

T_i = all vertical reactive forces with adjacent wedge

S_i = resisting shear force acting at critical potential failure plane

U_i = uplift force acting under the wedge on the critical potential failure plane = uplift pressure × area of critical potential failure plane

A_i = area of critical potential failure plane

N_i = the normal force acting on the critical potential failure plane

α_i = the angle between the inclined plane of critical potential failure and the horizontal ($\alpha > 0$ for upslope sliding; $\alpha < 0$ for downslope sliding)

k = the number of wedges in the failure mechanism or number of planes making up the critical potential failure surface

i = the subscript associated with planar segments along the critical potential failure surface

Requirements for Equilibrium of a Wedge

3. Refer to Figure A1. Note that subscripts are not used below where only one typical wedge is considered. Subscripts will necessarily be introduced later when overall equilibrium of a system of wedges is considered. Vertical equilibrium requires that

$$V + \Delta T + S \sin \alpha - N \cos \alpha - U \cos \alpha = 0 \tag{A4}$$

Substituting τA for S, substituting Equation A3 for τ, substituting N for σA, and solving for N yields

$$N = \frac{V + \Delta T + \frac{cA \sin \alpha}{FS} - U \cos \alpha}{-\frac{\sin \alpha \tan \phi}{FS} + \cos \alpha} \tag{A5}$$

Horizontal equilibrium requires that

$$\Delta P = H - N \sin \alpha - U \sin \alpha - S \cos \alpha \tag{A6}$$

Substituting τA for S, substituting Equation A3 for τ, and substituting N for σA yields

$$\Delta P = H - U \sin \alpha - \frac{cA \cos \alpha}{FS} - N \left(\sin \alpha + \frac{\cos \alpha \tan \phi}{FS} \right) \tag{A7}$$

Substituting Equation A5 into Equation A7 yields

$$\Delta P = H - U \sin \alpha - \frac{cA \cos \alpha}{FS} - \frac{(V + \Delta T) \sin \alpha - U \cos \alpha \sin \alpha}{\cos \alpha - \frac{\sin \alpha \tan \phi}{FS}} + \frac{\frac{cA \sin^2 \alpha + (V + \Delta T) \cos \alpha \tan \phi - U \cos^2 \alpha \tan \phi}{FS} + \frac{cA \sin \alpha \cos \alpha \tan \phi}{FS^2}}{\cos \alpha - \frac{\sin \alpha \tan \phi}{FS}} \tag{A8}$$

Algebraic and trigonometric manipulation of Equation A8 results in the simplified Equation A9:

$$\Delta P = H - \frac{(V + \Delta T)\ (FS \sin \alpha + \cos \alpha \tan \phi) - U \tan \phi + cA}{FS \cos \alpha - \sin \alpha \tan \phi} \qquad (A9)$$

Equation A9 satisfies both vertical and horizontal equilibrium.

Case 1: Single-Plane Failure Surface

4. Where the critical potential failure surface is defined by a single plane at the interface between the structure and foundation material with no embedment, there are no adjacent wedges to produce reactive forces and Equation A9 can be written as:

$$0 = H - \frac{FS\ V \sin \alpha + V \cos \alpha \tan \phi - U \tan \phi + cA}{FS \cos \alpha - \sin \alpha \tan \phi} \qquad (A10)$$

Equation A10 can be solved for FS , resulting in Equation A11, which provides direct solution for FS in this case:

$$FS = \frac{cA + (V \cos \alpha - U + H \sin \alpha) \tan \phi}{H \cos \alpha - V \sin \alpha} \qquad (A11)$$

Case 2: Multiple-Plane Failure Surface

5. Equilibrium of a system of wedges requires that $\sum_{i=1}^{k} \Delta P_i = 0$.

Applying this summation using Equation A9 would not result in an expression such that a solution for FS could be effected. However, Equation A9 can be rewritten as:

$$\Delta P = H - \frac{(V + \Delta T) \frac{\sin \alpha}{\cos \alpha} (FS \cos \alpha - \sin \alpha \tan \phi)}{FS \cos \alpha - \sin \alpha \tan \phi}$$

$$- \frac{(V + \Delta T) \left(\frac{\sin^2 \alpha \tan \phi}{\cos \alpha} + \cos \alpha \tan \phi \right)}{FS \cos \alpha - \sin \alpha \tan \phi} - \frac{cA - U \tan \phi}{FS \cos \alpha - \sin \alpha \tan \phi} \qquad (A12)$$

$$\Delta P = H - (V + \Delta T) \tan \alpha \frac{cA - U \tan \phi + (V + \Delta T) \tan \phi \left(\frac{\sin^2 \alpha + \cos^2 \alpha}{\cos \alpha}\right)}{FS \cos \alpha - \sin \alpha \tan \phi} \quad \text{(A13)}$$

$$\Delta P = H - (V + \Delta T) \tan \alpha - \frac{\frac{1}{FS}\left[cA \cos \alpha + (V + \Delta T - U \cos \alpha) \tan \phi\right]}{\cos^2 \alpha - \frac{\sin \alpha \cos \alpha \tan \phi}{FS}} \quad \text{(A14)}$$

Equation A14 is such that an implicit solution for FS can be effected by

$$\sum_{i=1}^{k} \Delta P_i = 0$$

Note that:

$$\cos^2 \alpha - \frac{\sin \alpha \cos \alpha \tan \phi}{FS} = \frac{1 - \frac{\tan \alpha \tan \phi}{FS}}{\sec^2 \alpha} = \frac{1 - \frac{\tan \alpha \tan \phi}{FS}}{1 + \tan^2 \alpha}$$

Introduce the notation:

$$n_\alpha = \frac{1 - \frac{\tan \alpha \tan \phi}{FS}}{1 + \tan^2 \alpha} \quad \text{(A15)}$$

Then, using Equation A14,

$$\sum_{i=1}^{k} \Delta P_i = 0 = \sum_{i=1}^{k} \left[H_i - (V_i + \Delta T_i) \tan \alpha_i\right]$$

$$- \frac{1}{FS} \sum_{i=1}^{k} \frac{c_i A_i \cos \alpha_i + (V_i + \Delta T_i - U_i \cos \alpha_i) \tan \phi_i}{n_{\alpha i}} \quad \text{(A16)}$$

$$FS = \frac{\sum_{i=1}^{k} \frac{c_i A_i \cos \alpha_i + (V_i + \Delta T_i - U_i \cos \alpha_i) \tan \phi_i}{n_{\alpha i}}}{\sum_{i=1}^{k} \left[H_i - (V_i + \Delta T_i) \tan \alpha_i\right]} \quad \text{(A17)}$$

If T is assumed to equal 0:

$$FS = \frac{\sum_{i=1}^{k} \frac{c_i A_i \cos \alpha_i + (V_i - U_i \cos \alpha_i) \tan \phi_i}{n_{\alpha i}}}{\sum_{i=1}^{k} (H_i - V_i \tan \alpha_i)} \qquad \text{(A18)}$$

which is the general form of the equation for solution of FS by the WES method of analysis, as displayed in the main text. The assumption of $\Delta T = 0$ is analogous to Bishop's approach where vertical forces between slices are assumed to equal zero. This is a reasonable assumption since usually $\Delta T << V$ and since this assumption tends to result in a lower calculated value of FS. Equation A18 is implicit in FS (except when $\phi = 0$ or $\alpha = 0$) since n_α is a function of FS. Therefore, the solution for FS requires an iteration procedure in which an initial estimate of FS is made to determine a value for n_α, and FS is calculated; the calculated FS is then used for a second approximation of n_α; and the process is repeated until the value of FS converges. Experience shows that convergence is rapid. Figure A2 shows a plot of n_α and α for values of $\tan \phi/FS$.

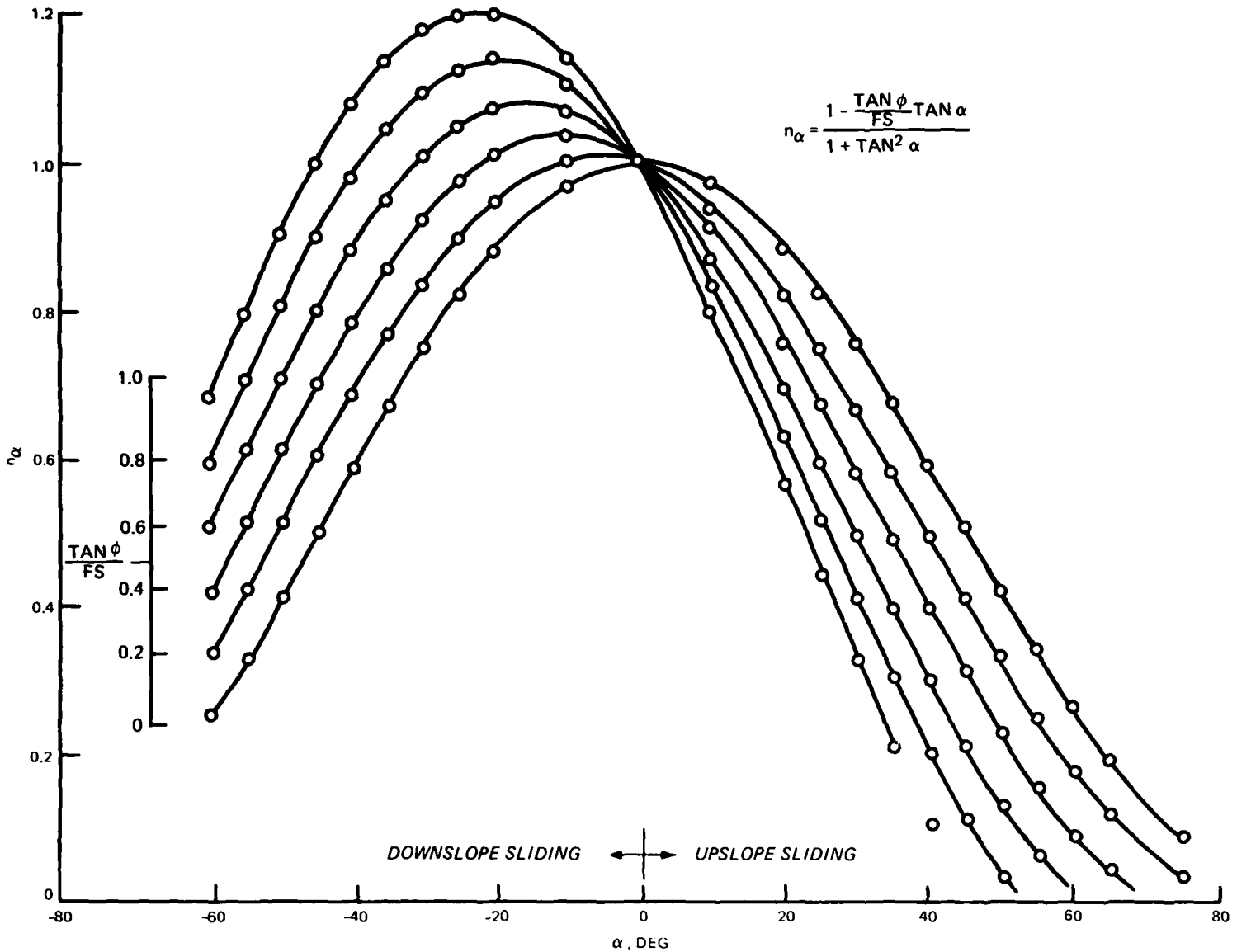

Figure A2. Plot of n_α and α for values of tan ϕ/FS

APPENDIX B: EQUIVALENCY OF LIMIT EQUILIBRIUM METHODS

1. The general wedge equation for equilibrium of a wedge (Equation 13), displayed below as Equation B1, results directly from summation of forces parallel to the failure plane and subsequent solution for $P_{i-1} - P_i$. In applying this equation to a system of wedges, summation of horizontal forces is used. Hence, the general wedge method (ETL 1110-2-256) requires equilibrium in two different directions within a vertical plane orientated in the direction of impending motion.

2. The alternate equation (Equation 15) for equilibrium of a system of wedges was derived from summation of vertical and horizontal forces on each wedge, and the requirement that summation of horizontal forces be zero for the system of wedges. In both methods, summation of forces in more than one direction within the same vertical plane is required; i.e., equilibrium in that plane is to be satisfied. In both methods differential vertical forces between wedges are neglected when considering overall equilibrium. It would, therefore, be expected that the two methods would yield the same result, even though the mechanics of calculation are quite different.

3. It shall be shown below that the alternate equation for equilibrium of a wedge (Equation 13) taken together with the stated conditions necessary for a system of wedges to act as an integral failure mechanism is mathematically equivalent to the alternate equation (Equation 15) for equilibrium of a system of wedges.

4. The general wedge equation for equilibrium of a wedge (Equation 13) is given below as Equation B1:

$$P_{i-1} - P_i = \frac{\left[\left(W_i + V_i\right)\cos\alpha_i - U_i + \left(H_{i-1} - H_i\right)\sin\alpha_i\right]\frac{\tan\phi_i}{FS_i}}{\cos\alpha_i - \frac{\sin\alpha_i \tan\phi_i}{FS_i}} + \frac{\left(W_i + V_i\right)\sin\alpha_i - \left(H_{i-1} - H_i\right)\cos\alpha_i + \frac{C_i L_i}{FS_i}}{\cos\alpha_i - \frac{\sin\alpha_i \tan\phi_i}{FS_i}} \quad \text{(B1)}$$

Using the following notation definitions, the terms of Equation B1 may be converted to their equivalent terms where differences in notation definition exist with the alternate equation. Converting Equation B1 to equivalent notation results in Equation B2:

H_i = all applied horizontal forces acting on an individual wedge

V_i = all applied vertical forces (body and surcharge) acting on an individual wedge

P_i = horizontal reactive forces with adjacent wedge

A_i = area of critical potential failure plane

$$\Delta P_i = \frac{\left(V_i \cos \alpha_i - U_i + H_i \sin \alpha_i\right) \frac{\tan \phi_i}{FS_i} + V_i \sin \alpha_i - H_i \cos \alpha_i + \frac{c_i A_i}{FS_i}}{\cos \alpha_i - \frac{\sin \alpha_i \tan \phi_i}{FS_i}} \qquad \text{(B2)}$$

Subscripts will not be used below where only one typical wedge is considered. Subscripts will necessarily be employed, later, when overall equilibrium of the system of wedges is considered. Equations B3 through B6 follow directly from Equation B2.

5. With the substitution $\cos \alpha = \frac{(\sin^2 \alpha - 1)}{\cos \alpha}$ and rearrangement of terms, Equation B2 becomes:

$$\Delta P = \frac{V \sin \alpha - H \cos \alpha + \frac{H \sin \alpha \tan \phi}{FS_i} - \frac{V (\sin^2 \alpha - 1) \tan \phi}{FS_i \cos \alpha} - \frac{U \tan \phi}{FS_i} + \frac{cA}{FS_i}}{\cos \alpha - \frac{\sin \alpha \tan \phi}{FS_i}} \qquad \text{(B3)}$$

Equation B3 can be rewritten as:

$$\Delta P = \frac{V \sin \alpha - H \cos \alpha + \frac{H \sin \alpha \tan \phi}{FS_i} - \frac{V \sin^2 \alpha \tan \phi}{FS_i \cos \alpha}}{\cos \alpha - \frac{\sin \alpha \tan \phi}{FS_i}} \qquad \text{(B4)}$$

$$+ \frac{\frac{cA \cos \alpha + (V - U \cos \alpha) \tan \phi}{FS_i \cos \alpha}}{\cos \alpha - \frac{\sin \alpha \tan \phi}{FS_i}}$$

The first four terms of the numerator of Equation B4 factor are as shown:

$$\Delta P = \frac{\left(V \frac{\sin \alpha}{\cos \alpha} - H\right)\left(\cos \alpha - \frac{\sin \alpha \tan \phi}{FS_i}\right) + \frac{cA \cos \alpha + (V - U \cos \alpha) \tan \phi}{FS_i \cos \alpha}}{\cos \alpha - \frac{\sin \alpha \tan \phi}{FS_i}} \tag{B5}$$

$$\Delta P = V \tan \alpha - H + \frac{cA \cos \alpha + (V - U \cos \alpha) \tan \phi}{FS_i \left(\cos^2 \alpha - \frac{\sin \alpha \cos \alpha \tan \phi}{FS_i}\right)} \tag{B6}$$

Note that:

$$\cos^2 \alpha - \frac{\sin \alpha \cos \alpha \tan \phi}{FS_i} = \frac{1 - \frac{\tan \alpha \tan \phi}{FS_i}}{\sec^2 \alpha} = \frac{1 - \frac{\tan \alpha \tan \phi}{FS_i}}{1 + \tan^2 \alpha}$$

Introduce the notation

$$n_\alpha = \frac{1 - \frac{\tan \alpha \tan \phi}{FS_i}}{1 + \tan^2 \alpha} \tag{B7}$$

Consider a system of wedges of k elements and the requirement that $\sum_{i=1}^{k} \Delta P_i = 0$ (See Equation 14). Then from Equation B6,

$$\sum_{i=1}^{k} \Delta P_i = 0 = \sum_{i=1}^{k} (V_i \tan \alpha_i - H_i) + \sum_{i=1}^{k} \frac{c_i A_i \cos \alpha_i + (V_i - U_i \cos \alpha_i) \tan \phi_i}{FS_i \, n_{\alpha i}} \tag{B8}$$

FS_i is considered constant in the limit equilibrium solution and may be solved for directly from Equation B8:

$$FS_i = \frac{\sum_{i=1}^{k} \frac{c_i A_i \cos \alpha_i + (V_i - U_i \cos \alpha_i) \tan \phi_i}{n_{\alpha i}}}{\sum_{i=1}^{k} (H_i - V_i \tan \alpha_i)} \tag{B9}$$

which is the general form of the equation for solution of FS by the alternate method of analysis, as given by Equation 15 in the main text.